

REPORT
UCB/SEMM-2001/05

STRUCTURAL ENGINEERING
MECHANICS AND MATERIALS

SHEAR STRENGTH OF R/C MEMBERS
WITHOUT TRANSVERSE REINFORCEMENT

By

MADHUSUDAN KHUNTIA
BOZIDAR STOJADINOVIC

MAY 2001

DEPARTMENT OF CIVIL ENGINEERING
UNIVERSITY OF CALIFORNIA
BERKELEY, CALIFORNIA

ABSTRACT: A simplified analytical model to compute the shear strength of reinforced concrete members without stirrups is presented in this report. This model is founded in the basic principles of mechanics of beams. The main variables considered during model development were the compressive strength of concrete, the longitudinal reinforcement ratio, and the shear span-to-effective depth ratio. In addition, the effects of member size, axial load, type of loading and support conditions on shear strength were considered. Using the proposed simplified analytical model an evaluation procedure, a parametrically derived equation, and a simplified design equation are proposed to calculate the shear strength. The evaluation procedure and equations were compared with numerous test data and found to be in good agreement. In addition, the approach is shown to be accurate, yet simpler than a number of commonly used empirical and analytical expressions. Changes to shear strength expressions in ACI Code are proposed.

Key words: shear strength, diagonal tension, reinforced concrete members, high strength concrete, effective shear depth, loading type, support conditions.

M. Khuntia is a structural engineer with S. K. Ghosh Associates Inc., Northbrook, IL, a firm specializing in structural, seismic and code consulting. He was formerly an Assistant Professor at Indian Institute of Technology, Delhi, INDIA. He received his Ph.D. from the University of Michigan, Ann Arbor in 1998. His research interests include behavior and design of RC and Steel-Concrete Composite Structures under seismic loading. He is a member of ACI Committees 335.

B. Stojadinovic is an Assistant Professor at the University of California, Berkeley. He received his Ph.D. from the same University in 1995. His research interests include behavior and performance-based design of Composite Structures under seismic loading. He is a member of ACI Committees 335, 341, 374 and 445.

INTRODUCTION

During the last 25 years significant advances have been made to design reinforced concrete (RC) members under shear in a more rational manner. Nevertheless, there is still a considerable amount of research effort going on in the area of shear design. The motivation for this work is the persistent difference between test data and shear strength expressions proposed by different investigators and code equations. Even though the principal reason for such differences is the considerable scatter of experimentally observed shear strengths, investigation of shear strength is important because of the brittle nature of shear failure. Another area of current shear strength research is the shear behavior of high-strength reinforced concrete members due to rapid growth of high-strength concrete application in construction practice.

It is believed that the shear failure of RC members without stirrups initiates when the principal tensile stress within the shear span exceeds the tensile strength of concrete and a diagonal crack propagates through the beam web. In other words, the diagonal cracking strength of RC members depends on the tensile strength of concrete, which in turn is related to its compressive strength. This belief is expressed in the fundamental shear strength model for concrete and the basic ACI Code (1999) equation.

However, the relation between concrete compressive strength and concrete shear strength is not that simple. Experimental studies by many investigators show that the present ACI design procedure can be quite unconservative when applied to very high-strength concrete. Similarly, RC beams with low reinforcement ratio were found to have substantially lower shear strength than that commonly assumed. There is now substantial evidence that, for reinforced concrete (RC) members without stirrups, the shear stress at failure decreases as the member becomes larger (Collins and Kuchma 1999; Kani 1967; Shioya et. al. 1989). Thus, the current ACI Code (1999) shear design procedures can be unconservative if applied to large RC members, especially when they are lightly reinforced. The current ACI empirical expression for the decrease in shear strength caused by axial tension is, in most situations, excessively conservative. While the Code procedure is intended for "members subjected to significant axial tension," it is based upon tests of members that were not reinforced for axial tension (Bhide and Collins 1989). Test results also show that RC members with uniform loading are likely to have greater shear strength than those with point loads (Krefeld and Thurston 1966). It may be noted that most of the shear tests conducted in laboratory by various investigators are subjected to point loads, whereas most of the loading encountered in practice is generally distributed in nature. Similarly, most of the shear tests conducted so far are simply supported, mainly for convenience. However, most support conditions encountered in practice are either rigid or semi-rigid.

Research Significance

As has been said many years ago, "Nothing is more practical than a simple theory." The purpose of this report is to present a simplified approach to compute the shear strength of RC members without stirrups. Current ACI simplified shear design procedure does not recognize the influence of member size, type of loading (point load or uniform loading) and support conditions (pinned or fixed) on the shear strength of the RC

members. The influence of axial load (tension or compression), longitudinal reinforcement ratio and concrete strength is also not appropriately accounted for. The effects of all these parameters are addressed in a more rational manner in a model for shear strength of reinforced concrete members without transverse reinforcement proposed in this report.

MODELING APPROACH

The goal of this study is to represent the shear strength of RC members without transverse reinforcement as:

$$v_c = k (f_c')^\alpha \quad (1)$$

a product of a factor k and an exponential function of the nominal concrete strength. Shear strength factor k is a function of the geometry of the beam, its longitudinal reinforcement, and the applied load. This model is a generalization of many existing models. For example, the fundamental ACI Code shear strength equation (1999):

$$v_c = 2\sqrt{f_c'}$$

is in this format, with $k = 2$ and $\alpha = 0.5$. Similarly, in the general shear design method based on the Modified Compression Field Theory (MCFT) (Collins et al. 1996), shear strength

$$v_c = 0.9\beta\sqrt{f_c'}$$

making factor k a function of the tensile stress factor β , defined by Collins et al. (1996), and $\alpha = 0.5$. Appendix III gives a summary of the general shear design method for RC members without stirrups.

SIMPLIFIED SHEAR STRENGTH MODEL

All theoretical models contain simplifying assumptions, with the test of the theory being that it should be simple enough to be used in practice, but complex enough to capture what happens in reality (Collins 1998). The following assumptions are made in the proposed simplified shear strength model:

A cross section that was plane before loading remains plane under load. This means that the distribution of longitudinal strain on a beam cross section (Fig. 1) is linear as shown in Fig. 2b. Thus, this model is not applicable to very deep members (with shear span-to-depth ratios of less than 2) for which longitudinal strain distribution is not linear.

For shear resistance, the cross section is effective over its uncracked depth c_1 (called as effective shear depth) as shown in Figs. 2c and 3a. The magnitude of c_1 is slightly larger than the neutral axis depth c (Fig. 2). Note that the sections with flexural cracks have less shear capacity than those without flexural cracks.

The shear stress distribution is modeled as parabolic over the effective shear depth (Fig. 3a) with the maximum value at the neutral axis, as shown in Fig. 3b. Thus, the magnitude of shear resistance over the effective cross section equals $(2/3) \tau_{\max} b_w c_1$.

where b_w is width of the section (Fig. 2a) and τ_{\max} is the shear stress at neutral axis. Note that the gradient of shear stress is different on either sides of neutral axis.

For simplicity and conservatism, the shear resistance due to dowel action of longitudinal reinforcement for flexure is neglected.

The proposed model considers the stress conditions just prior to diagonal cracking but after the formation of flexural cracking, whereas most conventional approaches and MCFT consider the stress conditions after the formation of diagonal cracking. The latter approaches may be less efficient due to many unreliable shear-resisting mechanisms (such as aggregate interlock and frictional resistance) involved along the cracking plane.

The model is based on considering the stress condition at the neutral axis of the cross section. It should be noted that the general shear design method (Collins et al. 1996) based on MCFT considers the stress conditions at the level of longitudinal steel for flexure. The stresses at these locations are always in the higher longitudinal strain region than other locations closer to the neutral axis. Note, however, that a major portion of the cross section considered to carry the shear force is under compression (Fig. 3a). In addition, prior to diagonal cracking, the shear stress at the neutral axis is higher than at other points of the cross section.

The material at the neutral axis is under pure shear (Fig. 3d), regardless of the magnitude of axial force. This stress-state is equivalent to a principal tension-compression stress state, as shown in Fig. 3e. The shear stress on the principal planes shown in Fig. 3e does not exist. Thus, a diagonal tension crack occurs when the principal tensile stress (σ_1) at the neutral axis attains the tensile strength (f_t) of concrete.

The shear strength of RC members is conservatively taken as the diagonal cracking strength. For slender RC beams without transverse reinforcements, this assumption is quite reasonable, as shown by experimental results (Yoon et al. 1996, Cassio and Siess 1960) for example. This assumption becomes more conservative (i.e., the ultimate shear strength becomes greater than the diagonal cracking strength) with decreasing shear span due to arch action. Based on numerous experimental results, Zsutty (1968) reported that the ultimate strength of RC members without stirrups is about 7% higher than their diagonal cracking strength.

From the above assumptions it can be inferred that when the principal tensile stress at the neutral axis reaches the tensile strength of concrete (Fig. 3e) a diagonal tension crack forms, thereby initiating the shear failure of the beam. Mathematically, at diagonal shear cracking the shear stress at neutral axis:

$$\tau_{\max} = f_t \quad (2)$$

where f_t is the tensile strength of concrete. Diagonal cracking shear strength of a beam cross section, is (note the parabolic distribution of shear stress over c_1)

$$V_{cr} = \frac{2}{3} b_w c_1 \tau_{\max} = \frac{2}{3} f_t b_w c_1 = \frac{2}{3} f_t \frac{c_1}{d} b_w d = v_{cr} b_w d \quad (3)$$

where d is the effective depth and v_{cr} is the diagonal cracking shear stress of the member given by

$$v_{cr} = \frac{2}{3} \frac{c_1}{d} f_t \quad (4)$$

If the shear strength of concrete v_{cr} is taken as $k\sqrt{f'_c}$, then Eq. (4) reduces to:

$$k = \frac{2}{3} \frac{c_1}{d} \frac{f_t}{\sqrt{f'_c}} \quad (5)$$

Equation 4 shows that the magnitude of v_{cr} depends on the tensile strength of concrete and the effective shear depth c_1 of the beam cross section under consideration. The tensile strength of concrete is a property of the material, and is generally related to its compressive strength. On the other hand, the effective shear depth c_1 depends on the factored bending moment M_u and factored axial load P_u at the section and can be calculated from force and moment equilibrium conditions (Figs. 1 and 2). For example, if the effective shear depth c_1 is $0.45d$ under a given loading condition, and the tensile strength of concrete is taken as $6.7\sqrt{f'_c}$, the shear strength of section computed using Eq. 4 would be $2\sqrt{f'_c}$, identical to simplified ACI Code Equation.

As shown in Eq. 4, to compute the shear strength of RC beams under given loading, it is only necessary to compute the value of effective shear depth c_1 . This value can be obtained from axial force equilibrium (Fig. 2). Corresponding moment capacity (M or M_u) can be obtained from moment equilibrium. The critical shear span-to-depth ratio $(M_u/V_u d)_{cr}$ ($M_u/V_{cr} d$ for shear failure) can then be computed, taking V_{cr} as the diagonal cracking shear strength computed by using Eq. 3 at the critical section. The critical shear section is defined as the section where diagonal cracking occurs first following flexural cracking (Fig. 1). At that section, the shear force due to external loading V_u equals the shear resistance V_{cr} , while the magnitude of V_u is less than V_{cr} at other sections. Note that along the shear span, shear force V_u can remain constant or vary depending on the type of loading whereas the cracking shear strength V_{cr} is proportional to effective shear depth c_1 .

From the above procedure, it can be seen that the proposed simple model cannot predict the shear deformation of the member after formation of diagonal cracking. This can be achieved using MCFT. However, shear deformation for RC members without transverse reinforcement is of little practical importance because the strength of such members after first diagonal cracking tends to deteriorate very rapidly leading to quick collapse.

Proposed Procedure for Computing the Shear Strength of RC Members without Stirrups

Step 1: At the design section under the factored bending moment M_u and axial load P_u , calculate the effective shear depth c_1 , as shown in Fig. 2 using strain compatibility and equilibrium conditions. Thus,

$$c_1 = c + c_2 = c \left(1 + \frac{\epsilon_{cr}}{\epsilon_c} \right) \quad (6)$$

Step 2: The shear strength of the RC member is (Eq. 4):

$$v_{cr} = \frac{2}{3} \frac{c_1}{d} f_t$$

where d is the effective depth of the section and f_t is the tensile strength of concrete.

PARAMETRIC STUDY

The two-step procedure for evaluating the shear strength of RC beams proposed above was evaluated in a parametric study. This study has three objectives.

First, the shear strength computed by the proposed procedure was compared to nine shear strength equations listed in Table 1. These expressions are empirical in nature because they are derived by regression of numerous experimental data. They are, also, quite good. For example, empirical expressions proposed by Zsutty (1968), Okamura and Higai (1980) and ASCE-ACI (1973) (shown in Table 1) were stated to be quite reliable in a study presented in the State-of-the-Art Report on Shear Strength of Concrete (ASCE-ACI Committee 445 Report, 1998).

Second, the sensitivity of the shear strength values was computed using the proposed procedure to changes in 3 primary and 4 secondary parameters. The primary parameters are: (1) critical shear span-to-depth ratio $M_u/V_{cr}d$ (ranging from 1 to 5); (2) main longitudinal reinforcement ratio ρ (ranging from 0.5 to 3.0%); and (3) compressive strength of concrete f_c' (ranging from 4000 to 12,000 psi). The secondary parameters are: (1) axial stress (-500 psi tension to 2500 psi compression); (2) member size; (3) type of loading (point vs. uniform loading); and (4) type of support conditions (pinned vs. fixed). As explained later, the range of 1 to 5 for critical shear span-to-depth ratio $M_u/V_{cr}d$ is equivalent to a range of 2 to 6 for customary shear span-to-depth (a/d or $L/2d$) ratio, depending on the type of loading and support conditions. Note that none of the empirical expressions in Table 1 considers all 7 parameters simultaneously.

Third, the parametric study was used to determine values of the shear strength factor k and exponent α in Eq. 1 to account for the effect of the 7 considered parameters.

Material Properties of Concrete

Tensile strength of concrete f_t was taken equal to split cylinder strength (f_{cr}). The split cylinder tensile strength (f_{cr}) was considered in two different ways.

The first option is to assume concrete split cylinder strength (f_{cr}) proportional to $(f_c')^{0.5}$. A value of splitting tensile strength equal to $6.7\sqrt{f_c'}$ is suggested in ACI 318 Sec. R11.2.1.1 (1999). The average split cylinder strength of normal weight concrete with f_c' between 3,000 and 12,000 psi of $7.4\sqrt{f_c'}$, with a lower limit of approximately $6.7\sqrt{f_c'}$ for lower compressive strength, is suggested in ACI Manual of Concrete Practice (2001), as shown in Fig. 4a. Experimental results from five different investigations (Bhide and Collins 1989, Yoon et. al. 1996, Rajagopalan and Fergusson 1968, Halladin et. al. 1971, and Adebar and Collins 1996) were compiled in this study (Table 2). The average split

cylinder strength of concrete was found to be $6.4\sqrt{f_c'}$, close to the ACI 318 value. Therefore, tensile strength of concrete equal to $6.7\sqrt{f_c'}$ was adopted as a good average value for all concrete strengths, and will be used in the following parametric study.

The second option is to assume concrete split cylinder strength (f_{cr}) proportional to $(f_c')^{0.67}$. Table 2 shows that adopting concrete tensile strength $f_{cr} = 1.5(f_c')^{2/3}$ is quite reasonable. It may be noted that some European investigators take tensile strength proportional to $(f_c')^{0.67}$ rather than to $\sqrt{f_c'}$. For example, Reineck (1991) used a value of $1.23(f_c')^{0.67}$ for direct tensile strength of concrete. The effect of these two options is examined later in this report.

Elastic modulus of concrete, E_c was taken as

$$E_c [\text{psi}] = 40,000\sqrt{f_c'} + 1,000,000 [\text{psi}] \quad (7)$$

following the recommendation in ACI Manual of Concrete Practice (2001). This expression applies to a wide range of compressive strengths of concrete ($3000 \text{ psi} < f_c' < 12,000 \text{ psi}$) for normal weight concrete (Fig. 4b). Elastic modulus of concrete is needed to calculate the cracking strain (Fig. 2b). It may be emphasized that the assumption of taking E_c according to ACI 318 (1999) will give almost identical results.

A common stress-strain relation for concrete in compression was adopted for all concrete strengths. It was a second-order parabola, given by the following equation:

$$f_c = f_c' \left\{ 2 \left(\frac{\epsilon_c}{\epsilon_o} \right) - \left(\frac{\epsilon_c}{\epsilon_o} \right)^2 \right\} \quad (8)$$

where f_c is the compressive stress in concrete corresponding to concrete strain ϵ_c . Strain at peak concrete stress ϵ_o is assumed to be equal to 0.002.

This choice of expressions for concrete tensile strength, concrete modulus of elasticity and stress-strain relation in compression was made for the parametric study. However, the method for evaluating beam shear strength presented herein is general in the sense that other expression for concrete strength and stiffness can be used. For example, a better compression stress-strain equation (Eq. 8a), applicable for all concrete strengths, suggested by Khuntia and Goel (1999), can be used in place of Eq. 8.

$$f_c = E_c \epsilon_c \left\{ Q + \frac{1-Q}{\left[1 + \left(\frac{E_c \epsilon_c}{2.85 f_c'} \right)^N \right]^{1/N}} \right\} \quad (8a)$$

In this equation, Q and N are non-dimensional factors taken as $Q = -0.9Z^{2.1}$ and $N = 1.5 + (Z-1)^{0.8}$ while $Z = f_c'/4000$ (f_c' in psi). Figure 5 shows typical stress-strain curves for different concrete strengths based on Eq. 8a. Note that the stress-strain curve for high

strength concrete is not a 2nd order parabola as predicted by Eq. 8, whereas this feature is captured by Eq. 8a. For a given concrete strength Eq. 8a can be easily simplified into a second- or third-order equation for use in nonlinear analysis. For example, a second-order equation $f_c = f_c'(A\varepsilon_c + B\varepsilon_c^2)$ can be generated from Eq. 8a, where A and B are constants depending on concrete strength.

RESULTS OF PARAMETRIC STUDY

The effect of each parameter was studied by varying its magnitude while maintaining the values of other six parameters constant. In each case, the proposed two-step procedure was applied. First, the value of effective shear depth of the beam c_1 was calculated by solving the equilibrium equations using a computer spreadsheet. Second, the shear strength v_{cr} and the corresponding k-value were computed by using Eqs. 4 and 5. In addition, the corresponding critical shear span-to-depth ratio $M_u/V_{cr}d$ was computed by using Eq. 3.

The results of data regression are presented using the format of Eq. 1 by specifying the shear strength factor k. The exponent α is fixed at 0.5, in compliance with the adopted expression for tensile strength of concrete $f_t = 6.7\sqrt{f_c'}$ (first option discussed above).

Influence of Critical Shear Span-to-Depth Ratio on Shear Strength

At any section of the RC member, the depth of the flexural crack is expected to increase (i.e., the magnitude of the effective shear depth c_1 is expected to decrease) with increasing bending moment M_u . Thus, the cracking shear strength V_{cr} decreases with increasing bending moment. Failure occurs at the section where V_{cr} equals V_u , the shear force due to applied member load. In this parametric study, the shear strength was found to be proportional to $(M_u/V_{cr}d)^{-0.13}$ for the considered ranges of concrete strength and longitudinal reinforcement ratio. For example, the shear strength factor k for a beam with $f_c' = 4000$ psi and $\rho = 1\%$ can be computed using the following equation, obtained by curve-fitting the data computed using the proposed two-step procedure:

$$k = 2.02 \times (M_u / V_{cr}d)^{-0.13} \quad (9)$$

The effect of critical shear span-to-depth ratio ($M_u/V_{cr}d$) on the shear strength is illustrated in Fig. 6. It shows that Eq. 9 matches closely and conservatively the data obtained by the two-step procedure. It should be emphasized that $M_u/V_{cr}d$ is not equal to a/d (shear span-to-depth ratio). As explained later, $M_u/V_{cr}d$ can be taken equal to $(a/d-1)$ for simply supported beams with point loading, while it varies in the case of uniform loading.

For deep beams with smaller a/d ratios (a/d less than 2.5, i.e. $M_u/V_{cr}d$ less than 1.5 for simply supported beams with point loading), Eq. 9 may give very conservative results (Fig. 6). It should be noted that the ultimate shear strength of a deep beam is considerably higher than its shear strength at diagonal cracking, due mainly to arching action. Properly designed strut and tie models are likely to give more accurate capacity estimates for such members.

Influence of Longitudinal Reinforcement Ratio on Shear Strength

The effective shear depth c_1 increases when the amount of tensile reinforcement increases to maintain axial force equilibrium, thereby increasing the shear strength of the member (Eq. 4). The proposed two-step procedure replicates this trend, even though it shows that the increase of shear strength is not directly proportional to the increase in the amount of longitudinal reinforcement. The computed shear strength is proportional to $(\rho)^{0.37}$ for the ranges of concrete strength and critical shear span-to-depth ratios considered in this study. It should be noted that in empirical expressions suggested (Table 1) by Zsutty (1968), Okamura and Higai (1980), JSCE (1986), and CEB-FIP Model Code (1993) for normal strength concrete, and by Ahmad et al. (1986) for high-strength concrete, shear strength is taken as proportional to $(\rho)^{1/3}$. Another experimental study involving high strength concrete by Kim and Park (1994) suggests that shear strength is proportional to $(\rho)^{0.31}$. In this study, the shear strength factor k for RC beams with critical shear span-to-depth ratio $M_u/V_{cr}d$ equal to 3 and concrete strength of 4000 psi is:

$$k = 1.75 \times (\rho)^{0.37} \quad (10)$$

The effect of reinforcement ratio (ρ) on the shear strength is illustrated in Fig. 7. This figure shows that shear strength values obtained using Eq. 10 compare very well with values obtained from the proposed two-step method.

Influence of Compressive Strength of Concrete on Shear Strength

When high-strength concrete is used in place of normal concrete, the neutral axis depth (and the effective shear depth c_1) decreases to maintain force equilibrium (Fig. 2). Thus, the shear strength factor k is expected to decrease, too. Using the proposed two-step procedure, it was found that shear strength factor k is proportional to $(f_c')^{-0.32}$ for the ranges of reinforcement ratios and critical shear span-to-depth ($M_u/V_{cr}d$) ratios considered in this study. A simplified expression is obtained by fitting the proposed two-step procedure results for a beam with a 1% longitudinal reinforcement ratio and a critical shear span-to-depth ratio $M_u/V_{cr}d$ equal to 3:

$$k = 1.75 \times \left(\frac{4000}{f_c'} \right)^{0.32} \quad (11)$$

The data obtained from Eq. 11 is compared to the proposed procedure data in Fig. 8. The match is quite good.

It is interesting to construct the entire shear strength equation using the format specified in Eq. 1. Such equation derived using Eq. 11 (for $\rho = 1\%$ and $M_u/V_{cr}d = 3$) is:

$$v_{cr} = k(f_c')^{0.5} = 24.9 \times (f_c')^{0.18} \quad (12)$$

i.e., v_{cr} is proportional to $(f_c')^{0.18}$. Note how the effective shear depth c_1 and tensile strength of concrete f_t combine to give such exponential relation between v_{cr} and f_c' .

Conducting the same parametric study assuming that tensile strength f_t is proportional to $(f_c')^{0.67}$ instead of $\sqrt{f_c'}$ (2nd option as discussed above), shows that the shear strength

v_{cr} is proportional to $(f_c')^{0.32}$. This is similar to the equations proposed by Zsutty, Okamura and Higai, JSCE, and CEB-FIP Model (Table 1). Mphonde and Frantz (1984) suggested that v_{cr} is proportional to $(f_c')^{0.33}$ using an experimental study of normal and high-strength concrete beam shear strengths.

Evidently, whether the shear strength v_{cr} is proportional to $(f_c')^{0.18}$ or to $(f_c')^{0.32}$ depends very much on the assumed relationship between tensile strength f_t and compressive strength f_c' of concrete. Furthermore, one selected relation may not hold for the entire range of concrete compressive strength. Indeed, test results on high strength concrete (by Yoon et. al. 1996, for example) indicate a need to reduce the shear strength factor k below the customary ACI value of 2, i.e. to assume that the exponent α in Eq. 1 is less than the customary 0.5. Such reduction in shear strength is commonly explained by decrease in shear resistance attributed to aggregate friction/interlock. This is because in high-strength concrete cracks pass through the aggregate, resulting in crack surfaces that are relatively smooth (Collins and Kuchma 1999). However, as explained in the assumptions of this study and corroborated by test results, shear capacity of a concrete beam just prior to diagonal cracking (where aggregate interlock has no role to play) is almost equal to that after diagonal cracking. Therefore, the smooth crack surface concept may not entirely explain the reduction in shear strength of high-strength concrete. On the other hand, the interpretation presented herein, based on formation of longer flexural crack and correspondingly smaller effective shear depth c_1 for high-strength concrete, is believed to be more logical. Furthermore, the two-step procedure is applicable to any concrete strength as long as a suitable concrete stress-strain relation, such as the one suggested by Khuntia and Goel (Eq. 8a) and a suitable split-cylinder tensile strength are used.

Proposed Equation for Computing the Shear Strength of RC Members without Stirrups

Regression of shear strength data computed using the proposed two-step shear strength procedure in the parametric study presented above makes it possible to formulate a simplified shear strength equation to replace the two-step procedure for codified design applications. Combining Eqs. 9 through 12, the shear strength of an RC member without stirrups can be expressed as:

$$v_{cr} = 28.7\rho^{0.37} \left(\frac{V_{cr}d}{M_u} \right)^{0.13} (f_c')^{0.18} \quad (13)$$

where the longitudinal reinforcement ratio ρ is expressed in percent and concrete compressive strength f_c' is in psi. In SI units, (f_c' in MPa), Eq. 13 is:

$$v_{cr} = 3.34\rho^{0.37} \left(\frac{V_{cr}d}{M_u} \right)^{0.13} (f_c')^{0.18} \quad (13a)$$

Note that Eq. 13 was obtained using the proposed two-step procedure (Eq. 4 and Eq. 6) based on principles of beam mechanics and reasonable assumptions about mechanical characteristics of concrete. Therefore, Eq. 13 is not empirical in the same sense as the empirical shear strength equations listed in Table 1. The proposed equation accounts only

for the effects of three primary parameters: $M_u/V_{cr}d$, f_c' and ρ . The form of the shear strength model equation (Eq. 1) is preserved: the shear strength factor k is a function of longitudinal reinforcement ρ and critical shear span-to-depth ratio $M_u/V_{cr}d$, while the exponent $\alpha = 0.18$. The exponents associated with each parameter in Eq. 13 show that beam shear strength is approximately twice as sensitive to variation of the longitudinal reinforcement ratio than to the variation of shear span-to-depth ratio or the variation of compressive strength of concrete.

Eq. 13 can be further simplified to:

$$v_{cr} = 34 \sqrt[3]{\rho \left(f_c' \frac{V_{cr}d}{M_u} \right)^{0.5}} \quad (14)$$

The data shown in Table 3 shows that the predicted ratio of shear strength computed by using Eq. 14 to Eq. 13 for wide range of f_c' (4000 to 12000 psi), ρ (1 to 3%) and $M_u/V_{cr}d$ (1 to 5) has a mean of 1.00 and a standard deviation of 0.03. In the following, Eq. 13 is referred to as the “parametric equation”, while Eq. 14 is called the “simplified equation”.

VERIFICATION USING EXPERIMENTAL DATA

A suite of 127 beam shear strength tests from 8 different investigators, listed in Table 4, are used to check the validity of the proposed two-step procedure, reduced parameter equation (Eq. 13), and proposed simplified equation (Eq. 14) for computing the shear strength of RC members. The shear strength values computed using the two-step proposed procedure and the proposed equations are also compared to those calculated using other empirical expressions (Table 1) and the Modified Compression Field Theory (Appendix III).

Table 4 shows the geometric and material properties of concrete beams considered by various investigators. The test data includes concrete strengths ranging from 2,300 psi to 13,300 psi, shear span-to-depth ratio of 2.5 to 7.3, reinforcement ratio of 0.47% to 6.6%, and effective beam depth up to 15.9 in. All specimens were simply supported beams loaded by transverse point loads. None of the specimens had any axial load.

In Table 4, the cracking shear strength is taken equal to ultimate shear strength, unless reported otherwise. The critical shear span-to-depth ratio for a beam with a point load and simple supports is computed as:

$$\frac{M_u}{V_{cr}d} = \frac{a}{d} - 1 \quad (15)$$

In other words, it is assumed that the critical shear section is at one beam depth away from the point load. However, as explained later in this report the location of critical shear section may be different for other loading and support conditions.

The shear strength was calculated using each method and compared to the measured test values. The mean and standard deviation of the test/prediction ratios for all methods are reported in Table 4. Table 5 shows the summary of this comparison. Figures 9

through 14 also show the test/prediction ratios computed using the proposed procedure, proposed parametric equation (Eq. 13), proposed simplified equation (Eq. 14), ACI-Simplified, ACI-Detailed procedure, and MCFT, respectively. The ratios computed using other empirical and code equations are illustrated in Figs. 15 through 20.

The results presented in Table 5 show that the proposed simplified procedure and the parametrically derived equation (Eq. 13), as well as the proposed simplified equation (Eq. 14) fit experimental data well and are statistically similar. Among other methods, MCFT (Fig. 12), and CEB-FIP Model Code (Fig. 18) are found to be very reliable for design purposes (with mean minus one standard deviation being close to 1.0 and with a small scatter). The predictions by JSCE Method (Fig. 19) and ACI-Detailed equation (ACI 318-99 Eq. 11-5) are also reasonable. However, it may be noted that the magnitude of $M_u/V_{cr}d$ while using ACI-Detailed Equation (Table 1) is taken as $(a/d-1)$. Using $M_u/V_{cr}d = 1$ (i.e., assuming critical shear section at a distance of d from the support), the mean and the standard deviation of test/predicted ratio for the above data set by ACI-Detailed procedure are 0.93 and 0.15, respectively.

The predictions by ACI-Simplified and ASCE-ACI Committee are found to be very conservative for beams with higher reinforcement ratio (Fig. 13 and Fig. 17). The prediction by Kim et al. (Table 1) was found to be very unconservative. It overestimates the influence of the tensile steel ratio (Fig. 20). The predictions by Zsutty and by Okamura show less scatter than the others (Fig. 15, Fig. 16 and Table 5). However, their predictions can be unconservative for many test cases (Table 4). For design purposes, their equations need to be multiplied by an appropriate safety factor. For example, a factor of 1.14 for Zsutty's equation will make the mean and standard deviation of the test/predicted ratio equal to 1.13 and 0.13, respectively. Similarly, a factor of 1.22 with Okamura's equation will make the mean and standard deviation of the test/predicted ratio equal to 1.12 and 0.12, respectively (Table 5).

Following important points should be noted about the two-step procedure, MCFT and equations presented in Table 1:

1. Only the proposed two-step procedure, the parametric and simplified equations (Eqs. 13 and 14) and the MCFT procedure are based on rational shear resistance models. Other equations are empirical in nature.
2. Comparing the proposed two-step procedure with MCFT and considering the influence of longitudinal reinforcement ratio (ρ), critical shear span-to-depth ratio ($M_u/V_{cr}d$), and compressive strength of concrete (f'_c) only, note that both predict a decrease in shear strength v_{cr} with a decrease in ρ and an increase in $M_u/V_{cr}d$, albeit at somewhat different rate. The major difference between the two procedures is the relation between shear strength and concrete compressive strength.
3. The expressions by Zsutty, Kim et al., ACI-Simplified, ACI-Detailed, and ASCE-ACI Committee do not take the size effect into account. As suggested by Collins and Kuchma (1999) and explained in this report, shear stress at failure decreases with increase in member size. By including the size effect with the proposed simplified equation (Eq. 14) for the above data set, the mean and standard deviation of test/predicted ratio were found to be 1.10 and

0.14, respectively, compared to 1.14 and 0.16 by ignoring the size effect. This difference is small because the beams in this data set were not too deep (the depth of beams in this data set did not exceed 16 in.).

INFLUENCE OF SECONDARY PARAMETERS

A group of four secondary parameters was also considered in this parametric study. These parameters were: member axial load, member size, type of member loading, and member support conditions. The principal findings of the parametric study are presented below.

Influence of Axial Load

In general, when an RC member is subjected to axial compression, effective shear depth c_1 (Fig. 2) will increase, thereby increasing the shear strength of the member (Eq. 4). The reverse is true in case of axial tension. However, the rate change of v_{cr} with respect to axial load magnitude is different for different concrete strengths, reinforcement ratios, and critical shear span-to-depth ($M_u/V_{cr}d$) ratios (Fig. 21). Therefore, no simple equation can accurately predict the influence of axial tension and compression on shear strength. It is suggested to use the proposed two-step procedure (Eq. 4) to predict the shear strength of RC member in presence of axial load more accurately.

There are only a few shear tests on RC beams with axial load. One of these investigations (Mattock 1969) is considered in this study for comparison. Table 6 gives the details of the variables and the test results from Mattock's study. The principal variable was axial stress, varied from -250 psi in tension to 400 psi in compression. Other variables include: concrete strength (ranging between 2200 psi and 8000 psi), longitudinal reinforcement ratio (ranging between 1% and 3.1%), and shear span-to-depth ratio (ranging between 2.74 and 5.14). The shear strength at diagonal cracking is taken for comparison. It is important to note that the magnitude of ultimate shear strength is almost equal to the diagonal cracking shear strength: the ratio of ultimate to cracking strength has a mean value of 1.05 and a standard deviation of 0.09 (Table 6).

These test results were compared to the proposed two-step procedure, MCFT, and the ACI-Simplified method (Fig. 22). The ACI Simplified expressions are:

$$v_c = 2 \left(1 + \frac{N_u}{2000A_g} \right) \sqrt{f'_c} \quad (16)$$

in case of axial compression (ACI Eq. 11-4), and

$$v_c = 2 \left(1 - \frac{N_u}{500A_g} \right) \sqrt{f'_c} \quad (17)$$

in case of axial tension (ACI Eq. 11-7). In both of these equations, N_u is positive in compression, while stress-related quantities $\sqrt{f'_c}$, N_u/A_g , 500, and 2000 are in psi.

The results show very good correlation of the proposed two-step procedure predictions (Eq. 4) to experiment data. The proposed two-step procedure yields an

average test/prediction ratio of 1.18 and a standard deviation of 0.13. The prediction by MCFT is less accurate but reasonable with test/prediction ratio of 1.43 and a standard deviation of 0.17 (Table 6). On the other hand, the predictions by the simplified ACI Code method (ACI Sec.11.3.1.2) are more scattered (with the average test/prediction ratio of 1.58 and a standard deviation of 0.40) and more conservative for members with significant axial tension (N_u/A_g between -100 to -300 psi). As can be seen from Fig. 21, the predictions by simplified ACI code method is likely to give very conservative results for low axial tension (N_u/A_g less than 150 psi tension). Bhide and Collins (1989) and Adebar and Collins (1996) also noted such conservativeness of the ACI method for shear strength of beams under axial tension. Parametric analysis using the two-step procedure shows that there is rapid degradation in shear strength when axial tension stress becomes significant. See Fig. 21 for the case when N_u/A_g is more than 150 psi in tension. This occurs because the effective shear depth c_1 becomes very small. Therefore, the conservativeness of the ACI approach may be justified for axial tension forces producing tensile stresses larger than 150 psi.

It is sometimes suggested to summarily neglect the shear strength contribution of concrete when axial tension stress exceeds 300 psi. However, it may be more appropriate to use the following equation (Eq. 18), when the member is subjected to an axial tension stress (N_u/A_g) of less than or equal to 150 psi:

$$v_c = 2 \left(1 + \frac{N_u}{1000A_g} \right) \sqrt{f_c'} \quad (18)$$

Using Eq. 18 in lieu of Eq. 17 for members with axial tension stress $N_u/A_g \leq 150$ psi tension gives an average test/predicted ratio of 1.53 instead of 1.58 for the limited data set shown in Table 6. Also shown in Table 6 and reported by Gupta and Collins (2001), the simplified ACI Eq. 11-4 (Eq. 16 above) gives a conservative estimate for shear strength of RC members under axial compression. This is also the case for the majority of the data shown in Fig. 22. Therefore, Eq. 16 is recommended for simplicity and conservatism when there is axial compression and when accuracy is a not very significant factor.

As expected, shear strength of an RC beam grows with increasing axial compression. However, there is a limit to the concrete shear strength. Equation 4 shows that for a given section, the maximum value of effective shear depth c_1 will be the total member depth h . Assuming concrete tensile strength f_t of $6.7\sqrt{f_c'}$ and h/d of 1.15 (h/d ranges between 1.1 and 1.2 in practical cases), the maximum shear strength is:

$$(v_{cr})_{\max} = \frac{2}{3} \frac{(c_1)_{\max}}{d} f_t = \frac{2}{3} \frac{h}{d} \times 6.7\sqrt{f_c'} \approx 5.0\sqrt{f_c'} \quad (19)$$

Equation 19 indicates that the shear strength of RC members will never exceed $5.0\sqrt{f_c'}$, even when the member is subjected to excessive axial compression. This value corresponds to an axial compressive stress (N_u/A_g) of 3000 psi in Eq. 16 (ACI Simplified Equation). It is interesting to note similar conclusions by Gupta and Collins (2001). Based on an extensive experimental study and comparison of test results with MCFT and

ACI Code methods, Gupta and Collins (2001) recommend: “when using ACI Simplified Equation, the term for axial compression (N_u/A_g) not be taken greater than 3000 psi.”

Influence of Member Size

The proposed two-step procedure does not capture the effect of increasing member depth on its shear strength. Test results by many investigators (Kani 1967, Kim and Park 1994, Collins and Kuchma 1999, Shioya et. al. 1989) show that the shear strength of RC beams decreases with increasing member depth. This phenomenon is often referred to as the size effect in shear strength of RC beams.

There are three major reasons for shear strength decrease with increasing member depth. The first reason is material-related size effect: tensile strength of concrete decreases with increasing specimen size. This is expected, given the relation between the tensile and compressive strength and the fact that compressive strength of concrete also diminishes with increasing specimen size. For example, test results show that the compressive strength of a 6 x 12 in. cylinder is about 92 percent of that of a 3 x 6 in. cylinder (Mphonde and Frantz 1984).

The second reason is a decrease in concrete strength in the upper layers of the section when concrete is cast from above (typical for deep beams). It should be noted that the ACI Code (1999) Equation (Eq. 12-1) for reinforcement development length considers a reinforcement location factor of 1.3 (test result mean being 1.2) when more than 12 in. of fresh concrete is cast below the rebar. Thus, the ACI Code indirectly considers a reduction of compressive strength in the upper layers of a member because rebar bond strength is taken proportional to $\sqrt{f_c}$. This reduction is approximately 40% (i.e., $1 - 1/1.3^2$). Thus, the actual concrete strength in the compression zone of large-size beams is expected to be smaller than that in normal-size beams.

The third reason for reduction in shear strength is attributed to a possible change of the critical section location with increasing beam depth. Test results by Kani (1967) show that the decrease in shear strength as depth increases is more prominent for beams with lower shear span-to-depth (a/d) ratio than for beams with higher a/d ratio (Fig. 23). It has also been reported (Kani 1967) that the spacing of flexural-shear cracks is almost constant, independent of the beam depth. Based on these observations, it is believed that the critical section for point loading, which is taken at a distance d from the load point for normal size beams under point loads (Eq. 15), would be closer to the load point (i.e., to a location of higher $M_u/V_{cr}d$) for large-size beams. In other words, effective shear depth c_1 and corresponding shear strength are likely to decrease for deeper beams. For example, the critical shear span-to-depth ratio ($M_u/V_{cr}d$) of 4 for a normal-size beam changes to 4.5 for a large-size beam (leading to about 1% decrease in shear strength per Fig. 6) while $M_u/V_{cr}d$ of 1 for normal-size beam changes to 1.5 for a large-size beam (leading to about 10% decrease in shear strength per Fig. 6). The test results by Kani (1967) shows similar trend (Fig. 23).

Recently, based on a series of test results Collins and Kuchma (1999) reported that longitudinal reinforcement uniformly distributed over the cross section depth slows the rate the shear strength reduction in large-size beams without stirrups. Longitudinal reinforcement in more layers distributed over the depth resist diagonal tension better and

enhances the dowel-mechanism resistance. Collins and Kuchma (1999) suggested the following simplified predictive equation (hereafter known as Modified ACI or MACI) for shear strength of large beams without stirrups:

$$v_c = \frac{57.5}{(50 + S_e)} \times 2\sqrt{f'_c} \quad (20)$$

The parameter S_e is a function of maximum aggregate size a and crack spacing S_x for normal strength concrete, and a function of S_x only for high-strength concrete, where S_x is the largest vertical distance between adjacent layers of longitudinal reinforcements (Fig. 24). Mathematically,

$$S_e = \frac{1.38S_x}{(a + 0.63)} \quad (20a)$$

In Eq. 20a, aggregate size a is taken to be zero for high strength concrete. This is based on the assumption that shear cracks pass through the aggregate thereby making the size of aggregate meaningless in high-strength concrete.

As reported by ASCE-ACI Committee 445 on Shear and Torsion (1998), the expression by Okamura and Higai (Table 1) represents a reasonable lower bound for capturing the size effect. The European (CEB-FIP 1993) and Japanese (JSCE 1986) Code Equations (Table 1) also incorporate the size effect in their shear strength expressions.

Keeping the above reasons and a large number of experimental results in view, the following expression is suggested to modify the proposed two-step procedure and simplified equations (Eq. 14) to account for the size effect.

$$\frac{(v_{cr})_{\text{WITH-SIZE-EFFECT}}}{(v_{cr})_{\text{WITHOUT-SIZE-EFFECT}}} = \left(\frac{12}{S}\right)^{(1/6)} \quad (21)$$

where S is the longitudinal web reinforcement parameter defined in Fig. 24. Note that S of Eq. 21 is identical to S_x of Eq. 20a used in MACI and general shear design method (Collins et al. 1996).

Combining Eq. 21 with Eq. 14, the proposed simplified equation for RC beams (without axial load) can be expressed as:

$$v_{cr} = 34 \rho^{1/3} \left(f'_c \frac{V_{cr} d}{M_u} \right)^{1/6} \left(\frac{12}{S} \right)^{(1/6)} \quad (22)$$

To test the accuracy of the proposed equation (Eq. 22) and to compare to other empirical expressions and MCFT, 94 test results from 7 investigations were considered. Table 7 gives the summary of their test programs, test results, and predictions by various methods. The shear strength at diagonal cracking is taken for comparison. In the cases where diagonal cracking strength is not specified for RC members without transverse reinforcement, the failure load is considered for comparison. The principal variable, the member depth, varies from 4.3 in. to 43.2 in. Other variables include concrete strength (ranging between 3200 and 14,330 psi), longitudinal reinforcement ratio (ranging

between 0.5% and 4.7%), and shear span-to-depth ratio (ranging between 2.9 and 8). Predictions by MACI and MCFT were compared by setting the maximum aggregate size equal to zero for concrete stronger than 6000 psi. Table 7 shows the comparison of test results with the proposed simplified equation (Eq. 14), the proposed simplified equation including size effect (Eq. 22), other empirical expressions, and MCFT. First-order statistics of the test/predicted ratio are summarized in Table 8. Figures 25 through 36 give the graphical comparison of results by proposed equations, MCFT and other empirical expressions.

Table 8 shows that the proposed simplified equation without size effect correction (i.e., Eq. 14), Zsutty's expression, ACI-Code expressions, and ASCE-ACI expression can be quite unconservative for large members. The predictions by Kim et. al. is very unconservative. It may be noted that the above five expressions do not take size effect into account. Okamura and Higai expression is unconservative irrespective of member size due mainly to an overestimate of the influence of a/d ratio in their equations. On the other hand, the proposed equation with size effect correction (Eq. 22), the JSCE, and CEB-FIP equations are in good agreement with the test results. Predictions by MCFT and MACI are generally more conservative, the latter being more scattered. Such scatter is expected since the MACI equation does not take the reinforcement ratio and critical shear span-to-depth ratio into account.

The proposed equation for size effects (Eq. 21) has two major differences with respect to MACI equation (Eq. 20). Figure 37 shows the variation of shear strength with beam size (containing different aggregate sizes) by both equations. Note that the proposed equation is independent of aggregate size and the value of maximum aggregate size is zero in MACI equation (Eq. 20a) for high-strength concrete. First, the reduction in shear strength in large size beams using the MACI equation is considerably higher (more being for small size aggregates) than that using Eq. 22 (Fig. 37). The MACI equation is mainly based on the test results by the authors themselves (Collins and Kuchma 1999) and observation of test results from Shioya et. al. (1989). Test results by Shioya et. al. on large size beams show a significant reduction in shear strength. However, note that these beams have a small reinforcement ratio equal to 0.4%. Analysis (Eq. 10) and test results (Table 4) show that the shear strength of beams with 0.4% reinforcement ratio is approximately 70% of that with 1% reinforcement ratio. Therefore, part of the shear strength reduction in tests by Shioya (1989) can be attributed to low reinforcement ratio. On the other hand, the test data by the authors of MACI include only a limited number of variables. Most data for simply supported beams have an a/d ratio of 3 and ρ of 1%. Therefore, the application of MACI Equation (Eq. 20) to all ranges of a/d ratio and reinforcement ratio may not be quite appropriate (Khuntia 2000). Test results by Kani (1967) show that the decrease in shear strength with beam size is not significant for shear span-to-depth ratio (a/d) more than 4 and is appreciable for a/d ratio less than or equal to 3 (Fig. 23).

As shown in Fig. 37, the reduction in shear strength for high strength RC beams is significantly low using MACI method compared to that by the proposed method (Eq. 21). The higher reduction by MACI is due to the assumption of maximum aggregate size as zero in Eq. 20a. However, it is believed that higher reduction in shear strength for high-

strength concrete is mainly due to reduction in effective shear depth c_1 , as explained under the section on influence of concrete strength.

The other major difference between Eq. 20 (MACI) and Eq. 21 (proposed) is the consideration of aggregate size a . As explained in the assumptions of this study, and corroborated by test results, the shear capacity of slender RC beams just prior to diagonal cracking (where size of aggregate and its frictional resistance have no role to play) is almost equal to that after formation of diagonal cracking. Therefore, the reduction in shear strength may not depend on aggregate size at all.

Using “S” instead of “ S_e ” in the proposed equation (Eq. 22) did not affect the accuracy of the prediction (Table 7). In general, consideration of aggregate size makes the calculation more complex.

In general, the comparison with test data (Table 4 and Table 7) shows that the error in disregarding size effect is negligible when effective member depth is less than 18 in. For large beams, the size effect can be neglected if the longitudinal reinforcements are distributed over the web region at a distance not more than 12 in. (Fig. 24).

Influence of Type of Loading

Two types of loading commonly encountered in practice are considered in this parametric study. They are: concentrated loading and uniformly distributed loading (Fig. 38). The major difference between the shear strength of a beam under these two types of loading is the location of critical section for diagonal cracking, which corresponds to the $M_u/(V_{cr}d)$ ratio. The case of simply supported beams (Fig. 38a and b) is considered first. The influence of other types of support conditions will be discussed later.

For simply supported beams, the critical section for point loading is closer to the location of maximum moment. The critical shear section can be taken approximately at a distance of d from the load point. This is because this section has the same shear force, and a higher bending moment than other sections in the shear span and, thus, develops longest flexural cracks and has the smallest effective shear depth c_1 (Fig. 38a). The critical shear span-to-depth ratio ($M_u/V_{cr}d$) for point loading can be expressed using Eq. 15. For a member with central point load, Eq. 15 is reduced to:

$$\frac{M_u}{V_{cr}d} = \frac{L}{2d} - 1 \quad (23)$$

However, the above situation is different in the case of uniform loading (Fig. 38b). Under uniform loading, although bending moment increases away from supports (thereby decreasing the magnitude of c_1 in Eq. 4), the corresponding shear force also decreases away from supports. For uniform loading, the critical shear span-to-depth ratio is:

$$\frac{M_u}{V_{cr}d} = \frac{x(L-x)}{d(L-2x)} \quad (24)$$

where x is the distance between the critical shear section and the support. Using Eq. 24 for different beam L/d ratios, $M_u/V_{cr}d$ can be calculated for varying x/d ratios and the corresponding shear strength can be computed using the proposed procedure (Eq. 4) for a given ρ and f'_c . Figure 39 shows the variation of shear strength for beams with different

L/d ratios. It may be noted that the shear force due to external loading V_u equals the shear capacity V_{cr} only at one location (i.e., at critical shear section). Also note that V_u is a linear relation of L/d with zero at mid-span, and V_{cr} is not linear with L/d (Fig. 39). The critical shear section location for the beam with a given L/d ratio can be found by drawing a tangent to the shear strength curve from a point where $x = L/2$ (i.e., the point where $V_u = 0$). Using this method and Fig. 39, the x/d ratio is found to vary between 0.8 to 2.0 depending upon L/d ratio, the ratio (x/d) being higher for higher L/d ratios. The analysis shows that the location of the critical shear section for a simply supported beam with uniform loading can be found using:

$$\frac{x}{d} = 0.14 \frac{L}{d} \geq 0.8 \leq 2.0 \quad (25)$$

Test results on beams under uniform loading (Krefeld and Thurston 1966) show a similar trend: the critical section moves away from the support with increasing L/d ratio. They suggested the variation of x/d from 0.8 to 2 depending on L/d ratio.

Using Eq. 25 in Eq. 24, the critical shear span-to-depth ratio ($M_u/V_{cr}d$) for simply supported beams under uniform loading can be expressed as:

$$\frac{M_u}{V_{cr}d} = \frac{L}{6d} \quad (26)$$

In general, for all practical slender beams failing in shear (L/d between 5 to 10) the x/d ratio varies from 0.80 to 1.40 per Eq. 25. Assumption of x/d = 1.5 is generally conservative for design purposes.

By combining Eq. 23 and Eq. 26 with Eq. 14 for a simply supported beam under uniform loading, it can be shown that:

$$\frac{(v_{cr})_{UNIFORM}}{(v_{cr})_{POINT}} = \left\{ \frac{3(L/d - 2)}{L/d} \right\}^{(1/6)} \quad (27)$$

The magnitude of Eq. 27 for different span-to-depth ratio (L/d) is graphically shown in Fig. 40. The increase in shear strength under uniform loading is 10 to 17% higher than under central point loading depending upon the L/d ratio (Fig. 40). The experimental study by Krefeld and Thurston (1966) confirms this observation. Using the available data at the time, Kani (1966) pointed out that it is slightly conservative if the design requirements for beams under point loadings are extended to beams under uniformly distributed loads.

Test data reported by Krefeld and Thurston (1966), consisting of 28 data points, were used to compare the proposed simplified Eq. 14 (with $M_u/V_{cr}d$ from Eq. 26) with other empirical equations of Table 1 and MCFT. Table 9 gives the details of the experimental program. The shear strength at diagonal cracking is taken for comparison. The variables include longitudinal reinforcement ratio (ranging between 1.3% and 4.3%), and span-to-depth ratio (ranging between 4.7 and 12.2). Note that the critical shear section in the above comparison is taken at 0.14L from supports. The effect of considering critical section at d from support ($x = d$) is explained later.

Table 10 gives the summary of test/predicted ratios by various models. It shows that the predictions by proposed simplified equation (Eq. 14) with appropriate $M_u/V_{cr}d$ (Eq. 26) are in very good agreement with the experimental results. The predictions by Zsutty and Okamura are also good. However, it may be noted that the equations by Zsutty and Okamura give unconservative results for beams under point loading (Table 5). The predictions by CEB-FIP, JSCE are also quite reasonable. The predictions by ACI-Detailed equation are slightly unconservative for many test cases. The predictions by MCFT, ACI-Simplified and ASCE-ACI are more scattered, although on the conservative side. Figures 41 through 49 show the comparison of test results to various models.

Table 11 shows similar comparison among various methods with the assumption that critical shear section is at a distance of d ($x = d$) from the supports, as generally used in design. It shows that the predictions by all methods, in general, are more scattered than those assuming x of $0.14L$. More over, if the ultimate shear strength is taken for comparison, all the methods give overly conservative results. Note that unlike the present method which gives a correction for ultimate shear strength for beams under uniform loading (explained later), no other method or MCFT distinguish between the cracking and ultimate shear strength.

Relation between ultimate (V_{ult}) and cracking (V_{cr}) shear strength also depends on the type of beam loading. Test data for 21 beams under point loading (Mattock 1969) are shown in Table 6. The ratio of ultimate to cracking shear strength (V_{ult}/V_{cr}) has a mean of 1.05 and a standard deviation of 0.09, showing that for point loading the beams have little or no shear strength reserve after diagonal shear cracking. Similar trend has also been observed by Zsutty (1968, 1971). However, the loading condition is not similar for beams under uniform loading. The critical section for such beams is approximate distance d to $1.5d$ from supports compared to a distance d from load point under point loading. Unlike point loading case where the portion between the support and critical shear section is free from external loading, that portion is subjected to applied loads in case of uniform loading. In other words, in uniformly loaded beams, arching action occurs in the region between the critical section and the support. It substantially increases the ultimate shear strength of the beam. Experimental results by Krefeld and Thurston (1966) support this observation. The comparison between the ultimate and cracking shear strengths for the test data are plotted in Fig. 50. Also plotted is the proposed lower bound equation:

$$1 \leq \left(\frac{V_{ult}}{V_{cr}} \right) = 2.5 - \frac{L}{8d} \leq 2.0 \quad (28)$$

As can be seen from Fig. 50, the difference between the ultimate shear strength and diagonal cracking shear strength can be as high as 50% for uniformly loaded beams. Based on the above discussion, the proposed procedure and simplified equation can be used directly to estimate the ultimate shear strength of RC members without stirrups in case of point loading, but must be corrected using Eq. 28 in case of uniform loading. Combining Eq. 28 with Eq. 14, the expression for ultimate shear strength for RC beams under uniform loading can be expressed as (neglecting size effect):

$$v_{cr} = 34 \rho^{1/3} \left(f_c' \frac{V_{cr}d}{M_u} \right)^{1/6} \left(1 \leq 2.5 - \frac{L}{8d} \leq 2 \right) \quad (29)$$

If size correction is needed, Eq. 29 can be combined with Eq. 21 in a similar way. Table 11 shows a comparison of ultimate shear strength between the test results and the predictions by proposed simplified equation (Eq. 29), MCFT and other empirical expressions (Table 1). It shows grossly conservative predictions by all other models except the proposed simplified equation (Eq. 29).

Influence of Support Conditions

The influence of support conditions on the shear strength of RC beams without stirrups is expressed through the effect of support conditions on the magnitude of bending moment and shear force at the critical section.

Four common cases are considered to examine the influence of support conditions. They are: (1) simply supported beam with central point loading (2) fixed beam with central point loading; (3) simply supported beam with uniform loading; and (4) fixed beam with uniform loading (Fig. 38). The bending moment and shear force diagrams for each case are also shown.

For beams with point loading, the critical shear section is at a distance d from the load point for both pinned and fixed supports. Although the magnitude of shear force is the same in both cases, bending moment at the critical section for the beam with fixed supports (Fig. 38c) is substantially smaller than the moment for the beam with pinned supports (Fig. 38a). Thus, the flexural crack is shorter (making the effective shear depth c_1 larger) for the fixed support case, thereby yielding higher shear strength compared to the simply supported case. Simple static analysis yields Eq. 15 for critical shear span-to-depth ratio ($M_u/V_{cr}d$) for point loading with simple supports considered as default in the proposed procedure. For a fixed beam with central point loading:

$$\frac{M_u}{V_{cr}d} = \frac{a}{2d} - 1 \quad (30)$$

Thus, the ratio of shear strength for fixed and simple supported beams under center-point loading (using Eqs. 15 and 30 with Eq. 14) is:

$$\frac{(v_{cr})_{FIXED}}{(v_{cr})_{SIMPLE SUPPORT}} = \left\{ \frac{(a/d - 1)}{(a/2d - 1)} \right\}^{1/6} \quad (31)$$

Equation 31 is plotted in Fig. 51. It shows that the shear strength computed assuming simple support condition is always conservative for point loading, more so for beams with smaller L/d ratios.

However, the situation is different for beams with uniform loading. For fixed-end beams under uniform loading (Fig. 38d), the critical shear section can be taken at a distance $0.8d$ or simply d from the support as both shear force and bending moments are highest at that location. Static analysis shows that for uniform loaded beam with fixed supports the critical shear span-to-depth ratio is:

$$\frac{M_u}{V_{cr}d} = \frac{\frac{1}{6}(L/d)^2 - (L/d) + 1}{(L/d) - 2} \quad (32)$$

As explained earlier (Eq. 26), the $M_u/V_{cr}d$ for simply supported beam under uniform loading is $L/6d$ (critical section being 0.8 to $2d$ from support). Although the magnitude of shear force at the critical section is similar for both fixed and simply supported beams, bending moment at the critical section for the beam with fixed supports can be larger or smaller than the moment for the beam with simple supports depending on the span-to-depth (L/d) ratio. Mathematically, the ratio of shear strengths of fixed and simple supported beam with uniform loading is:

$$\frac{(v_{cr})_{FIXED}}{(v_{cr})_{SIMPLESUPPORT}} = \left\{ \frac{(L/d - 2)(L/6d)}{\left(\frac{1}{6}[L/d]^2 - L/d + 1 \right)} \right\}^{1/6} \quad (33)$$

Equation 33 is plotted in Fig. 52. It shows that the shear strength computed assuming simple support condition is always conservative for uniform loading, more so for beams with smaller L/d ratios. It is interesting to note that the cracking shear strength under uniform loading may be 5 to 10% smaller for fixed-end beams where L/d ratio more than 11 if the critical shear section is assumed at a distance of d from support (Fig. 52). Similar increase in shear strength may be obtained using MCFT or ACI-Detailed Equation. However, no empirical expressions (Table 1) specifically consider the influence of support conditions on shear strength. Thus, no comparison can be made. In general, it may be appropriate to use Eq. 31 for point loading and Eq. 33 for uniform loading for beams with L/d ratio of less than 8, if more accuracy in determining shear strength is desired.

CONCLUSIONS

Based on a parametric study and comparisons to numerous experimental results, different code provisions, empirical expressions, and Modified Compression Field Theory the following conclusions can be drawn about the proposed shear strength evaluation procedure and a simplified equation derived from it:

1. The approach can be applied to members with any shear span-to-depth ratio, reinforcement ratio, concrete strength, presence of axial compression/tension, member size, loading type and support conditions.
2. The shear strength of RC members without transverse reinforcement can be conveniently predicted using the proposed simplified procedure (Eq. 4) based on the basic principles of mechanics.
3. A simplified expression (Eq. 14) is suggested for design purposes. It is virtually as accurate as the proposed procedure considering the data set used for comparison.
4. The influence of longitudinal reinforcement is more significant than those of concrete strength and span-to-depth ratio.
5. Corrections for size effects are not needed if longitudinal reinforcements are distributed over the entire web region when member depth exceeds 18 in.

6. Correction for uniform loading should be used if more accuracy is desired. In general, the proposed method is conservative for beams with uniform loading. In addition, the ultimate shear strength compared to diagonal cracking strength is significantly higher, especially for short spans.
7. Correction for support conditions is generally not needed for design purposes as any support type other than simple supports yields conservative results.
8. Corrections for axial tension or compression can be properly accounted for using the proposed procedure, if more accuracy is desired. ACI Code equation, in its present form, is generally conservative.
9. The present ACI Code Equation for evaluating the shear strength of RC members needs to be modified to include the effect of concrete strength, critical shear span-to-depth ratio, tensile reinforcement ratio, and size effect in an appropriate manner, as suggested in this report.

APPENDIX I. NOTATION

a	=	shear span, ft (also aggregate size, in.)
a/d	=	shear span-to-depth ratio
A_s	=	area of main reinforcement, sq. in.
A_g	=	gross section, sq. in.
A_{sw}	=	area of longitudinal web reinforcement in each layer, sq. in.
b_w	=	width of beam, in.
c	=	depth of neutral axis, in.
c_1	=	effective shear depth, in.
c_2	=	uncracked depth on tension side, in.
C_c	=	compressive force due to concrete, kips
d	=	effective depth, in.
d_v	=	effective shear depth in MCFT, in.
E_c	=	modulus of elasticity of concrete, psi
E_s	=	modulus of elasticity of steel, psi
f_c	=	compressive strength in concrete corresponding to a strain of ϵ_c , psi
f_c'	=	compressive strength of concrete, psi
f_{cr}	=	split cylinder tensile strength of concrete, psi
f_s	=	tensile stress in main reinforcing steel, psi
f_t	=	tensile strength of concrete, psi
f_y	=	yield strength of steel, ksi
h	=	total depth of beam, in.
k	=	shear strength factor
l_d	=	development length of rebar, in.
L	=	span length, ft
L/d	=	span-to-depth ratio
M, M_x	=	bending moment, kip-in.
M_u	=	ultimate bending moment, kip-in.
$M_u/V_{cr}d$	=	critical shear span-to-depth ratio, both M_u and V_{cr} at critical section
P, P_x	=	axial load, kips
P_u	=	ultimate axial load, kips
Q, N, Z	=	nondimensional factors, used in Eq. 8a
S	=	longitudinal web reinforcement parameter, in.
S_e	=	crack spacing parameter (used in MCFT), in.
S_x	=	crack spacing, in.
T_c	=	tensile force due to concrete, kips
T_s	=	tensile force due to main steel, kips
v_{cr}, v_c	=	shear stress at diagonal cracking, psi
V, V_x	=	shear force, kips
V_{cr}	=	shear strength at diagonal cracking, kips
V_u	=	ultimate shear force, kips
V_{ult}	=	ultimate shear strength, kips
w_u	=	factored gravity (dead and live) load, klf
x	=	distance of critical shear section from support under uniform loading, ft
α	=	exponent to compressive strength of concrete

β	=	tensile stress factor, used in MCFT
ϵ_c	=	compressive strain in concrete, in/in
ϵ_{cr}	=	cracking strain in concrete, in/in
ϵ_o	=	compressive strain in concrete at peak stress, in/in
ϵ_s	=	longitudinal strain in tensile steel, in./in.
ϵ_s	=	longitudinal strain in tensile steel (used in MCFT), in./in.
ρ	=	longitudinal reinforcement ratio, in decimals
σ_1, σ_2	=	principal stresses, psi
τ	=	shear stress in effective shear depth, psi
τ_{max}	=	maximum shear stress in effective shear depth, psi
θ	=	angle of inclination of compressive stress in cracked concrete (in MCFT)

APPENDIX II. REFERENCES

- Adebar, P., and Collins, M. (1996). "Shear strength of members without transverse reinforcement." *Canadian J. Civ. Eng.*, 23, pp. 30-41.
- Ahmad, S.H., Khaloo, A.R., and Proveda, A. (1986). "Shear Capacity of Reinforced High-Strength Concrete Beams." *ACI Journal*, V. 83(2), pp. 297-305.
- ACI Committee 318. (1999). "Building Code Requirements for Structural Concrete (ACI 318-99) and Commentary (ACI 318R-99)." ACI, Farmington Hills, 391 pp.
- ACI Manual of Concrete Practice (2001). "State of Art Report on High-Strength Concrete." Reported by ACI Committee 363, ACI, Farmington Hills, MI.
- ASCE-ACI Committee 426. (1973). "The shear strength of RC members." *J. of Str. Dvn., ASCE*, V. 99(6), pp. 1091-1187. – *Referred in ASCE-ACI Committee 445 (1998)*.
- ASCE-ACI Committee 445 on Shear and Torsion. (1998). "Recent Approaches to Shear Design of Structural Concrete." *J. of Str. Engrg., ASCE*, V. 124(12), pp. 1375-1417.
- Bhide, S.B. and Collins, M.P. (1989). "Influence of Axial Tension on the Shear Capacity of Reinforced Concrete Members." *Structural Journal, ACI*, V. 86(5), pp. 570-581.
- Bresler, B. and Scordelis, A.C. (1963). "Shear Strength of Reinforced Concrete Beams." *ACI Journal*, V. 60(4), pp.51-73.
- Cassio, R.D.D., and Siess, C.P. (1960). "Behavior and Strength in Shear of Beams and Frames without Web Reinforcement." *ACI*, 1960-Feb., pp. 695-735.
- CEB -FIP Model Code Final Draft (1993). Bulletin d'Information No. 203-205. – *Referred in "Size effect in RC members subjected to shear loading" by McCabe and Niwa (1994). Also referred in the paper by Kim and Park (1994)*.
- Collins, M.P. (1998). "Procedure for Calculating the Shear Response of RC Elements: A Discussion." An opinion paper, *J. of Str. Engrg., ASCE*, V. 124(12), pp. 1485-1488.
- Collins, M.P., Mitchell, D., Adebar, P., and Vecchio, F.J. (1996). "A General Shear Design Method." *Structural Journal, ACI*, V. 93(1), pp. 36-45.
- Collins, M.P., and Kuchma, D. (1999). "How Safe are Our Large Lightly Reinforced Slabs and Footings ?" *ACI Journal*, V. 96(4), pp.482-490.
- Elzanaty, A.H., Nilson, A.H., and Slate, F.O. (1986). "Shear Capacity of Reinforced Concrete Beams using High-Strength Concrete." *ACI Journal*, V. 83(2), pp.290-296.
- Gupta, P. R., and Collins, M. P. (2001). "Evaluation of Shear Design Procedures for RC Members under Axial Compression." *ACI Journal*, V. 98(4), pp.537-547.
- Halladin, M.J., Hong, S.T., and Mattock, A.H. (1971). "Stirrup Effectiveness in RC Beams with Axial Force." *J. of Str. Dvn., ASCE*, V. 97(ST9), pp. 2277-2297.
- Johnson, M.K., and Ramirez, J.A. (1989). "Minimum Shear Reinforcement in Beams with Higher Strength Concrete." *Structural Journal, ACI*, V. 86(4), pp.376-382.
- JSCE (1986) Standard Specification for Design and Construction of Concrete Structures, Part 1 (Design), 1st Edition. - *Referred in "Size effect in RC members subjected to shear loading" by McCabe and Niwa (1994)*.
- Kani, G.N.J. (1966). "Basic Facts Concerning Shear Failure." *ACI J.*, V, 63, June, pp. 675-690.
- Kani, G.N.J. (1967). "How Safe are our Large Concrete Beams ?." *ACI Journal*, V, 64(3), March, pp. 128-141.
- Kim, D., Kim, W., and White, R.N. (1999). "Arch Action in RC Beams – A Rational Prediction of Shear Strength." *ACI Journal*, V. 96(4), pp.586-593.

- Kim, J.K., and Park Y.D. (1994). "Shear Strength of Reinforced High Strength Concrete Beams without Web Reinforcement." *Magazine of Concrete Research*, 46 (166), pp.7-16.
- Khuntia, M. (2000). Discussion on the paper "How Safe are our Large, Lightly RC Beams, Slabs and Footing?" by Collins and Kuchma (June 1999 ACI Str. J.), *ACI Str. J.*, May-June.
- Khuntia, M., and Goel, S. C. (1999). "Analytical Study of FRC-Encased Steel Joist Composite Beams." *J. of Str. Engrg., ASCE*, V. 125(5), pp. 503-509.
- Krefeld, J.K., and Thurston, C.W. (1966). "Studies of the Shear and Diagonal Tension Strength of Simply Supported Reinforced Concrete Beams." *ACI Journal*, V. 63(4), pp.450-475.
- Mathey, R.G., and Watstein (1963). "Shear Strength of Beams without Web Reinforcement containing Deformed bars of Different Yield Strengths." *ACI Journal*, 1963-Feb., pp. 183-206.
- Mattock, A. H. (1969). "Diagonal Tension Cracking in Concrete Beams with Axial Forces." *Journal of Str. Dvn.*, V. 95, ST9, September, pp. 1887-1899.
- McCabe, S.L., and Niwa, J. (1994). "Size Effect in RC Members subjected to Shear Loading." *Size Effect in Concrete Structures*, Edited by Mihashi, Okamura and Bazant.
- Moody, K.G., Viest, M., Elstner, R.C., and Hognestad, E. (1954). "Shear Strength of RC Beams: Part 1 – Tests of Simple Beams." *ACI Journal*, V. 26, No. 4, December, pp. 317-332.
- Mphonde, A.G., and Frantz, G.C. (1984). "Shear Tests of High and Low-Strength concrete Beams without Stirrups." *ACI Journal*, V. 81(4), pp. 350-357.
- Okamura, H. and Higai, T. (1980). "Proposed Design Equation for Shear Strength of RC Beams without Web Reinforcement." *Proceedings, Japanese Soc. of Civil Engrg.*, 300, 131-141 - referred in *ASCE-ACI Committee 445 on Shear and Torsion. (1998)*.
- Rajagopalan, K.S., and Ferguson, P.M. (1968). "Exploratory Shear Tests Emphasizing Percentage of Longitudinal Steel." *ACI Journal*, Aug., pp. 634-638.
- Reineck, K.H. (1991). "Ultimate Shear Force of Structural Concrete Members without Transverse Reinforcement derived from a Mechanical Model." *Structural Journal, ACI*, V. 88(5), pp. 562-602.
- Shioya, T., Iguro, M., Akiyama, H., and Okada, T. (1989). "Shear Strength of Large Reinforced Concrete Beams." *Fracture Mechanics: Application to Concrete*, SP-118, V.C. Li and Z.P. Bazant, eds. ACI, Detroit, pp. 259-279.
- Taylor, H.P.J. (1972). "Shear strength of large beams." *Journal of Str. Dvn.*, ASCE, V. 98, ST 11, pp. 2473-2490.
- Vecchio, F.J. and Collins, M.P. (1986). "The Modified Compression Field Theory for RC Elements Subjected to Shear." *ACI Journal*, V. 83(4), pp. 219-231.
- Vecchio, F.J. and Collins, M.P. (1988). "Predicting the Response of RC Beams Subjected to Shear using Modified Compression Field Theory." *Str. Journal, ACI*, V. 85(3), pp. 258-268.
- Yoon, Y.S., Cook, W.D., and Mitchell, D. (1996). "Minimum Shear Reinforcement in Normal, and High-strength Concrete Beams." *Structural Journal, ACI*, V. 93(5), pp. 576-584.
- Zsutty, T. (1968). "Beam Shear Strength Prediction by Analysis of Existing Data." *ACI Journal*, V. 65(11), pp. 943-951.
- Zsutty, T. (1971). "Shear Strength Prediction for Separate Categories of Simple Beam Tests." *ACI Journal*, V. 68(2), pp. 138-143.

APPENDIX III. SHEAR STRENGTH COMPUTED BY THE GENERAL SHEAR DESIGN METHOD BASED ON MODIFIED COMPRESSION FIELD THEORY (MCFT)

The general shear design method (Collins et al. 1996) is based on MCFT (Vecchio and Collins 1986). It is a rational approach to shear design of RC members. In this context, it is appropriate to compare the results from the proposed shear strength prediction procedure to those predicted by MCFT. The shear strength of concrete without stirrups is computed as:

$$V_c = \beta \sqrt{f'_c} b_w d_v \quad (\text{III-1})$$

where: β is the tensile stress factor; d_v is the effective shear depth which can be taken as $0.9d$; b_w is the effective web width. For design purposes, Collins et al. (1996) and Collins-Kuchma (1999) suggested to use a simplified table or graph for β (Fig. III-1). In these design aids, β is a function of two variables: (1) S_e , the crack spacing parameter (which is a function of crack spacing S_x and maximum aggregate size "a") as defined in the report, and (2) ϵ_x , the longitudinal strain at the level of main flexural reinforcements. The strain ϵ_x can be obtained using the following expression for non-prestressed members in absence of any other axial load:

$$\epsilon_x = \frac{\left(\frac{M_u}{d_v} \right) + 0.5V_u \cot\theta}{E_s A_s} \quad (\text{III-2})$$

where: M_u , and V_u are the factored moment and shear force; and θ is the angle of inclination of compressive stress in cracked concrete. Rearranging the terms with $d_v = 0.9d$, noting that at failure $V_u = V_c$, Eq. III-2 can be reduced to:

$$\epsilon_x = \frac{0.9 \times \beta \sqrt{f'_c} \times \left(1.11 \frac{M_u}{V_u d} + 0.5 \cot\theta \right)}{\rho E_s} \quad (\text{III-3})$$

The influence of different parameters on concrete shear strength v_c can be reasonably predicted by using Eqs. III-1 and III-3 and the table/graph (Fig. III-1) for β suggested by Collins et al. (1996) and Collins and Kuchma (1999). It should be noted that the MCFT method involves trial and error procedure and is considerably more complex than the traditional ACI Equation.

APPENDIX IV. EVALUATION OF THE PROPOSED ACI COMMITTEE EQUATION TO INCLUDE SIZE EFFECT AND REINFORCEMENT RATIO

Recently, there is a discussion within ACI Committee 445 on proposal to include the size effect and reinforcement ratio in the following manner:

$$V_c = \alpha \sqrt{f_c'} b_w d_v \quad (\text{IV-1})$$

$$\text{For members with } \rho \geq 1.5\%, \alpha = 2.0 \quad (\text{IV-2})$$

$$\text{For members with } \rho < 1.5\%, 1.0 \leq \alpha = (1.1 + \rho) \left\{ \frac{46}{40 + \frac{d}{a + 0.6}} \right\} \leq 2.0 \quad (\text{IV-3})$$

The above proposal is mainly based on the test results by Kani (1967), Taylor (1972), Shioya (1989), Collins and Kuchma (1999), and Krefeld and Thurston (1966). The results from above Eq. IV-2 and Eq. IV-3 were compared with the test results reported in Table 4. These 127 data set includes maximum aggregate size of 0.5 to 1.0 in., when reported in the investigation. When the test data do not report the aggregate size, the default value is taken to be 0.75 in. In addition, the maximum beam depth in Table 4 was not more than 16 in. The mean and standard deviation of test/predicted ratio using Eqs. IV-2 and -3 are found to be 1.32 and 0.28, respectively (Fig. IV-1). It is interesting to note that the mean and standard deviation of test/predicted ratio using ACI-Simplified equation for the same data set are found to be 1.30 and 0.30, respectively. The proposed ACI-Committee equation was also used to compare with the test results of Table 7 (i.e., influence of size effect). These 94 data set include aggregate size from 0.1 to 1.5 in., most data with 0.39 to 1.00 in. The mean and standard deviation of test/predicted ratio using ACI-Committee 445 equation are found to be 1.19 and 0.25, respectively (Fig. IV-2). For the same data set, ACI-Simplified equation gives mean and standard deviation of test/predicted ratio as 1.13 and 0.28, respectively. Therefore, the proposed equation by ACI committee 445 does not give any appreciable accurate results than the current ACI-Simplified expression, whereas it is more complex than the latter.

Figure IV-3 shows the influence of member depth and aggregate size by ACI-Committee proposal. It is compared with the proposed equation (Eq. 21) on size effect. The proposed Committee equation gives similar drastic reduction in shear strength with member size, more so with small size aggregate. The variation is similar to that suggested by MACI method of Collins and Kuchma (1999). See Fig. 37 for details. As explained earlier, the drastic reduction of shear strength with beam size is too conservative. The other shortcoming of the proposed ACI is the upper limit of k-factor being 2.0. However, as numerous test results pointed out (Table 4 and Table 7), the upper limit of k can go up to 3.0 in many practical cases. Therefore, the proposed Committee expression is, in general, is very conservative. Note that the equation proposed in this report is more rational and accurate than the one proposed by the ACI Committee.

APPENDIX V. EXAMPLES USING THE PROPOSED TWO-STEP PROCEDURE AND SIMPLIFIED EQUATIONS

The following examples are provided to show the application of proposed two-step procedure and simplified equations to shear design of RC members without stirrups. For comparison purposes, corresponding design by ACI Code method is also illustrated.

Example 1.

Calculate the design shear strength of a RC beam shown in Fig. V-1. The beam is simply supported and uniformly loaded with a factored dead and live load of 4.5 klf. Assume $f_c' = 4000$ psi and $f_y = 60$ ksi.

Solution:

$$\begin{aligned} \text{Area of reinforcement } A_s &= 3 \times 0.6 = 1.8 \text{ sq. in.} \\ \text{Reinforcement ratio } \rho &= A_s/b_w d = 1.8/(10 \times 12) = 1.5\% \\ \text{Span-to-depth ratio } L/d &= 12 \times 12/12 = 12 \end{aligned}$$

1. Check for Flexure:

$$\text{Factored maximum bending moment } M_u = w_u L^2/8 = 4.5 \times 12^2 \times 12/8 = 972 \text{ k-in.}$$

Design moment capacity was found to be 1012 k-in. > 972 k-in. (O.K.)

Therefore, no flexural failure of the beam will occur.

2. Check for shear by proposed method:

The critical shear section per the proposed model (Eq. 25) is at 0.14L from support (Fig. V-2).

$$\text{At the critical location, applied shear force } V_u = 4.5 \times 12(1/2 - 0.14) = 19.44 \text{ kips}$$

Nominal cracking shear stress by proposed simplified equation is given by Eq. 14 as shown below:

$$v_{cr} = 34 \sqrt[3]{\rho \left(f_c' \frac{V_{cr} d}{M_u} \right)^{0.5}}$$

Size effect can be neglected as beam is not large (effective depth is less than 18 in.).

$$M_u/V_{cr}d \text{ for the example beam (under uniform loading)} = L/6d = 2 \text{ (Eq. 26).}$$

$$\text{Cracking shear resistance } V_{cr} = 34 \times (1.5)^{1/3} (4000/2)^{1/6} \times 10 \times 12 = 16.58 \text{ kips}$$

The ultimate shear strength may be higher than cracking strength for beams under uniform loading as given in Eq. 24. Note that for beams under point loading there is negligible difference between ultimate and cracking shear strength.

$$\text{Magnification factor} = 2.5 - L/8d = 1.0. \quad (\text{Eq. 28})$$

$$\text{Therefore, ultimate nominal shear strength of the beam} = 16.58 \times 1.0 = 16.58 \text{ kips.}$$

Note that the ultimate shear strength can be higher than cracking shear strength for beams under uniform loading with L/d ratio less than 12.

$$\text{Design shear strength } \phi V_{ult} = 0.85 \times 16.58 = 14.1 \text{ kips} < V_u (=19.44 \text{ kips})$$

Provide transverse reinforcement.

3. Check for shear by ACI -Simplified method:

The critical shear section per the ACI Code method is at d from support.

$$\text{At the critical location, applied shear force } V_u = 4.5 \times 12/2 - 4.5 \times 1 = 22.5 \text{ kips.}$$

ACI Code does not distinguish between cracking and ultimate shear strength irrespective of type of loading. Ultimate shear stress is given by:

$$v_{cr} = 2\sqrt{f_c'}$$

Therefore, ultimate nominal shear strength of the beam $V_{ult} = 2\sqrt{4000} \times 10 \times 12 = 15.2$ kips.

Design shear strength $\phi V_{ult} = 0.85 \times 15.2 = 12.9$ kips $< V_u (=22.5$ kips)

Provide transverse reinforcement.

4. Comments:

The design shear force by ACI Code method ($V_u=22.5$ kips) is about 16% higher than that by proposed method ($V_u=19.44$ kips). In addition, the design shear strength by ACI Code method ($\phi V_{ult}=12.9$ kips) is about 9% lower than that by proposed method ($\phi V_{ult}=14.1$ kips). Therefore, by using ACI Code method underestimates the shear design by about 25%.

Example 2.

Calculate the shear strength of the RC beam in Example 1 if the compressive strength of concrete is increased from 4000 to 10,000 psi.

Solution:

1. Using the proposed simplified equation, shear resistance

$V_{ult} = V_{cr} = 34 \times (1.5)^{1/3} (10000/2)^{1/6} \times 10 \times 12 = 19.3$ kips. This is 16% higher than that with 4000 psi concrete.

2. Using the ACI Code simplified equation, shear resistance

$V_{ult} = V_{cr} = 2(10000)^{1/2} \times 10 \times 12 = 24.0$ kips. This is 58% higher than that with 4000 psi concrete.

3. Comments:

ACI Code method overestimates the shear strength for beams with high-strength concrete. As many test results pointed out, the increase in shear strength is marginal with increase in concrete strength.

Example 3.

Calculate the shear strength of the RC beam in Example 1 if the effective depth is increased from 12 in. to 24 in. along with an increase in area of steel reinforcement from 3 to 6 #7 bars. The factored gravity load is increased from 4.5 to 6 klf. Assume shear failure will govern.

Solution:

Longitudinal reinforcement ratio ρ is same as in Example 1. However, the value of L/d decreased from 12 to $12/2 = 6$ in this example.

1. Using the proposed simplified equation

Applied shear force at critical location $V_u = 19.44 \times 6/4.5 = 25.92$ kips.

$M_u/V_{cr}d$ for the example beam $= L/6d = 1$ (Eq. 22).

Size effect needs to be considered as $d > 18$ in.

Web reinforcement parameter $S = 0.9 \times 24 = 21.6$ in.

$$V_{cr} = 34 \times (1.5)^{1/3} (4000/1)^{1/6} (12/21.6)^{1/6} \times 10 \times 24 = 33.74 \text{ kips. (Eq. 21)}$$

Without considering size effect the strength is 10% more.

$$V_{ult} = V_{cr} \times (1 \leq 2.5 - L/8d \leq 2.0) = 33.74 \times 1.75 = 59.0 \text{ kips}$$

Design shear strength $\phi V_{ult} = 0.85 \times 59.0 = 50.1$ kips $> V_u (= 25.92$ kips)

Transverse reinforcement is NOT needed anywhere along the beam.

2. Using the ACI Code simplified equation

Applied shear force at critical location $V_u = 22.5 \times 6/4.5 = 30.0$ kips.

$$V_{ult} = V_{cr} = 2(4000)^{1/2} \times 10 \times 24 = 30.4 \text{ kips.}$$

Note that ACI code does not consider size effect.

Design shear strength $\phi V_{ult} = 0.85 \times 30.4 = 25.84$ kips $< V_u (= 30.0$ kips)

Transverse reinforcement is needed.

3. Comments:

The ACI Code method does not consider the influence of critical shear span-to-depth ratio as well as the type of loading. Therefore, in spite of minor decrease in shear strength due to size effect, the computed shear strength by proposed simplified equation was found to be significantly higher than that by the ACI Code method.

Example 4.

Calculate the shear strength of the RC beam in Example 1 if the beam is subjected to an axial tension of (a) 14 kips (or 100 psi axial stress), (b) 28 kips (or 200 psi axial stress).

Solution:

When a RC member is subjected to axial load, it is recommended to use proposed two-step procedure, as no simplified equation can predict accurately the change in shear strength.

1. Using the proposed procedure (Eq. 4)

Using method of strain compatibility and equilibrium conditions, the effective shear depth c_1 was found to be 4.3 in. and 5.4 in. under axial tension of 28 and 14 kips, respectively. The corresponding cracking shear stress can be given as:

$$v_{cr} = \frac{2}{3} \frac{c_1}{d} f_t = \frac{2}{3} \times \frac{4.3}{12} \times 6.7 \sqrt{f_c'} = 1.6 \sqrt{f_c'} \text{ for beam under axial tension of 28 kips.}$$

Similarly, the cracking shear stress under axial tension of 14 kips was found to be $2.0 \sqrt{f_c'}$

Note that a value of critical shear span-to-depth ratio ($M_u/V_{cr}d$) of 2 (as calculated in Example 1) is used in the procedure. The magnitude of c_1 would change for different $M_u/V_{cr}d$ ratios.

2. Using the ACI Code procedure

Per ACI Code the shear strength under axial tension can be given as:

$$v_{cr} = 2.0\sqrt{f'_c} \left\{ 1 + \frac{N_u}{500A_g} \right\}$$

The above equation will give a value of $1.8\sqrt{f'_c}$ under axial tension of 14 kips and a value of $1.6\sqrt{f'_c}$ under an axial tension of 28 kips.

3. Comments:

As pointed out in the report, ACI Code method gives conservative result for RC members under low axial tension.

Example 5.

Calculate the shear strength of the RC beam located in a framed building shown in Fig. V-3 and Fig. V-4. The beam is uniformly loaded with a factored dead and live load of 4.5 klf. Assume $f'_c = 5000$ psi and $f_y = 60$ ksi. Assume no flexural failure.

Solution:

The important aspect of this type of practical frame is to locate the critical shear section. As can be seen from Fig. V-3, although maximum bending moment occurs at mid-span of beam, the applied shear force is quite small at nearby locations. The critical section will occur at a distance of d from the support.

1. Check for shear by proposed method:

The critical shear section per the proposed model is at d from support (Fig. V-3).

At the critical location, applied shear force $V_u = 4.5 \times (18/2 - 1.5) = 33.75$ kips.

Bending moment at that location was found to be 48.25 k-ft.

$M_u/V_{cr}d$ at critical shear location = $48.25 / (33.75 \times 1.8) = 0.95$ (Use 1.0)

Longitudinal reinforcement ratio = $1.8 / (16 \times 18) = 0.625\%$

Cracking shear resistance $V_{cr} = 34 \times (0.625)^{1/3} (5000/1)^{1/6} \times 16 \times 18 = 34.7$ kips (Eq. 14)

The ultimate shear strength may be higher than cracking strength for beams under uniform loading as given in Eq. 28.

Per Eq. 28, magnification factor = $2.5 - L/8d = 1.0$. Note that in absence of test data for fixed beams under uniform loading, Eq. 28 (which is derived for simple support) can be used.

Therefore, ultimate nominal shear strength of the beam $V_{ult} = 34.7 \times 1.0 = 34.7$ kips.

Considering size-effect, the ultimate nominal shear strength of the beam

$$= 34.7 \times (12 / (0.9 \times 18))^{1/6} = 33.0 \text{ kips}$$

Design shear strength $\phi V_{ult} = 0.85 \times 33.0 = 28.0$ kips $< V_u (=33.75$ kips)

Provide transverse reinforcement.

2. Check for shear by ACI Code-Simplified method:

The critical shear section per the ACI Code method is at d from support.

At the critical location, applied shear force $V_u = 33.75$ kips.

Therefore, ultimate nominal shear strength of the beam $V_{ult} = 2\sqrt{5000} \times 16 \times 18 = 40.7$ kips.

Design shear strength $\phi V_{ult} = 0.85 \times 40.7 = 34.6$ kips $> V_u (= 33.75$ kips)

Theoretically, transverse reinforcement need NOT be provided.

3. Comments:

The design shear force by ACI Code method is about 24% higher than that by proposed method. This is mainly due to the fact that the ACI Code does not take the effects of reinforcement ratio and size effect into account.

Table 1. Empirical equations and code provisions for shear strength of RC beams

<i>Investigator</i>	<i>Predictive Equation</i>
Zsutty (1968)	$v_{cr} = 59 \times (f_c' \times \rho \times d/a)^{1/3}$
Okamura and Higai (1980)	$v_c = 64 \times (f_c' \times \rho)^{1/3} \times d^{-1/4} \times (0.75 + 1.4 d/a)$
ACI-Code (1999) – Simplified	$v_c = 2\sqrt{f_c'} \leq 200\text{psi}$
ACI-Code (1999) – Detailed	$v_c = 1.9\sqrt{f_c'} + 2500\rho \frac{V_u d}{M_u} \leq 3.5\sqrt{f_c'}$
ASCE-ACI Committee 426 (1973)	$v_c = (0.8 + 100\rho) \times \sqrt{f_c'} \leq 2.3 \times \sqrt{f_c'}$
CEB-FIP Model Code (1993)	$v_c = 27.67 \times (f_c' \times \rho \times d/a)^{1/3} \times (1 + \sqrt{8/d})$
Japanese Code (JSCE, 1986)	$v_c = 61.13 \times (f_c' \times \rho)^{1/3} \times d^{-1/4}$
Kim, Kim and White (1999)	$v_u = 0.2(1 - \sqrt{\rho}) \times \left(\frac{d}{a}\right)^r (12\sqrt{f_c'} + 147900\rho^{0.9}) \times \left(\frac{d}{a}\right)^{0.6}$ $r = \left(\frac{d}{a}\right)^{0.6} \rho^{-0.1} \leq 1$
Modified ACI (MACI) – suggested by Collins and Kuchma (1999)	$v_c = \frac{57.5}{50 + S_e} \times 2\sqrt{f_c'}$
<p>Note: All the above expressions are in U.S. customary (psi) units; f_c' in psi; d in in.; ρ is tensile steel ratio. The magnitudes of v_c and v_u are considered to be equal to v_{cr} in calculating shear strength.</p>	

Table 2. Relationship between split cylinder tensile strength and compressive strength of concrete

Sl. No.	Investigator	f_c' (psi)	f_{cr} (psi)	$f_{cr}/(f_c')^{0.5}$	$f_{cr}/(f_c')^{0.67}$	Sl. No.	Investigator	f_c' (psi)	f_{cr} (psi)	$f_{cr}/(f_c')^{0.5}$	$f_{cr}/(f_c')^{0.67}$
[1]	[2]	[3]	[4]	[5]	[6]	[1]	[2]	[3]	[4]	[5]	[6]
1		3756	431	7.03	1.78	41	Haddadin,	3750	457	7.46	1.89
2		3365	425	7.33	1.89	42	Hong, and	4275	345	5.28	1.31
3		2379	278	5.71	1.56	43	Mattock (1971)	4045	450	7.08	1.77
4		2567	263	5.18	1.40	44		4235	376	5.78	1.43
5		2930	318	5.87	1.55	45		4115	429	6.69	1.67
6		2959	287	5.28	1.39	46		4145	427	6.63	1.65
7		3481	344	5.83	1.49	47		4285	396	6.05	1.50
8		3394	384	6.60	1.70	48		3925	422	6.74	1.69
9		2959	342	6.29	1.66	49		3815	376	6.09	1.54
10		5569	425	5.69	1.35	50		3995	482	7.63	1.91
11	Bhide and	6048	400	5.15	1.20	51		3720	382	6.26	1.59
12	Collins (1989)	5961	497	6.44	1.51	52		4020	427	6.73	1.68
13		6033	438	5.64	1.32	53		4015	427	6.74	1.69
14		5497	438	5.91	1.40	54		3485	409	6.93	1.77
15		3669	341	5.63	1.43	55		3985	360	5.70	1.43
16		2901	339	6.30	1.66	56		3760	399	6.51	1.65
17		3147	371	6.62	1.72	57		4225	441	6.78	1.68
18		3292	355	6.19	1.60	58		4050	373	5.86	1.46
19		3162	358	6.37	1.66	59		4030	411	6.47	1.62
20		2553	270	5.34	1.44	60		4385	439	6.63	1.63
21		2988	345	6.32	1.66	61		3870	387	6.22	1.57
22		6033	458	5.90	1.38	62		3960	390	6.20	1.55
23		5888	463	6.03	1.41	63		3500	381	6.44	1.65
24		6280	538	6.79	1.58	64		4250	403	6.18	1.53
25		7614	624	7.15	1.61	65		4010	410	6.47	1.62
26		7150	653	7.72	1.75	66		3815	409	6.62	1.67
27	Adebar and	6701	624	7.62	1.75	67		3730	457	7.48	1.89
28	Collins (1996)	7469	537	6.21	1.40	68		4040	381	5.99	1.50
29		7223	566	6.66	1.51	69		4415	400	6.02	1.48
30		8542	812	8.79	1.94	70		4335	422	6.41	1.58
31	Rajagopalan	3440	414	7.06	1.81	71		4245	400	6.14	1.52
32	and Ferguson	5300	455	6.25	1.49	72		3795	381	6.18	1.56
33	(1968)	4800	462	6.67	1.62	73	Yoon, Cook	5221	450	6.22	1.49
34		4200	413	6.37	1.58	74	and Mitchell	9717	667	6.77	1.46
35		4800	396	5.72	1.39	75	(1996)	12618	885	7.88	1.63
36		4050	382	6.00	1.50						
37		3640	369	6.12	1.56						
38		4500	414	6.17	1.51						
39		4150	446	6.92	1.72						
40		4300	418	6.37	1.58						
								Average:		6.41	1.58
								Std.Deviation:		0.66	0.15

Table 3. Comparison of proposed simplified equation with two-step procedure

$M_u/V_c d$	ρ (%)	f'_c (psi)	k-Eq.13	k-Eq.14	Ratio
[1]	[2]	[3]	[4]	[5]	[6]=[5]/[4]
1	1	4000	2.02	2.14	1.06
1	1	8000	1.62	1.70	1.05
1	1	12000	1.42	1.49	1.05
1	2	4000	2.61	2.70	1.03
1	2	8000	2.09	2.14	1.02
1	2	12000	1.84	1.87	1.02
1	3	4000	3.03	3.09	1.02
1	3	8000	2.43	2.45	1.01
1	3	12000	2.13	2.14	1.00
3	1	4000	1.75	1.78	1.02
3	1	8000	1.40	1.42	1.01
3	1	12000	1.23	1.24	1.00
3	2	4000	2.26	2.25	0.99
3	2	8000	1.81	1.78	0.98
3	2	12000	1.59	1.56	0.98
3	3	4000	2.63	2.57	0.98
3	3	8000	2.11	2.04	0.97
3	3	12000	1.85	1.78	0.96
5	1	4000	1.64	1.64	1.00
5	1	8000	1.31	1.30	0.99
5	1	12000	1.15	1.14	0.99
5	2	4000	2.12	2.06	0.97
5	2	8000	1.70	1.64	0.97
5	2	12000	1.49	1.43	0.96
5	3	4000	2.46	2.36	0.96
5	3	8000	1.97	1.87	0.95
5	3	12000	1.73	1.64	0.95
				Mean =	1.00
				Std.Dev. =	0.03

Table 4. Summary of experimental program, results, and predictions

Test No.	Investigator	b _w in.	d in.	E _c psi	ρ %	a/d	V _{cr} kips	V _{cr} /b _w d(f _c ') ^{0.5} k-test	Proposed Procedure (Equation 4)		Parametric Equation (Equation 13)	
									k	Ratio	k	Ratio
[1]	[2]	[3]	[4]	[5]	[6]	[7]	[8]	[9]	[10]	[11]	[12]	[13]
1	Cassio and	6.00	9.94	5320	3.36	3.02	14.35	3.30	2.88	1.14	2.63	1.25
2	Siess (1960)	6.00	9.94	4060	3.36	4.02	12	3.16	2.83	1.11	2.73	1.16
3		6.00	9.94	3740	3.36	5.03	11.5	3.15	2.79	1.13	2.70	1.17
4		6.00	9.94	4050	3.36	6.04	11.4	3.00	2.71	1.11	2.55	1.18
5		6.00	10	2820	1	4.00	7.7	2.42	2.08	1.16	1.96	1.23
6		6.00	10	3890	1	5.00	7.9	2.11	1.79	1.18	1.70	1.24
7		6.00	10	3870	3.33	3.00	13.25	3.55	3.08	1.15	2.91	1.22
8		6.00	10	3210	3.33	4.00	10.55	3.10	2.99	1.04	2.93	1.06
9		6.00	10	3990	3.33	5.00	12.3	3.25	2.74	1.18	2.63	1.23
10		6.00	10	3630	3.33	6.00	11.1	3.07	2.78	1.10	2.64	1.16
11	Mathey and	8.00	15.86	4240	2.54	3.78	17.5	2.12	2.60	0.81	2.45	0.86
12	Watstein (1963)	8.00	15.86	3650	2.54	3.78	16.5	2.15	2.70	0.80	2.57	0.84
13		8.00	15.86	3410	0.93	3.78	12	1.62	1.92	0.84	1.81	0.89
14		8.00	15.86	3710	0.93	3.78	12.5	1.62	1.87	0.87	1.76	0.92
15		8.00	15.86	3790	0.84	2.84	12.5	1.60	1.95	0.82	1.78	0.90
16		8.00	15.86	3740	0.84	2.84	12	1.55	1.94	0.80	1.79	0.87
17		8.00	15.86	4430	0.84	2.84	13.5	1.60	1.85	0.86	1.69	0.94
18		8.00	15.86	3820	0.47	3.78	10.5	1.34	1.40	0.95	1.36	0.99
19		8.00	15.86	3740	0.47	3.78	9	1.16	1.41	0.82	1.37	0.85
20	Moody, Viest,	7.00	10.3	4400	2.17	3.06	13	2.72	2.59	1.05	2.38	1.14
21	Elstner and	7.00	10.5	4500	2.15	3.00	15	3.04	2.57	1.18	2.36	1.29
22	Hognestad (1954)	7.00	10.55	4500	2.22	2.99	14	2.83	2.60	1.09	2.39	1.18
23		7.00	10.63	4570	2.37	2.96	15	2.98	2.67	1.12	2.44	1.22
24		7.00	10.5	3070	1.62	3.00	11.45	2.81	2.56	1.10	2.40	1.17
25		7.00	10.55	3130	1.63	2.99	13.5	3.27	2.56	1.27	2.39	1.36
26		7.00	10.63	2790	1.6	2.96	12	3.05	2.61	1.17	2.47	1.24
27		7.00	10.69	2430	1.66	2.95	11.9	3.23	2.74	1.18	2.62	1.23
28		6.00	10.56	5320	1.89	3.41	11.5	2.49	2.26	1.10	2.08	1.20
29		6.00	10.56	2420	1.89	3.41	7.5	2.41	2.76	0.87	2.68	0.90
30		6.00	10.56	3740	1.89	3.41	11.5	2.97	2.48	1.20	2.33	1.27
31		6.00	10.56	2230	1.89	3.41	8.5	2.84	2.82	1.01	2.75	1.03
32		6.00	10.56	4450	1.89	3.41	10.5	2.48	2.36	1.05	2.20	1.13
33		6.00	10.56	2290	1.89	3.41	7.5	2.47	2.81	0.88	2.73	0.91
34		6.00	10.56	4480	1.89	3.41	10	2.36	2.38	0.99	2.20	1.07
35		6.00	10.56	5970	1.89	3.41	11.5	2.35	2.18	1.08	2.01	1.17
36		6.00	10.56	3470	1.89	3.41	9.5	2.55	2.52	1.01	2.39	1.07
37		6.00	10.56	5530	1.89	3.41	11	2.33	2.24	1.04	2.06	1.14
38		6.00	10.56	2930	1.89	3.41	10.5	3.06	2.65	1.16	2.52	1.22
39		6.00	10.56	5480	1.89	3.41	10	2.13	2.24	0.95	2.06	1.03
40		6.00	10.56	3270	1.89	3.41	9.7	2.68	2.57	1.04	2.43	1.10
41		6.00	10.56	5420	1.89	3.41	11.5	2.47	2.24	1.10	2.07	1.19
42		6.00	10.56	2370	1.89	3.41	8	2.59	2.77	0.94	2.70	0.96
43	Ahmad,	5.00	8	8823	3.93	4	13.0	3.46	2.48	1.39	2.26	1.53
44	Khaloo and	5.00	8	8823	3.93	3	14.0	3.73	2.73	1.36	2.38	1.57
45	Proveda (1986)	5.00	8	8823	3.93	2.7	14.0	3.73	2.84	1.31	2.43	1.53
46		5.00	8.19	8823	1.77	4	8.5	2.21	1.82	1.21	1.68	1.32
47		5.00	8.19	8823	1.77	3	9.5	2.47	2.00	1.24	1.77	1.40
48		5.00	8.19	8823	1.77	2.7	11.0	2.86	2.11	1.36	1.81	1.58
49		5.00	7.94	9715	5.04	4	11.5	2.94	2.64	1.11	2.40	1.23
50		5.00	7.94	9715	5.04	3	12.8	3.26	2.90	1.13	2.53	1.29
51		5.00	7.94	9715	5.04	2.7	14.0	3.58	3.04	1.18	2.58	1.39
52		5.00	8.19	9715	2.25	4	10.0	2.48	1.95	1.27	1.78	1.39
53		5.00	8.19	9715	2.25	3	10.5	2.60	2.14	1.22	1.88	1.39
54		5.00	8.19	9715	2.25	2.7	10.5	2.60	2.26	1.15	1.92	1.36
55		5.00	7.25	9329	6.64	4	12.0	3.43	2.91	1.18	2.69	1.27
56		5.00	7.25	9329	6.64	3	11.0	3.14	3.21	0.98	2.84	1.11
57		5.00	7.25	9329	6.64	2.7	9.0	2.57	3.37	0.76	2.90	0.89
58		5.00	8.13	9329	3.26	4	8.0	2.04	2.28	0.89	2.07	0.99
59		5.00	8.13	9329	3.26	3	10.0	2.55	2.50	1.02	2.18	1.17
60		5.00	8.13	9329	3.26	2.7	10.0	2.55	2.62	0.97	2.23	1.14

Table 4. (contd.) Summary of experimental program, results, and predictions

61	Krefeld and	6.00	12.36	4380	3.41	2.92	15	3.06	3.06	1.00	2.84	1.08
62	Thurston (1966)	6.00	9.36	4360	4.5	3.85	12.5	3.37	3.08	1.09	2.99	1.13
63		6.00	12.44	2800	2.68	2.9	13	3.29	3.12	1.06	3.00	1.10
64		6.00	12.44	2880	2.68	2.9	13	3.25	3.11	1.04	2.97	1.09
65		6.00	12.44	3280	2.68	2.9	12	2.81	2.99	0.94	2.85	0.98
66		6.00	12.44	3200	2.68	2.9	12	2.84	3.03	0.94	2.87	0.99
67		6.00	12.56	2890	0.8	2.86	8.5	2.10	2.05	1.03	1.90	1.10
68		6.00	9.56	3000	1.05	3.77	6	1.91	2.08	0.92	1.97	0.97
69		6.00	12.44	2920	1.34	2.9	9	2.23	2.46	0.91	2.29	0.97
70		6.00	12.44	3000	1.34	2.9	11	2.69	2.44	1.10	2.27	1.19
71		6.00	9.44	3220	1.77	3.81	8.5	2.64	2.47	1.07	2.34	1.13
72		6.00	9.56	3190	2.09	3.77	9	2.78	2.63	1.06	2.50	1.11
73		6.00	12.44	2870	2.68	2.9	12	3.00	3.09	0.97	2.98	1.01
74		6.00	9.44	2980	3.53	3.81	9.5	3.07	3.12	0.99	3.09	0.99
75		6.00	9.36	3050	4.52	3.85	10	3.22	3.31	0.97	3.36	0.96
76		6.00	9.36	2890	5.01	3.85	14	4.64	3.46	1.34	3.55	1.31
77		6.00	10	3340	1.32	4.8	7	2.02	2.12	0.95	1.99	1.01
78		6.00	10.06	3020	1.99	4.77	9	2.71	2.51	1.08	2.40	1.13
79		6.00	10	2390	2.63	4.8	8.5	2.90	2.93	0.99	2.86	1.01
80		6.00	9.94	2660	3.35	4.84	8.5	2.76	3.07	0.90	3.02	0.91
81		6.00	9.86	3310	4.3	4.87	12	3.53	3.12	1.13	3.09	1.14
82		6.00	10.06	2970	1.99	5.96	8	2.43	2.51	0.97	2.33	1.05
83		6.00	10.06	5010	1.99	3.58	12	2.81	2.30	1.22	2.14	1.31
84		6.00	10	4235	2.63	3.6	12.5	3.20	2.65	1.21	2.50	1.28
85		6.00	9.94	4760	3.35	3.62	12	2.92	2.81	1.04	2.64	1.11
86		6.00	9.86	4990	4.3	3.65	13	3.11	2.98	1.04	2.84	1.09
87		6.00	10.06	4620	1.99	4.77	11	2.68	2.21	1.21	2.09	1.28
88		6.00	10	4420	2.63	4.8	11	2.76	2.49	1.11	2.35	1.17
89		6.00	9.94	4760	3.35	4.83	11	2.67	2.63	1.02	2.51	1.07
90		6.00	9.86	4950	4.3	4.87	12	2.88	2.83	1.02	2.71	1.06
91		6.00	10	5570	2.63	6	11	2.46	2.26	1.09	2.11	1.17
92		6.00	9.94	5430	3.35	6.04	12	2.73	2.48	1.10	2.32	1.18
93		6.00	9.86	5570	4.3	6.09	11.5	2.60	2.66	0.98	2.52	1.03
94		6.00	9.94	5430	3.35	7.24	9	2.05	2.44	0.84	2.26	0.91
95		6.00	9.86	4990	4.3	7.3	9	2.15	2.72	0.79	2.54	0.85
96	Elzanaty,	7.00	10.5	3000	0.6	4	7.4	1.85	1.65	1.12	1.59	1.16
97	Nilson and	7.00	10.5	3000	1.2	4	9.8	2.44	2.17	1.13	2.05	1.19
98	Slate (1986)	7.00	10.5	3000	2.5	4	12.0	2.97	2.78	1.07	2.69	1.10
99		7.00	10.5	5800	1	4	10.1	1.80	1.64	1.10	1.55	1.16
100		7.00	10.5	5800	1.2	4	10.2	1.82	1.76	1.03	1.66	1.09
101		7.00	10.5	5800	2.5	4	14.3	2.55	2.34	1.09	2.18	1.17
102		7.00	10.5	9500	1.2	4	12.9	1.80	1.52	1.19	1.42	1.27
103		7.00	10.5	9500	2.5	4	14.8	2.06	2.03	1.01	1.86	1.11
104		7.00	10.5	9500	3.3	4	17.2	2.41	2.26	1.06	2.06	1.17
105		7.00	10.5	11500	1.2	4	13.8	1.75	1.42	1.23	1.34	1.31
106		7.00	10.5	11500	2.5	4	15.0	1.90	1.93	0.98	1.75	1.09
107		7.00	10.5	9200	1.2	6	9.6	1.37	1.38	0.99	1.34	1.02
108		7.00	10.5	9200	2.5	6	13.6	1.93	1.88	1.02	1.76	1.09
109	Mphonde and	6.00	11.75	3011	3.36	3.6	12.8	3.30	3.11	1.06	3.06	1.08
110	Frantz (1984)	6.00	11.75	5463	3.36	3.6	15.0	2.88	2.71	1.06	2.53	1.14
111		6.00	11.75	6037	3.36	3.6	14.0	2.56	2.64	0.97	2.45	1.05
112		6.00	11.75	10867	3.36	3.6	15.0	2.04	2.28	0.90	2.03	1.01
113		6.00	11.75	10825	3.36	3.6	15.0	2.05	2.28	0.90	2.03	1.01
114		6.00	11.75	11797	3.36	3.6	19.0	2.49	2.23	1.11	1.98	1.26
115		6.00	11.75	13319	3.36	3.6	21.5	2.64	2.17	1.22	1.90	1.39
116		6.00	11.75	2986	3.36	2.5	14.0	3.63	3.47	1.05	3.29	1.10
117		6.00	11.75	6549	3.36	2.5	18.0	3.15	2.98	1.06	2.56	1.23
118		6.00	11.75	11498	3.36	2.5	20.0	2.65	2.64	1.00	2.14	1.24
119		6.00	11.75	12148	3.36	2.5	24.0	3.08	2.60	1.19	2.10	1.47
120		6.00	11.75	10065	3.36	2.5	18.0	2.54	2.73	0.93	2.23	1.14
121	Rajagopalan and	5.99	10.43	3440	1.73	4.21	9	2.46	2.36	1.04	2.23	1.10
122	Fergusson (1968)	6.06	10.18	5300	1.42	3.92	8	1.78	1.96	0.91	1.83	0.97
123		6.06	10.44	4800	0.98	3.86	8.4	1.92	1.74	1.10	1.65	1.16
124		6.00	10.5	4200	0.81	4.18	6.99	1.71	1.66	1.03	1.58	1.08
125		6.00	10.56	4800	0.63	4.16	6.3	1.44	1.43	1.00	1.38	1.04
126		6.00	10.31	4050	0.53	4.26	7.55	1.92	1.40	1.37	1.36	1.41
127		5.98	10.3	3640	0.53	4.28	5.5	1.48	1.45	1.02	1.41	1.05

b_w = width; d = effective depth; f_c = compressive strength of concrete;

$a/d = M/Vd$, measured for maximum moment location; ρ = tensile steel ratio

$V_{cr} = V_u$ = shear force at diagonal cracking

Note: $M_u/V_{cr}d = a/d - 1$ for these test cases (simple support under point loading)

Average	1.06	1.14
Std.Dev.	0.13	0.16

Table 5. Summary of the comparison in Table 4

Method No.	Procedure/Equation	Test/Predicted Ratio	
		Mean	Std. Deviation
[1]	[2]	[3]	[4]
1	Proposed Procedure (Eq. 4)	1.06	0.13
2	Parametric Equation (Eq. 13)	1.14	0.16
3	Proposed Simplified Equation (Eq. 14)*	1.15	0.16
4	MCFT**	1.19	0.19
5	ACI	1.30	0.30
6	ACI-Detailed	1.14	0.20
7	Zsutty	0.98	0.12
8	Okamura**	0.92	0.10
9	ASCE-ACI	1.18	0.21
10	CEB**	1.11	0.12
11	JSCE**	1.10	0.14
12	Kim	0.81	0.16
13	MACI***	-	-

* By including the size effect, the mean and the standard deviation were 1.10 and 0.14, respectively.

** Includes size effect.

*** Identical to ACI Equation, unless size effect is considered.

Table 6. Summary of experimental program, results, and predictions for RC beams in presence of axial load based on tests by Mattock (1969)

Test No.	d in.	f' psi	ρ %	a/d	S _e in.	P/A _g psi	V _{cr} kips	V _{ult} kips	V _{ult} /V _{cr}	V _{cr} /bwdf' ^{0.5} k-test	Procedure (Eq. 4)		ACI-simplified		MCFT	
[1]	[2]	[3]	[4]	[5]	[6]	[7]	[8]	[9]	[10]	[11]	[12]	[13]	[14]	[15]	[16]	
											k	Ratio	k	Ratio	k	Ratio
1	10	2480	1.03	2.74	9.00	0	8	8.2	1.025	2.68	2.19	1.22	2.00	1.34	2.02	1.32
2	10	2250	1.03	2.74	9.00	190	9	9.2	1.022	3.16	2.85	1.11	2.19	1.44	2.27	1.39
3	10	6800	1.03	2.74	19.70	0	11.5	12.3	1.070	2.32	1.69	1.37	2.00	1.16	1.58	1.47
4	10	6700	1.03	2.74	19.70	-90	10	10	1.000	2.04	1.54	1.32	1.64	1.24	1.52	1.34
5	10	2330	2.07	2.74	9.00	-90	7.5	7.5	1.000	2.59	2.60	1.00	1.64	1.58	2.34	1.11
6	10	2660	2.07	2.74	9.00	190	11.5	12.1	1.052	3.72	3.26	1.14	2.19	1.70	2.59	1.44
7	10	2530	2.07	2.74	9.00	400	12.5	13.5	1.080	4.14	3.99	1.04	2.40	1.73	2.88	1.44
8	10	6340	2.07	2.74	19.70	190	17	20.8	1.224	3.56	2.58	1.38	2.19	1.62	2.07	1.72
9	10	6960	2.07	2.74	19.70	400	17.5	23.7	1.354	3.50	2.85	1.23	2.40	1.46	2.23	1.57
10	10	2690	3.1	2.74	9.00	0	11.5	12.6	1.096	3.70	3.15	1.17	2.00	1.85	2.63	1.40
11	10	2210	3.1	2.74	9.00	-190	9.5	9.5	1.000	3.37	2.60	1.29	1.24	2.72	2.52	1.33
12	10	2350	3.1	2.74	9.00	190	12.5	13.9	1.112	4.30	3.67	1.17	2.19	1.96	2.88	1.49
13	10	7220	3.1	2.74	19.70	190	18	20	1.111	3.53	2.84	1.24	2.19	1.61	2.25	1.57
14	10	7100	3.1	2.74	19.70	400	20	25	1.250	3.96	3.18	1.25	2.40	1.65	2.42	1.63
15	10	3750	1.03	5.14	9.00	0	7	7	1.000	1.91	1.77	1.08	2.00	0.95	1.59	1.20
16	10	4400	1.03	5.14	9.00	-150	6.3	6.3	1.000	1.58	1.43	1.11	1.40	1.13	1.51	1.05
17	10	4030	1.03	5.14	9.00	400	8	8.5	1.063	2.10	2.20	0.95	2.40	0.88	1.76	1.19
18	10	2620	2.07	5.14	9.00	0	8	8	1.000	2.60	2.56	1.02	2.00	1.30	1.99	1.31
19	10	2680	2.07	5.14	9.00	-90	9	9	1.000	2.90	2.41	1.20	1.64	1.77	1.94	1.49
20	10	7000	2.07	5.14	19.70	-90	13	13.000	1.000	2.59	1.81	1.43	1.64	1.58	1.52	1.70
21	10	7330	2.07	5.14	19.70	-190	12.8	12.8	1.000	2.49	1.68	1.49	1.24	2.01	1.48	1.68
22	10	2340	3.1	5.14	9.00	0	9	9	1.000	3.10	3.00	1.03	2.00	1.55	2.24	1.38
23	10	2680	3.1	5.14	9.00	-90	9.5	9.5	1.000	3.06	2.77	1.10	1.64	1.86	2.16	1.41
24	10	4230	3.1	5.14	9.00	0	11.8	11.8	1.000	3.02	2.55	1.19	2.00	1.51	2.07	1.46
25	10	4000	3.1	5.14	9.00	-150	11	11.5	1.045	2.90	2.41	1.20	1.40	2.07	2.04	1.42
26	10	4180	3.1	5.14	9.00	-250	9.5	9.5	1.000	2.45	2.24	1.09	1.00	2.45	1.99	1.23
27	10	4430	3.1	5.14	9.00	200	12	12	1.000	3.00	2.70	1.11	2.20	1.37	2.14	1.40
28	10	3520	3.1	5.14	9.00	400	11	11.8	1.073	3.09	3.08	1.00	2.40	1.29	2.31	1.34
29	10	7720	3.1	5.14	19.70	-90	15	15	1.000	2.85	2.07	1.37	1.64	1.73	1.69	1.69
30	10	8000	3.1	5.14	19.70	190	15	15	1.000	2.80	2.26	1.24	2.19	1.28	1.76	1.59
31	10	7640	3.1	5.14	19.70	400	15	15	1.000	2.86	2.45	1.17	2.40	1.19	1.85	1.54
Mean=										1.05	1.18		1.58		1.43	
Std.dev.=										0.09	0.13		0.40		0.17	

Table 7. Summary of experimental program, results, and predictions: influence of member size

Test No.	Investigator	b_w in.	d in.	f_c' psi	ρ %	a/d	a^* in.	S or S _r in.	S _e (MCFT) in.	V _{cr} kips	V _{cr} /b _w d ^{1.5} k-test	Proposed (Eq 14) k	Proposed (Eq 22) Ratio	Proposed (Eq 22) k	Proposed (Eq 22) ratio
[1]	[2]	[3]	[4]	[5]	[6]	[7]	[8]	[9]	[10]	[11]	[12]	[13]	[14]	[15]	[16]
1	Kani (1967)	5.92	5.3	3640	2.89	3.02	0.75	4.77	4.77	7.32	3.87	2.80	1.38	3.27	1.18
2		6	5.45	3600	2.69	3.93	0.75	4.91	4.91	6.5	3.31	2.58	1.28	2.99	1.11
3		5.95	5.25	3590	2.81	5.09	0.75	4.73	4.73	6.1	3.26	2.48	1.32	2.89	1.13
4		5.96	5.4	4060	2.73	5.92	0.75	4.86	4.86	6.54	3.19	2.28	1.40	2.66	1.20
5		6.14	10.68	3980	2.73	3.00	0.75	9.61	9.61	14.6	3.53	2.67	1.32	2.77	1.27
6		5.95	10.67	3980	2.83	4.01	0.75	9.60	9.60	12.45	3.11	2.53	1.23	2.62	1.19
7		6.04	10.8	3990	2.76	5.94	0.75	9.72	11.5	7.92	2.79	2.30	1.21	2.39	1.17
8		6.1	21.42	3970	2.66	2.99	0.75	19.28	19.28	22.95	2.79	2.65	1.05	2.45	1.14
9		6.08	21.37	3800	2.77	4.00	0.75	19.23	19.23	20.95	2.62	2.55	1.03	2.36	1.11
10		6.15	21.31	3830	2.75	6.02	0.75	19.18	19.18	20.4	2.52	2.33	1.08	2.15	1.17
11		6.03	21.9	3790	2.72	6.83	0.75	19.71	19.71	18.8	2.31	2.27	1.02	2.09	1.11
12		6.15	21.28	3730	2.75	8.01	0.75	19.15	19.15	17.75	2.22	2.22	1.00	2.05	1.08
13		6.05	43	3910	2.72	3.00	0.75	38.70	38.70	37.1	2.28	2.68	0.85	2.21	1.03
14		6	43.2	4280	2.73	3.97	0.75	38.88	38.88	35.75	2.11	2.44	0.86	2.01	1.05
15		6.1	43	4100	2.7	5.00	0.75	38.70	38.70	34.25	2.04	2.35	0.87	1.93	1.06
16		6.1	43.2	3870	2.72	7.00	0.75	38.88	38.88	34.65	2.11	2.24	0.94	1.84	1.15
17		6.1	43.1	3870	2.68	8.00	0.75	38.79	38.79	33.05	2.02	2.17	0.93	1.79	1.13
18	Johnson and Ramirez (1989)	12	21.21	5280	2.49	3.1	0.75	19.09	19.09	40.0	2.16	2.34	0.92	2.16	1.00
19		12	21.21	5280	2.49	3.1	0.75	19.09	19.09	40.0	2.16	2.34	0.92	2.16	1.00
20		12	21.21	10490	2.49	3.1	0.75	19.09	41.78	49.9	1.91	1.86	1.03	1.72	1.11
21		12	21.21	10490	2.49	3.1	0.75	19.09	41.78	48.1	1.85	1.86	0.99	1.72	1.07
22		12	21.21	8100	2.49	3.1	0.75	19.09	41.78	40.0	1.74	2.03	0.86	1.88	0.93
23		12	21.21	8100	2.49	3.1	0.75	19.09	41.78	43.0	1.88	2.03	0.93	1.88	1.00
24		12	21.21	7440	2.49	3.1	0.75	19.09	41.78	40.0	1.82	2.09	0.87	1.93	0.94
25		12	21.21	7440	2.49	3.1	0.75	19.09	41.78	44.0	2.01	2.09	0.96	1.93	1.04
26		Bresler and Scordelis (1963)	12	18.15	3270	1.81	3.97	0.75	16.34	16.34	30.0	2.41	2.33	1.03	2.21
27	12		18.35	3440	2.27	4.9	0.75	16.52	16.52	32.5	2.52	2.36	1.07	2.24	1.12
28	12		18.17	5450	2.74	6.94	0.75	16.35	16.35	35.0	2.17	2.01	1.08	1.91	1.14
29	12		18.35	3490	1.8	3.92	0.75	16.52	16.52	30.0	2.31	2.28	1.01	2.16	1.07
30	12		18.27	3520	2.28	4.93	0.75	16.44	16.44	27.5	2.11	2.34	0.90	2.22	0.95
31	9		18.15	3590	2.43	3.95	0.75	16.34	16.34	27.5	2.81	2.49	1.13	2.37	1.19
32	9		18.33	3360	2.43	4.91	0.75	16.50	16.50	27.5	2.88	2.43	1.18	2.31	1.25
33	6		18.25	4290	1.8	3.95	0.75	16.43	16.43	22.5	3.14	2.13	1.48	2.02	1.56
34	6		18.28	3450	3.66	4.93	0.75	16.45	16.45	17.5	2.72	2.76	0.98	2.62	1.04
35	Kim and Park (1994)	12	22	7400	1.87	3	1.00	19.80	43.34	51.3	2.26	1.92	1.18	1.76	1.28
36		12	36.5	7400	1.87	3	1.00	32.85	71.91	69.9	1.85	1.92	0.97	1.62	1.15
37		6.8	10.8	7400	1.87	3	1.00	9.72	21.28	16.5	2.61	1.92	1.36	1.98	1.32
38		6.8	10.8	7400	1.01	3	1.00	9.72	21.28	13.2	2.09	1.56	1.34	1.62	1.29
39		6.8	10.8	7400	3.35	3	1.00	9.72	21.28	18.4	2.91	2.33	1.25	2.41	1.21
40		6.8	10.2	7400	4.67	3	1.00	9.18	20.09	21.5	3.61	2.60	1.39	2.72	1.33
41		6.8	10.8	7400	1.87	4.5	1.00	9.72	21.28	15.1	2.39	1.74	1.37	1.81	1.32
42		6.8	10.8	7400	1.87	6	1.00	9.72	21.28	14.0	2.21	1.64	1.34	1.70	1.30
43		6.8	5.68	7400	1.87	3	1.00	5.11	11.19	9.4	2.82	1.92	1.47	2.21	1.28
44	Yoon, Cook, and Mitchell (1996)	14.76	25.8	5220	2.8	3.28	0.80	23.22	22.45	55.1	2.00	2.41	0.83	2.16	0.93
45		14.76	25.8	5220	2.8	3.28	0.80	23.22	22.45	58.5	2.12	2.41	0.88	2.16	0.98
46		14.76	25.8	5220	2.8	3.28	0.80	23.22	22.45	45.0	1.64	2.41	0.68	2.16	0.76
47		14.76	25.8	5220	2.8	3.28	0.80	23.22	22.45	57.1	2.08	2.41	0.86	2.16	0.96
48		14.76	25.8	9720	2.8	3.28	0.80	23.22	50.83	65.0	1.73	1.96	0.88	1.75	0.99
49		14.76	25.8	9720	2.8	3.28	0.80	23.22	50.83	65.0	1.73	1.96	0.88	1.75	0.99
50		14.76	25.8	9720	2.8	3.28	0.80	23.22	50.83	65.0	1.73	1.96	0.88	1.75	0.99
51		14.76	25.8	9720	2.8	3.28	0.80	23.22	50.83	65.0	1.73	1.96	0.88	1.75	0.99
52		14.76	25.8	12620	2.8	3.28	0.80	23.22	50.83	69.9	1.63	1.79	0.91	1.61	1.02
53		14.76	25.8	12620	2.8	3.28	0.80	23.22	50.83	69.9	1.63	1.79	0.91	1.61	1.02
54		14.76	25.8	12620	2.8	3.28	0.80	23.22	50.83	69.9	1.63	1.79	0.91	1.61	1.02
55		14.76	25.8	12620	2.8	3.28	0.80	23.22	50.83	75.1	1.76	1.79	0.98	1.61	1.09

Table 7. (contd.) Summary of experimental program, results, and predictions: influence of member size

56		15.7	36.8	4500	1.35	3	1.50	33.12	21.46	80.7	2.08	2.03	1.03	1.71	1.22
57		15.7	36.8	3920	1.35	3	0.75	33.12	33.12	73.9	2.04	2.12	0.96	1.79	1.14
58		7.85	18.4	4190	1.35	3	1.50	16.56	10.73	23.4	2.50	2.08	1.21	1.97	1.27
59		7.85	18.4	3820	1.35	3	0.75	16.56	16.56	19.6	2.20	2.14	1.03	2.03	1.08
60		7.85	18.4	4940	1.35	3	0.37	16.56	22.74	19.2	1.89	1.97	0.96	1.86	1.02
61		3.93	9.2	3940	1.35	3	0.75	8.28	8.28	5.1	2.23	2.12	1.05	2.25	0.99
62	Taylor (1972)	3.93	9.2	3940	1.35	3	0.37	8.28	11.37	5.4	2.37	2.12	1.12	2.25	1.05
63		3.93	9.2	4230	1.35	3	0.37	8.28	11.37	6.2	2.63	2.07	1.27	2.20	1.19
64		3.93	9.2	3200	1.35	3	0.37	8.28	11.37	5.1	2.47	2.27	1.09	2.42	1.02
65		3.93	9.2	3450	1.35	3	0.37	8.28	11.37	6.1	2.85	2.22	1.29	2.36	1.21
66		3.93	9.2	4440	1.35	3	0.10	8.28	15.65	6.2	2.57	2.04	1.26	2.17	1.18
67		2.36	5.52	4930	1.35	3	0.10	4.97	9.39	2.6	2.86	1.97	1.46	2.28	1.26
68		2.36	5.52	4930	1.35	3	0.10	4.97	9.39	2.7	2.97	1.97	1.51	2.28	1.31
69		2.36	5.52	4930	1.35	3	0.10	4.97	9.39	2.4	2.60	1.97	1.32	2.28	1.14
70		2.36	5.52	4930	1.35	3	0.10	4.97	9.39	2.6	2.80	1.97	1.42	2.28	1.23
71		12	36.4	5221	1.01	2.92	0.39	32.78	44.09	51	1.62	1.76	0.92	1.49	1.09
72		12	36.4	5221	1.01	2.92	0.39	32.78	44.09	57	1.80	1.76	1.02	1.49	1.21
73		12	36.4	5221	1.19	2.92	0.39	6.80	9.02	73	2.30	1.86	1.24	2.05	1.13
74		12	36.4	14213	1.01	2.92	0.39	32.78	71.65	53	1.01	1.26	0.80	1.07	0.94
75		12	36.4	14213	1.01	2.92	0.39	32.78	71.65	59	1.13	1.26	0.89	1.07	1.06
76		12	36.4	5656	1.01	2.92	0.39	32.78	44.09	51	1.55	1.72	0.90	1.45	1.07
77		12	36.4	5656	1.01	2.92	0.39	32.78	44.09	54	1.63	1.72	0.95	1.45	1.12
78	Collins and	12	36.4	5656	1.01	2.92	0.39	32.78	44.09	47	1.42	1.72	0.82	1.45	0.97
79	Kuchma (1999)	12	36.4	5395	0.76	2.92	0.39	32.78	44.13	44	1.36	1.59	0.85	1.34	1.01
80		12	17.7	5395	0.81	3	0.39	15.94	21.46	30	1.92	1.61	1.19	1.54	1.25
81		12	8.9	5395	0.89	3	0.39	7.97	10.75	17	2.12	1.66	1.28	1.78	1.19
82		12	4.3	5395	0.91	3.07	0.39	3.90	5.24	9	2.39	1.66	1.44	2.01	1.19
83		12	36.4	5395	1.19	2.92	0.39	6.80	9.02	59	1.82	1.84	0.99	2.03	0.90
84		12	17.7	5395	1.11	3	0.39	3.40	4.25	37	2.38	1.79	1.33	2.21	1.08
85		12	8.9	5395	1.31	3	0.39	1.60	2.13	25	3.26	1.89	1.73	2.64	1.23
86		12	36.4	14329	0.76	2.92	0.39	32.78	71.69	53	1.01	1.15	0.88	0.97	1.04
87		12	17.7	14329	0.81	3	0.39	15.94	34.88	36	1.40	1.16	1.21	1.11	1.27
88		12	8.9	14329	0.89	3	0.39	7.97	17.44	23	1.81	1.20	1.51	1.28	1.41
89		12	36.4	14329	1.19	2.92	0.39	6.80	14.65	76	1.45	1.33	1.09	1.46	0.99
90		12	36.4	14329	1.19	2.92	0.39	6.80	14.65	91	1.74	1.33	1.31	1.46	1.19
91		12	17.7	14329	1.11	3	0.39	3.40	6.89	53	2.06	1.29	1.60	1.59	1.30
92		12	17.7	14329	1.11	3	0.39	3.40	6.89	56	2.20	1.29	1.70	1.59	1.38
93		12	8.9	14329	1.31	3	0.39	1.60	3.46	30	2.39	1.36	1.75	1.91	1.25
94		12	36.4	13633	0.5	2.92	0.39	32.78	71.69	43	0.85	1.01	0.84	0.86	0.99

Notes: 1. $M_u/V_{ud} = a/d - 1$ for the above test cases (simple support under point loading)

* Max aggregate size "a" is taken as 0.75 in. when not available in literature

Mean =	1.11	1.12
Std. Deviation =	0.24	0.13

Table 7. (contd.) Summary of experimental program, results, and predictions: influence of member size

56	2.39	0.87	1.85	1.13	2.00	1.04	2.15	0.97	1.61	1.29	2.15	0.97	1.65	1.26	1.73	1.21	1.45	1.43	2.63	0.79
57	2.45	0.83	1.89	1.08	2.00	1.02	2.17	0.94	1.38	1.48	2.15	0.95	1.69	1.21	1.65	1.24	1.49	1.37	2.76	0.74
58	2.42	1.03	2.23	1.12	2.00	1.25	2.16	1.16	1.89	1.32	2.15	1.16	1.89	1.33	1.91	1.31	1.75	1.43	2.70	0.93
59	2.46	0.89	2.26	0.97	2.00	1.10	2.17	1.01	1.73	1.27	2.15	1.02	1.92	1.14	1.82	1.21	1.78	1.24	2.78	0.79
60	2.36	0.80	2.17	0.87	2.00	0.95	2.14	0.88	1.58	1.20	2.15	0.88	1.84	1.03	1.69	1.12	1.70	1.11	2.55	0.74
61	2.45	0.91	2.68	0.83	2.00	1.11	2.17	1.03	1.97	1.13	2.15	1.04	2.22	1.00	2.00	1.11	2.10	1.06	2.75	0.81
62	2.45	0.97	2.68	0.89	2.00	1.19	2.17	1.10	1.87	1.27	2.15	1.10	2.22	1.07	1.92	1.24	2.10	1.13	2.75	0.86
63	2.42	1.09	2.64	0.99	2.00	1.31	2.16	1.22	1.87	1.40	2.15	1.22	2.20	1.20	1.90	1.39	2.08	1.27	2.69	0.98
64	2.54	0.98	2.77	0.89	2.00	1.24	2.20	1.13	1.87	1.32	2.15	1.15	2.30	1.08	1.96	1.26	2.17	1.14	2.96	0.84
65	2.50	1.14	2.74	1.04	2.00	1.43	2.19	1.30	1.87	1.52	2.15	1.33	2.27	1.26	1.94	1.47	2.15	1.33	2.88	0.99
66	2.40	1.07	2.62	0.98	2.00	1.28	2.15	1.19	1.75	1.46	2.15	1.19	2.18	1.18	1.80	1.42	2.06	1.25	2.64	0.97
67	2.36	1.21	2.93	0.98	2.00	1.43	2.14	1.34	1.94	1.48	2.15	1.33	2.44	1.17	1.92	1.49	2.30	1.25	2.55	1.12
68	2.36	1.26	2.93	1.02	2.00	1.49	2.14	1.39	1.94	1.54	2.15	1.38	2.44	1.22	1.92	1.55	2.30	1.29	2.55	1.16
69	2.36	1.10	2.93	0.89	2.00	1.30	2.14	1.22	1.94	1.34	2.15	1.21	2.44	1.07	1.92	1.36	2.30	1.13	2.55	1.02
70	2.36	1.19	2.93	0.96	2.00	1.40	2.14	1.31	1.94	1.45	2.15	1.30	2.44	1.15	1.92	1.46	2.30	1.22	2.55	1.10
71	2.14	0.76	1.66	0.98	2.00	0.81	2.08	0.78	1.22	1.33	1.81	0.90	1.48	1.10	1.33	1.22	1.29	1.26	2.15	0.75
72	2.14	0.84	1.66	1.08	2.00	0.90	2.08	0.86	1.22	1.47	1.81	0.99	1.48	1.22	1.33	1.35	1.29	1.40	2.15	0.84
73	2.26	1.02	1.75	1.31	2.00	1.15	2.11	1.09	1.95	1.18	1.99	1.16	1.56	1.48	1.90	1.21	1.36	1.69	2.37	0.97
74	1.81	0.56	1.40	0.72	1.68	0.60	2.01	0.50	0.95	1.07	1.81	0.56	1.25	0.81	1.05	0.96	1.09	0.92	1.65	0.61
75	1.81	0.62	1.40	0.80	1.68	0.67	2.01	0.56	0.95	1.19	1.81	0.62	1.25	0.90	1.04	1.08	1.09	1.03	1.65	0.68
76	2.11	0.73	1.64	0.95	2.00	0.77	2.07	0.75	1.22	1.27	1.81	0.86	1.46	1.06	1.31	1.18	1.27	1.22	2.10	0.74
77	2.11	0.77	1.64	1.00	2.00	0.82	2.07	0.79	1.22	1.34	1.81	0.90	1.46	1.12	1.32	1.24	1.27	1.28	2.10	0.78
78	2.11	0.67	1.64	0.86	2.00	0.71	2.07	0.68	1.22	1.16	1.81	0.78	1.46	0.97	1.31	1.08	1.27	1.11	2.10	0.67
79	1.94	0.70	1.50	0.90	2.00	0.68	2.03	0.67	1.22	1.11	1.56	0.87	1.34	1.02	1.19	1.14	1.17	1.16	1.83	0.74
80	1.96	0.98	1.82	1.06	2.00	0.96	2.04	0.94	1.61	1.19	1.61	1.19	1.54	1.25	1.44	1.33	1.43	1.35	1.86	1.03
81	2.02	1.05	2.23	0.95	2.00	1.06	2.05	1.04	1.89	1.12	1.69	1.26	1.85	1.15	1.70	1.25	1.75	1.21	1.96	1.09
82	2.02	1.18	2.66	0.90	2.00	1.19	2.05	1.17	2.08	1.15	1.71	1.40	2.24	1.07	1.93	1.24	2.11	1.13	1.95	1.22
83	2.25	0.81	1.74	1.05	2.00	0.91	2.11	0.86	1.95	0.94	1.99	0.92	1.55	1.18	1.82	1.00	1.35	1.35	2.34	0.78
84	2.18	1.09	2.02	1.18	2.00	1.19	2.09	1.14	2.12	1.12	1.91	1.24	1.71	1.39	2.10	1.13	1.58	1.50	2.21	1.07
85	2.30	1.42	2.54	1.29	2.00	1.63	2.12	1.54	2.21	1.48	2.11	1.55	2.11	1.55	2.40	1.36	1.99	1.64	2.44	1.34
86	1.64	0.61	1.28	0.79	1.67	0.60	1.98	0.51	0.95	1.07	1.56	0.65	1.13	0.89	0.93	1.08	0.99	1.02	1.46	0.69
87	1.66	0.84	1.54	0.91	1.67	0.84	1.98	0.71	1.35	1.04	1.61	0.87	1.31	1.07	1.17	1.20	1.21	1.16	1.48	0.95
88	1.72	1.05	1.89	0.96	1.67	1.08	1.99	0.91	1.71	1.06	1.69	1.07	1.57	1.15	1.42	1.28	1.49	1.22	1.54	1.18
89	1.91	0.76	1.48	0.98	1.67	0.87	2.03	0.72	1.78	0.82	1.99	0.73	1.32	1.10	1.54	0.94	1.15	1.26	1.78	0.82
90	1.91	0.91	1.48	1.17	1.67	1.04	2.03	0.86	1.78	0.98	1.99	0.87	1.32	1.32	1.54	1.13	1.15	1.51	1.78	0.98
91	1.85	1.12	1.71	1.20	1.67	1.24	2.02	1.02	2.02	1.02	1.91	1.08	1.45	1.42	1.79	1.15	1.35	1.53	1.70	1.22
92	1.85	1.19	1.71	1.28	1.67	1.31	2.02	1.09	2.02	1.09	1.91	1.15	1.45	1.51	1.80	1.22	1.35	1.63	1.70	1.29
93	1.95	1.22	2.16	1.11	1.67	1.43	2.04	1.17	2.15	1.11	2.11	1.13	1.79	1.33	1.74	1.37	1.69	1.41	1.84	1.30
94	1.44	0.59	1.12	0.76	1.71	0.50	1.96	0.44	0.95	0.90	1.30	0.66	0.99	0.86	0.80	1.06	0.87	0.98	1.26	0.68
		0.92		0.97		1.13		1.02		1.40		1.03		1.14		1.27		1.18		0.82
		0.20		0.14		0.28		0.25		0.24		0.24		0.17		0.17		0.17		0.21

Table 8. Summary of comparisons in Table 7

Method No.	Procedure/Equation	Test/Predicted Ratio	
		Mean	Std. Deviation
[1]	[2]	[3]	[4]
1	Proposed Simplified Equation (Eq. 14)*	1.11	0.24
2	Proposed Simplified with Size Effect (Eq. 22)	1.12	0.13
3	MCFT	1.27	0.17
4	ACI-Simplified*	1.13	0.28
5	ACI-Detailed*	1.02	0.25
6	Zsutty*	0.92	0.20
7	Okamura	0.97	0.14
8	ASCE-ACI*	1.03	0.24
9	CEB	1.14	0.17
10	JSCE	1.18	0.17
11	Kim*	0.82	0.21
12	MACI	1.40	0.24

* These methods do not include size effect

Table 9. Summary of test program, results, and predictions: influence of type of loading based on tests by Krefeld and Thurston (1966)

Test No.	b_w in.	d in.	f_c' psi	ρ %	L/d	x/d	$M_u/V_{cr}d$	S or S_x in.	V kips	V_{ult} kips	V_{ult}/V	V_{cr} kips	$V_{cr}/b_wd(f_c')^{0.5}$ k-test	Simplified Eq. 14	
[1]	[2]	[3]	[4]	[5]	[6]	[7]	[8]	[9]	[10]	[11]	[12]	[13]	[14]	[15]	[16]
1	8.0	15.36	4070	2.06	4.7	0.80	1.01	13.82	40	95.8	2.40	26.4	3.37	2.71	1.24
2	8.0	15.36	4260	3.09	4.7	0.80	1.01	13.82	40	142.6	3.57	26.4	3.29	3.05	1.08
3	6.0	12.36	3910	3.41	5.84	0.82	1.00	11.12	25	60.1	2.40	18.0	3.88	3.25	1.19
4	8.0	15.36	4240	2.06	4.7	0.80	1.01	13.82	37.5	90.6	2.42	24.7	3.09	2.67	1.16
5	8.0	15.36	3990	2.06	4.7	0.80	1.01	13.82	42.5	98.1	2.31	28.0	3.61	2.72	1.33
6	8.0	15.36	4270	3.09	4.7	0.80	1.01	13.82	47.5	123.1	2.59	31.3	3.90	3.05	1.28
7	8.0	15.36	4290	3.09	4.7	0.80	1.01	13.82	42.5	140.1	3.30	28.0	3.48	3.04	1.14
8	6.0	9.56	3040	2.09	7.54	1.06	1.26	8.60	14	28.8	2.06	10.1	3.19	2.89	1.10
9	6.0	12.44	2780	1.34	5.8	0.81	1.00	11.20	16	34.8	2.18	11.5	2.93	2.67	1.10
10	6.0	9.44	3050	1.77	7.62	1.07	1.27	8.50	13	23.7	1.82	9.4	2.99	2.72	1.10
11	6.0	9.56	2660	2.09	7.54	1.06	1.26	8.60	13	27.5	2.12	9.4	3.16	3.02	1.05
12	6.0	12.44	2930	2.68	5.8	0.81	1.00	11.20	21	54.3	2.59	15.1	3.74	3.30	1.13
13	6.0	9.44	3080	3.53	7.62	1.07	1.27	8.50	19	36	1.89	13.7	4.35	3.42	1.27
14	6.0	9.36	3090	4.52	7.7	1.08	1.29	8.42	18	37.6	2.09	13.0	4.15	3.70	1.12
15	6.0	9.36	3080	4.93	7.7	1.08	1.29	8.42	27	50.6	1.87	19.4	6.24	3.81	1.64
16	6.0	10.06	3290	1.99	9.54	1.34	1.60	9.05	15	20.9	1.39	10.8	3.12	2.66	1.17
17	6.0	10	2590	2.63	9.6	1.34	1.61	9.00	15.5	20.4	1.32	11.2	3.65	3.16	1.16
18	6.0	9.94	2990	3.35	9.66	1.35	1.62	8.95	16	24.8	1.55	11.5	3.53	3.26	1.08
19	6.0	9.86	2990	4.3	9.86	1.38	1.65	8.87	17.5	28.3	1.62	12.6	3.89	3.53	1.10
20	6.0	10.06	2970	1.99	11.92	1.67	1.99	9.05	11	16.1	1.46	7.9	2.41	2.65	0.91
21	6.0	10	5280	2.63	7.2	1.01	1.20	9.00	20	41.2	2.06	14.4	3.30	2.61	1.26
22	6.0	9.86	4990	4.3	7.3	1.02	1.22	8.87	20	48.3	2.42	14.4	3.45	3.13	1.10
23	6.0	10	4590	2.63	9.6	1.34	1.61	9.00	17	26.4	1.55	12.2	3.01	2.61	1.15
24	6.0	9.94	4590	3.35	9.66	1.35	1.62	8.95	21	29.8	1.42	15.1	3.74	2.83	1.32
25	6.0	9.86	4950	4.3	9.74	1.36	1.63	8.87	20	34.8	1.74	14.4	3.46	2.99	1.16
26	6.0	10	4680	2.63	12	1.68	2.01	9.00	16.5	21.9	1.33	11.9	2.89	2.50	1.16
27	6.0	9.94	4680	3.35	12.08	1.69	2.02	8.95	19	21.4	1.13	13.7	3.35	2.71	1.24
28	6.0	9.87	5340	4.3	12.16	1.70	2.03	8.88	20.5	24.2	1.18	14.8	3.41	2.81	1.21

Note: x = distance of critical section from the support

V, V_{ult} are shear force at support; V_{cr} = shear resistance at critical section	Mean =	1.99	1.18
S_x = crack spacing (= $0.9d$ in these tests)	Std. Deviation =	0.60	0.13

Table 9. (contd.) Summary of test program, results, and predictions: influence of type of loading based on tests by Krefeld and Thurston (1966)

Test No.	Zsutty		Okamura		ACI-simplified		ACI-detailed		ASCE-ACI		CEB		MCFT		JSCE	
	k	Ratio	k	Ratio	k	Ratio	k	Ratio	k	Ratio	k	Ratio	k	Ratio	k	Ratio
[1]	[17]	[18]	[19]	[20]	[21]	[22]	[23]	[24]	[25]	[26]	[27]	[28]	[29]	[30]	[31]	[32]
1	3.04	1.11	2.98	1.13	2.00	1.68	2.71	1.24	2.30	1.46	2.46	1.37	2.35	1.43	2.12	1.59
2	3.45	0.95	3.39	0.97	2.00	1.64	3.09	1.06	2.30	1.43	2.79	1.18	2.59	1.27	2.40	1.37
3	3.37	1.15	3.42	1.13	2.00	1.94	3.26	1.19	2.30	1.69	2.85	1.36	2.74	1.42	2.66	1.46
4	3.02	1.02	2.96	1.04	2.00	1.55	2.70	1.15	2.30	1.34	2.44	1.27	2.35	1.32	2.10	1.47
5	3.05	1.18	2.99	1.21	2.00	1.81	2.72	1.33	2.30	1.57	2.47	1.46	2.37	1.53	2.12	1.70
6	3.45	1.13	3.38	1.15	2.00	1.95	3.09	1.26	2.30	1.70	2.79	1.40	2.61	1.50	2.40	1.62
7	3.45	1.01	3.38	1.03	2.00	1.74	3.09	1.13	2.30	1.51	2.79	1.25	2.58	1.35	2.40	1.45
8	2.74	1.16	2.95	1.08	2.00	1.59	3.09	1.03	2.30	1.39	2.46	1.29	2.50	1.27	2.51	1.27
9	2.62	1.12	2.66	1.10	2.00	1.46	2.54	1.15	2.14	1.37	2.22	1.32	2.28	1.28	2.06	1.42
10	2.58	1.16	2.79	1.07	2.00	1.50	2.92	1.02	2.30	1.30	2.33	1.28	2.40	1.25	2.38	1.26
11	2.80	1.13	3.02	1.05	2.00	1.58	3.18	1.00	2.30	1.38	2.52	1.26	2.55	1.24	2.57	1.23
12	3.27	1.14	3.32	1.13	2.00	1.87	3.14	1.19	2.30	1.63	2.77	1.35	2.67	1.40	2.57	1.46
13	3.25	1.34	3.50	1.24	2.00	2.18	3.50	1.24	2.30	1.89	2.93	1.49	2.85	1.53	2.99	1.45
14	3.51	1.18	3.80	1.09	2.00	2.08	3.50	1.19	2.30	1.80	3.17	1.31	3.02	1.38	3.26	1.27
15	3.61	1.73	3.91	1.59	2.00	3.12	3.50	1.78	2.30	2.71	3.27	1.91	3.10	2.01	3.35	1.86
16	2.46	1.27	2.63	1.19	2.00	1.56	3.28	0.95	2.30	1.36	2.19	1.43	2.34	1.34	2.41	1.30
17	2.80	1.30	3.00	1.22	2.00	1.83	3.50	1.04	2.30	1.59	2.49	1.47	2.59	1.41	2.75	1.33
18	2.96	1.19	3.18	1.11	2.00	1.77	3.50	1.01	2.30	1.54	2.64	1.34	2.68	1.32	2.92	1.21
19	3.20	1.22	3.44	1.13	2.00	1.95	3.50	1.11	2.30	1.69	2.85	1.37	2.85	1.37	3.18	1.23
20	2.32	1.04	2.53	0.95	2.00	1.20	3.50	0.69	2.30	1.05	2.06	1.17	2.27	1.06	2.45	0.98
21	2.74	1.21	2.92	1.13	2.00	1.65	2.99	1.10	2.30	1.44	2.44	1.36	2.47	1.34	2.45	1.35
22	3.24	1.06	3.46	0.99	2.00	1.72	3.50	0.98	2.30	1.50	2.89	1.19	2.82	1.22	2.92	1.18
23	2.55	1.18	2.73	1.10	2.00	1.51	3.46	0.87	2.30	1.31	2.27	1.33	2.40	1.25	2.50	1.20
24	2.76	1.36	2.96	1.26	2.00	1.87	3.50	1.07	2.30	1.63	2.46	1.52	2.55	1.47	2.72	1.38
25	2.95	1.17	3.17	1.09	2.00	1.73	3.50	0.99	2.30	1.50	2.63	1.31	2.69	1.29	2.92	1.18
26	2.36	1.23	2.57	1.13	2.00	1.45	3.50	0.83	2.30	1.26	2.10	1.38	2.29	1.26	2.50	1.16
27	2.55	1.31	2.78	1.20	2.00	1.68	3.50	0.96	2.30	1.46	2.27	1.48	2.44	1.38	2.71	1.24
28	2.71	1.26	2.96	1.15	2.00	1.71	3.50	0.97	2.30	1.48	2.41	1.41	2.55	1.34	2.88	1.18
			1.19	1.13	1.76	1.09	1.53	1.37	1.36	1.35	1.35	1.37	1.36	1.35	1.35	1.35
			0.14	0.12	0.34	0.20	0.29	0.14	0.16	0.19	0.14	0.16	0.16	0.16	0.19	0.19

Table 10. Summary of comparisons in Table 9 ($x = 0.14L$)

Method No.	Procedure/Equation	Test/Predicted Ratio	
		Mean	Std. Deviation
[1]	[2]	[3]	[4]
1	Proposed Simplified Equation (Eq. 14)	1.18	0.14
2	MCFT	1.36	0.16
3	ACI-Simplified	1.76	0.34
4	ACI-Detailed	1.09	0.20
5	Zsutty	1.19	0.14
6	Okamura	1.13	0.12
7	ASCE-ACI	1.53	0.29
8	CEB	1.37	0.14
9	JSCE	1.35	0.19
Note:	The critical shear section is taken at $0.14L$ from the supports (See Eq. 21)		

Table 11. Summary of comparisons in Table 9 ($x = d$)

Method No.	Procedure/Equation	Test/Predicted at Cracking**		Test/Predicted at Ultimate***	
		Mean	Std. Deviation	Mean	Std. Deviation
[1]	[2]	[3]	[4]	[5]	[6]
1	Proposed Simplified Equation (Eq. 14)*	1.17	0.14	1.51	0.18
2	MCFT	1.36	0.17	2.67	0.73
3	ACI-Simplified	1.79	0.37	3.48	0.99
4	ACI-Detailed	1.10	0.19	2.13	0.51
5	Zsutty	1.22	0.23	2.31	0.39
6	Okamura	1.15	0.18	2.21	0.42
7	ASCE-ACI	1.56	0.32	3.03	0.86
8	CEB	1.39	0.22	2.67	0.50
9	JSCE	1.36	0.14	2.68	0.75

Note: The critical shear section is taken at d from the supports

* For computing ultimate shear strength, Eq. 29 is used in place of Eq. 14

** At cracking shear strength V_{cr}

*** At ultimate shear strength V_{ult}

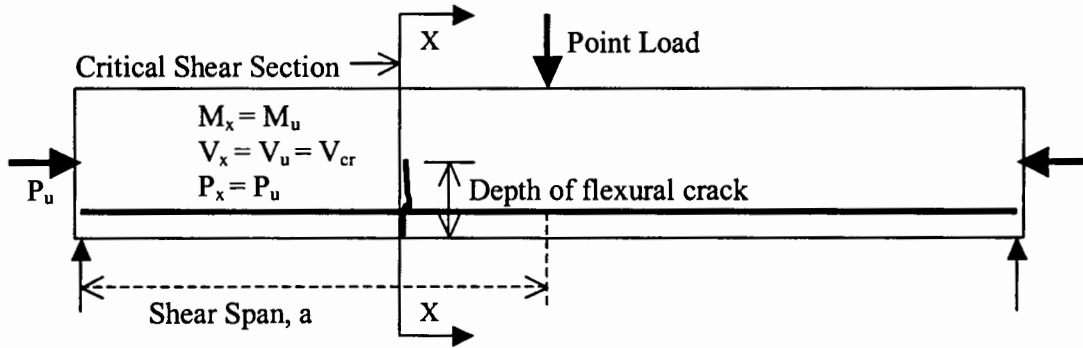


Fig. 1. A typical RC member under flexure and shear applied by a point load and axial load

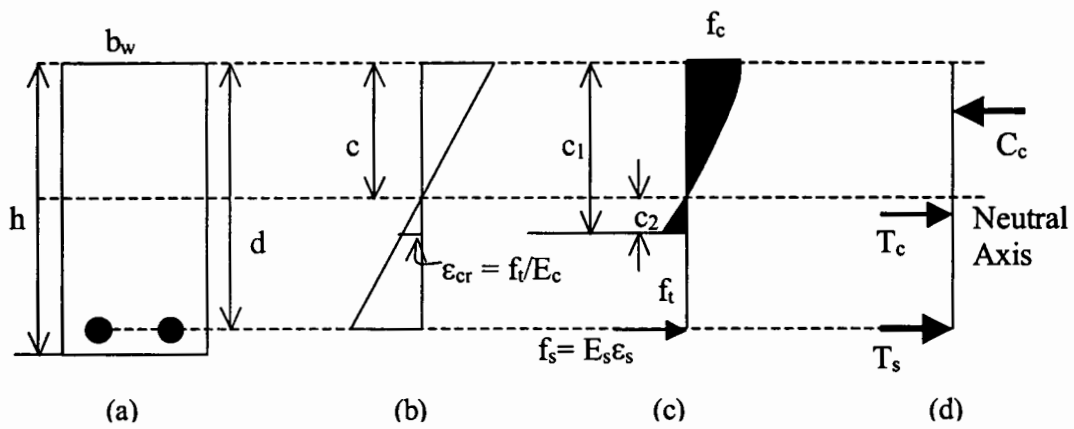


Fig. 2. Strain compatibility and force equilibrium at a section: (a) cross-section X-X; (b) strain distribution; (c) stress distribution; (d) cross-section force equilibrium

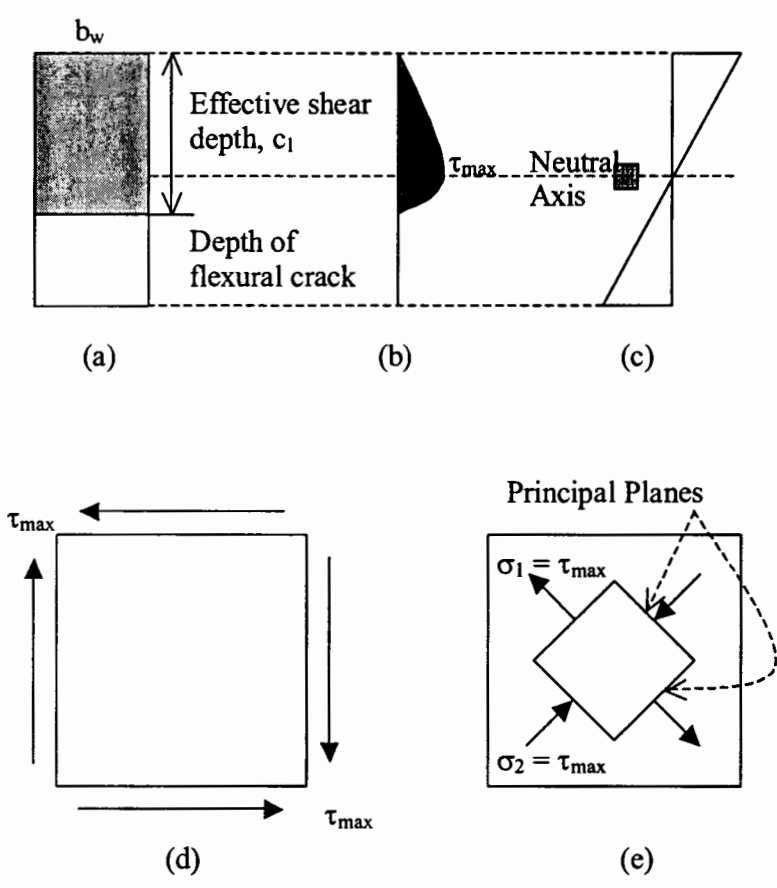


Fig. 3. Shear stress distribution and stress condition at neutral axis: (a) cross-section X-X; (b) shear stress distribution; (c) longitudinal strain distribution; (d) stress conditions at neutral axis; (e) diagonal cracking occurs when $\sigma_1 = f_t$

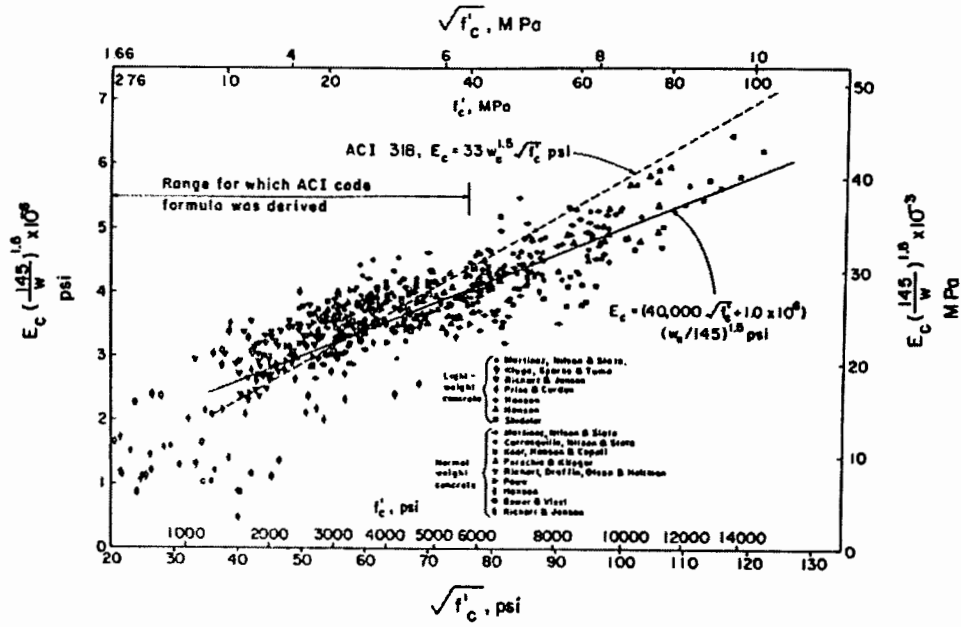


Fig. 4(a). Modulus of elasticity of concrete (ACI Manual of Concrete Practice 2001)

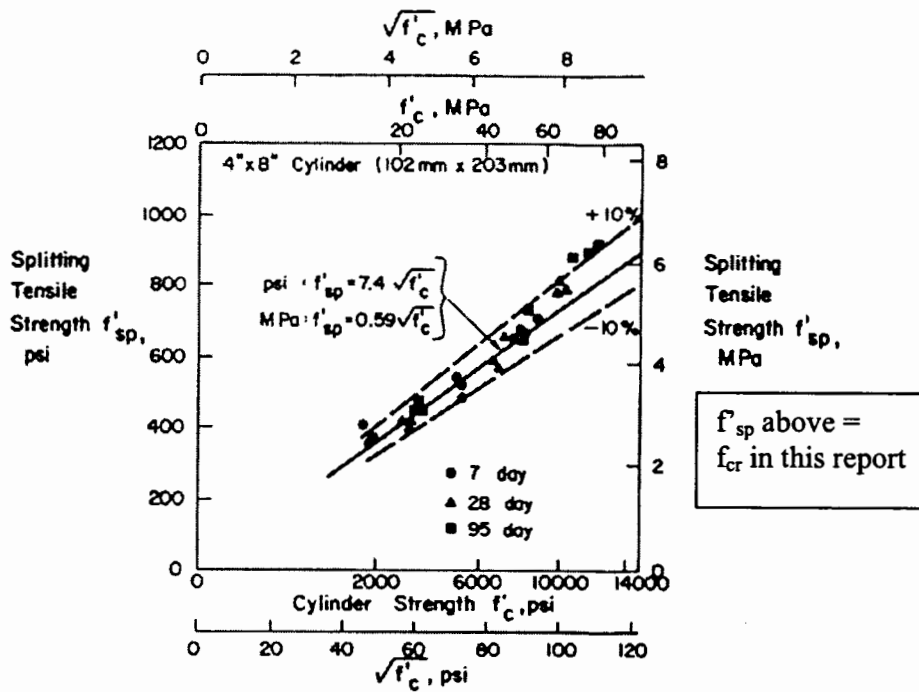


Fig. 4(b). Tensile strength based on split cylinder test

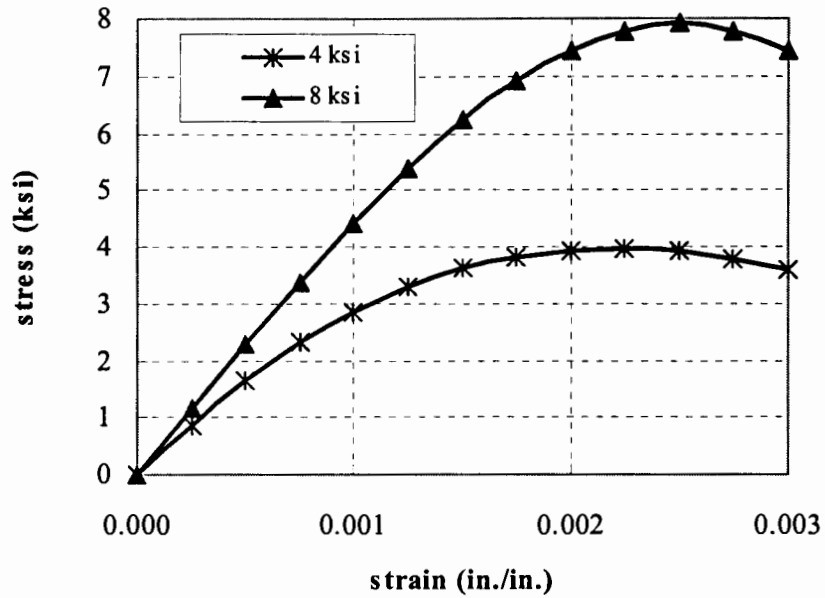


Fig. 5. A typical stress-strain curve given by Equation 8a for different concrete strengths in compression (Khuntia and Goel 1999)

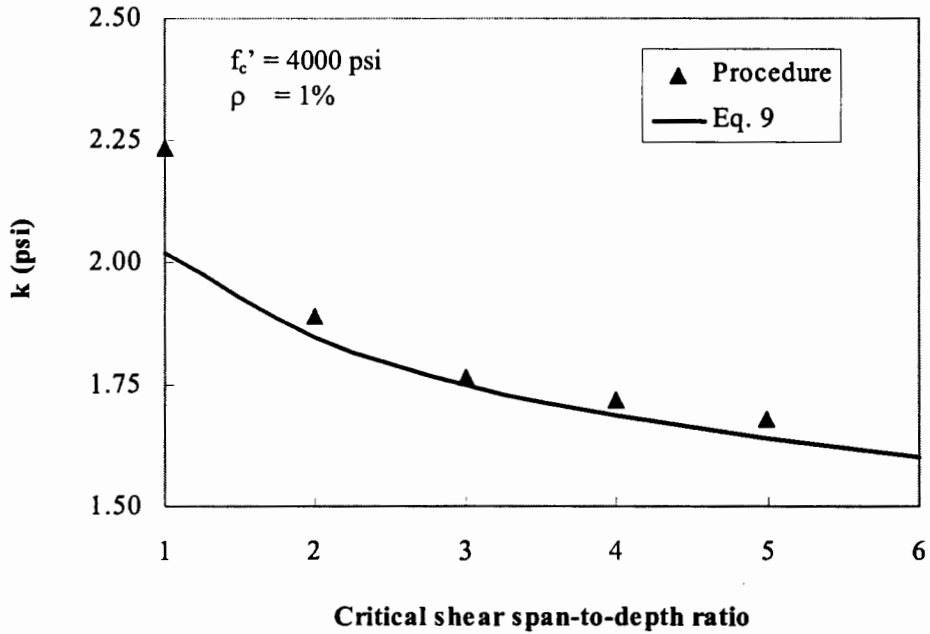


Fig. 6. Influence of critical shear span-to-depth ratio on shear strength

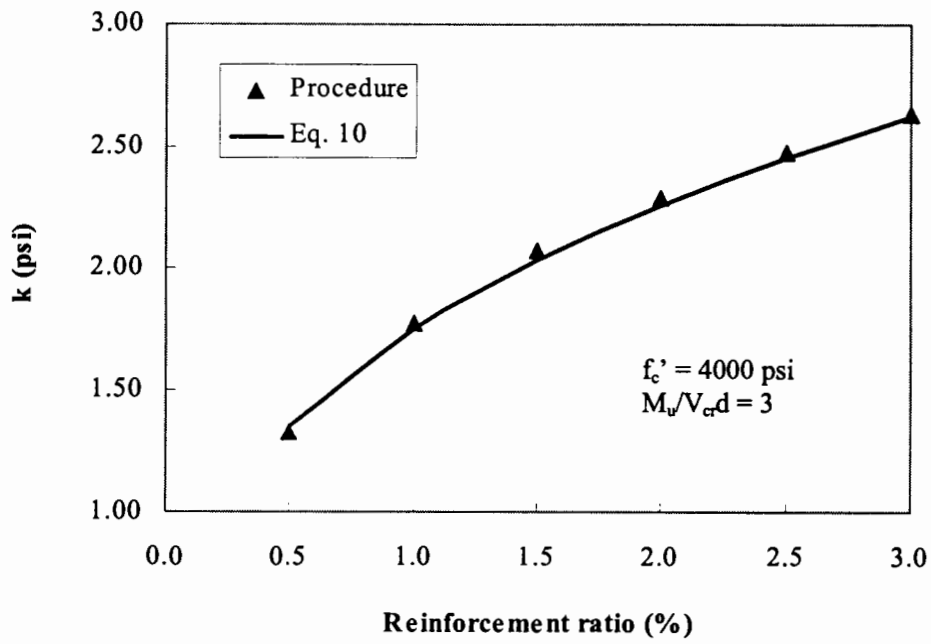


Fig. 7. Influence of reinforcement ratio on shear strength

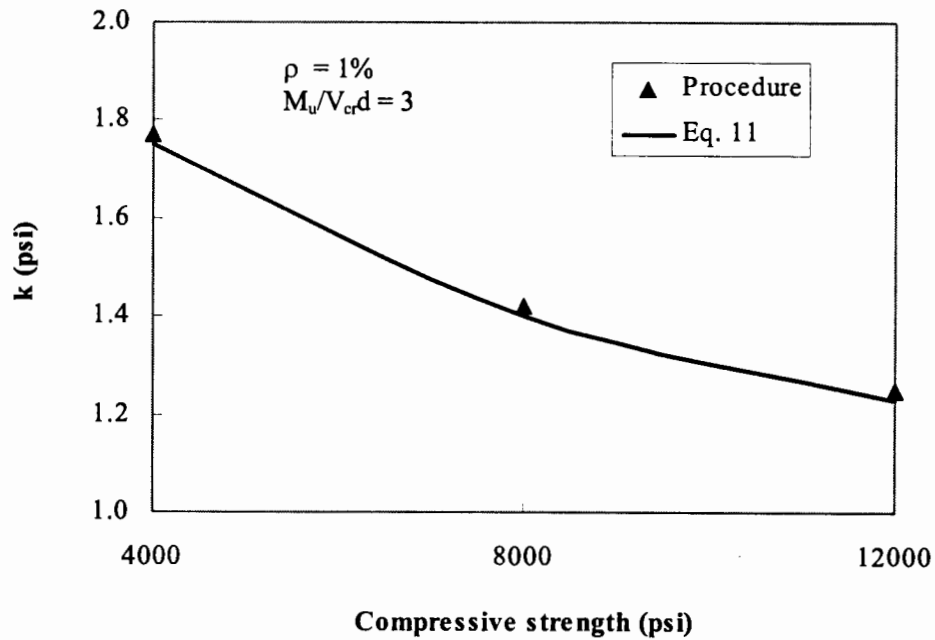


Fig. 8. Influence of concrete strength on shear strength

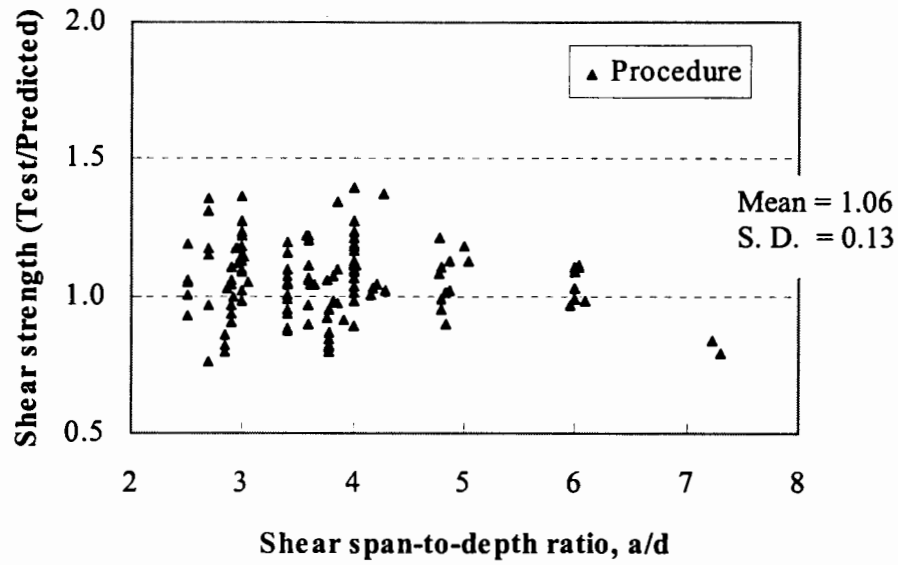


Fig. 9(a). Comparison of experimental results with proposed procedure - Influence of a/d ratio (Note: $M_u/V_{cr}d = a/d-1$ here)

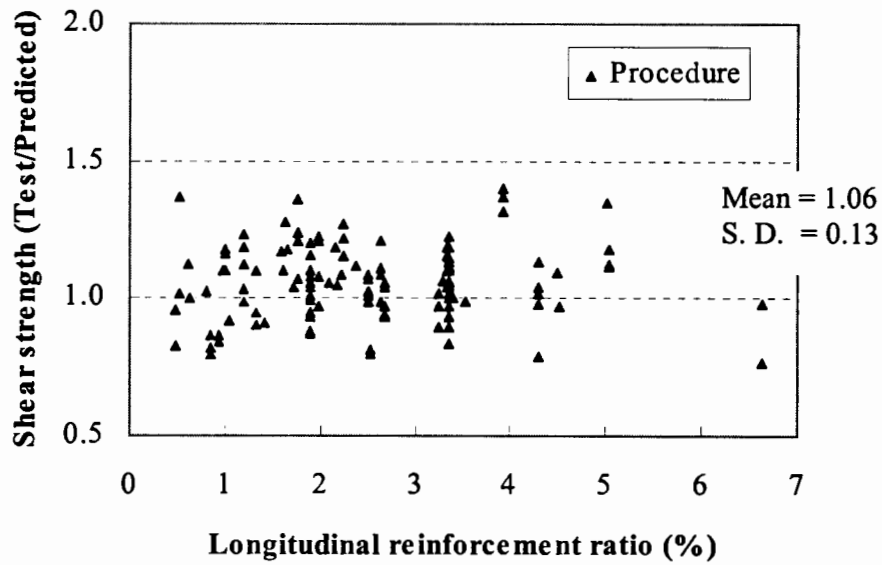


Fig.9(b). Comparison of experimental results with proposed procedure - Influence of longitudinal reinforcement ratio

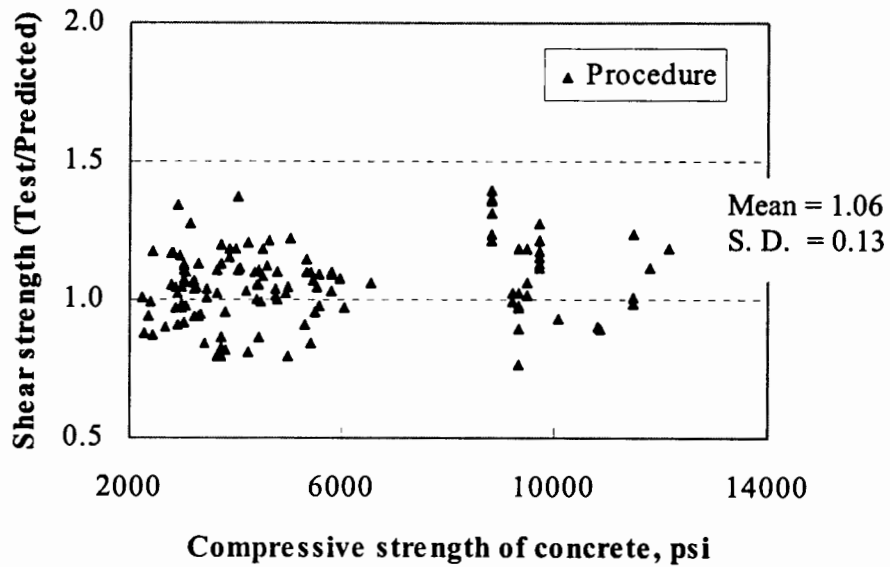


Fig. 9(c). Comparison of experimental results with proposed procedure - Influence of concrete strength

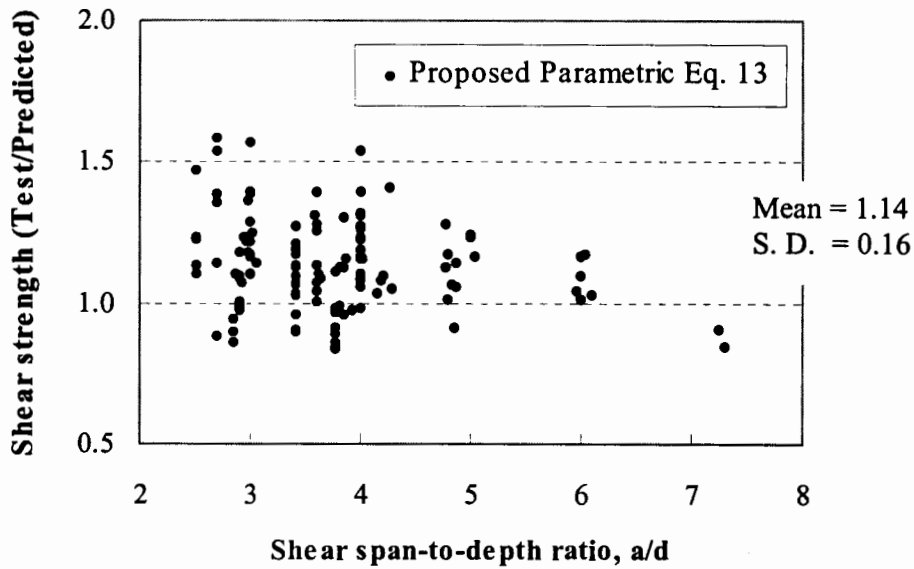


Fig.10(a). Comparison of experimental results with proposed parametric equation - Influence of a/d ratio

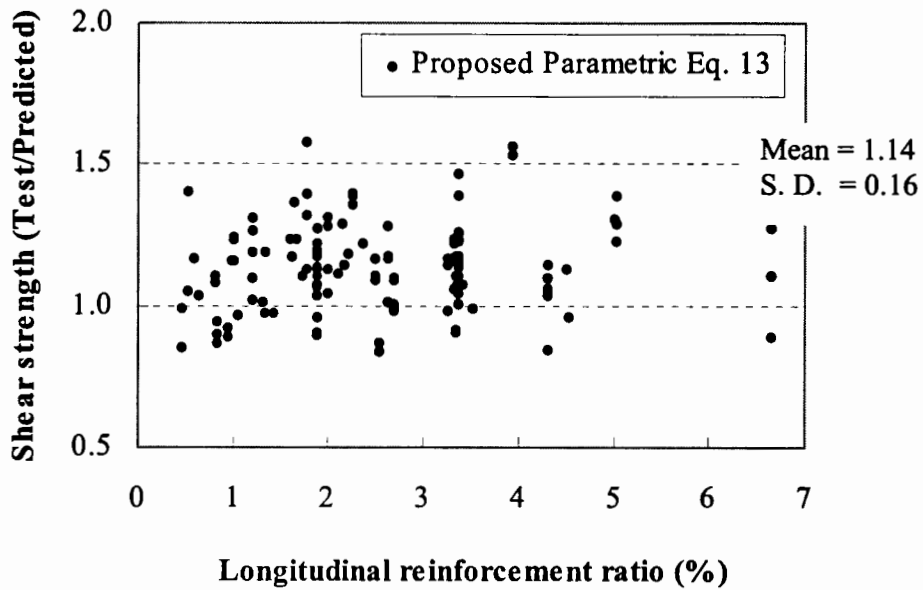


Fig.10(b). Comparison of experimental results with proposed parametric equation - Influence of longitudinal reinforcement ratio

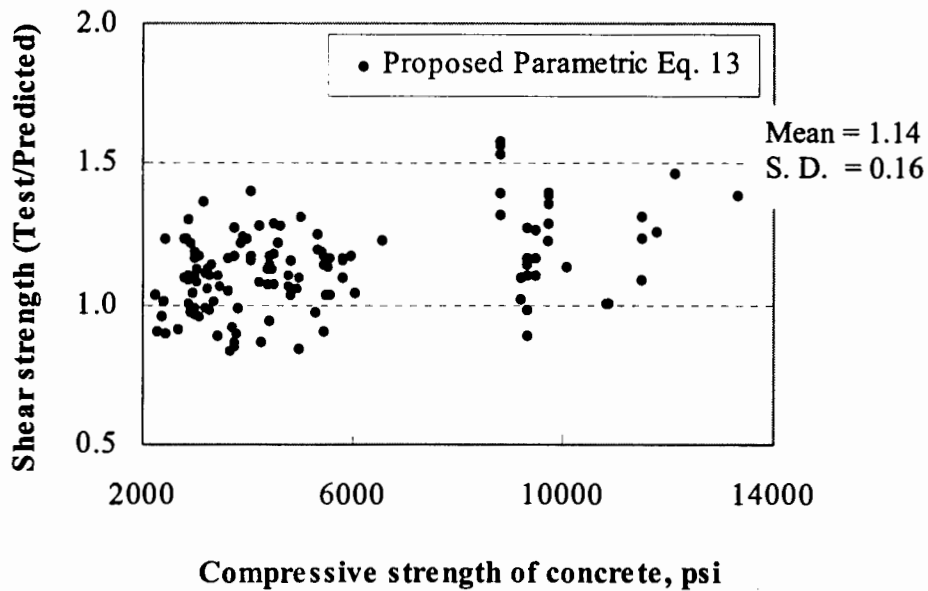


Fig.10(c). Comparison of experimental results with proposed parametric equation - Influence of concrete strength

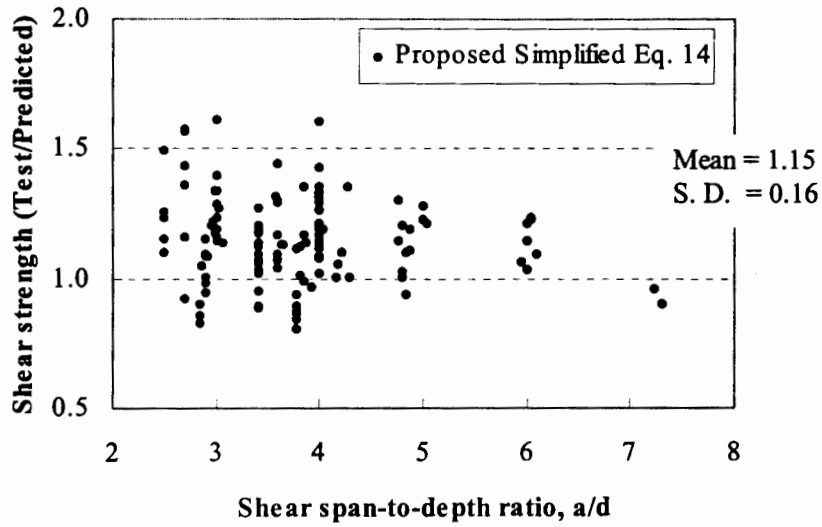


Fig.11(a). Comparison of experimental results with those predicted by proposed simplified equation - Influence of a/d ratio

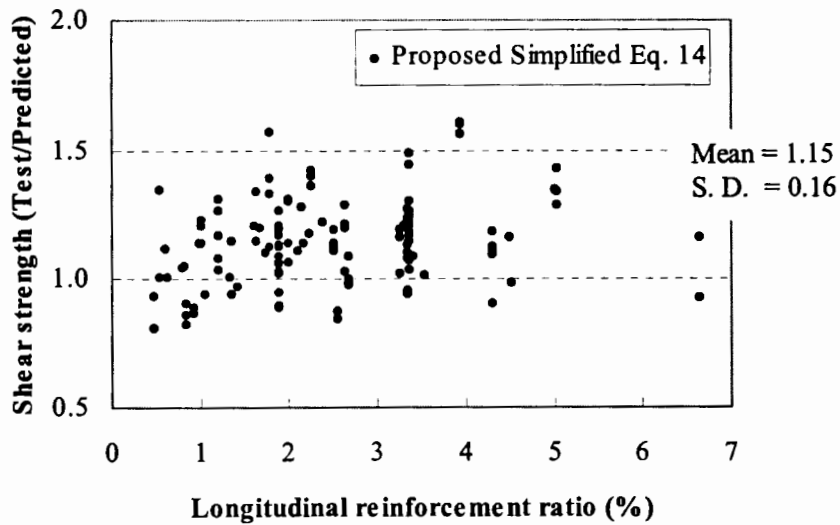


Fig.11(b). Comparison of experimental results with those predicted by proposed simplified equation - Influence of longitudinal reinforcement ratio

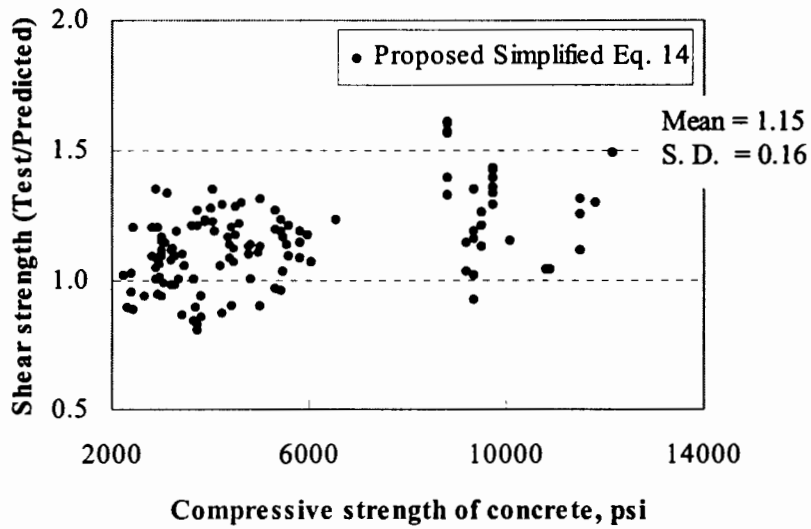


Fig.11(c). Comparison of experimental results with those predicted by proposed simplified equation - Influence of concrete strength

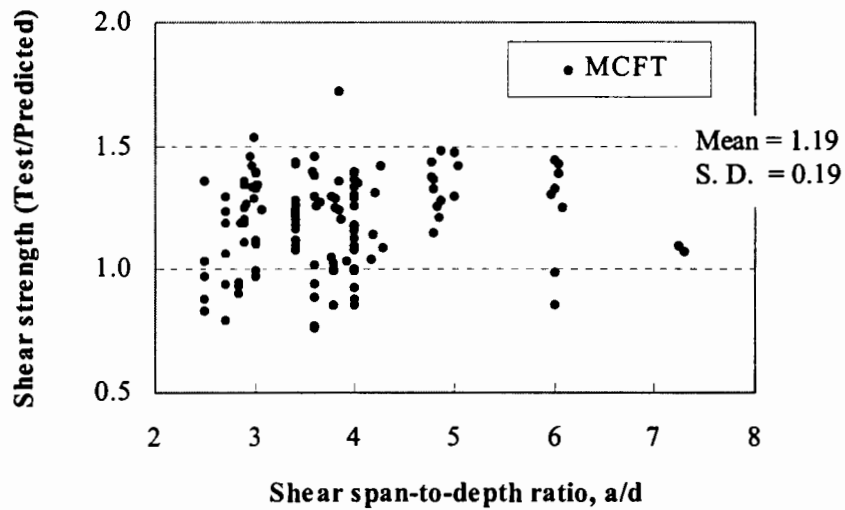


Fig. 12(a). Comparison of experimental results with those predicted by MCFT - Influence of a/d ratio

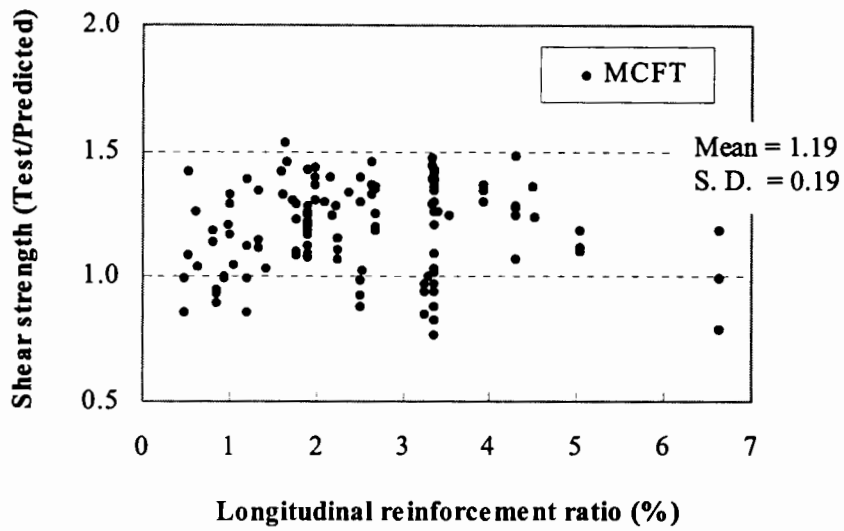


Fig.12(b). Comparison of experimental results with those predicted by MCFT - Influence of longitudinal reinforcement ratio

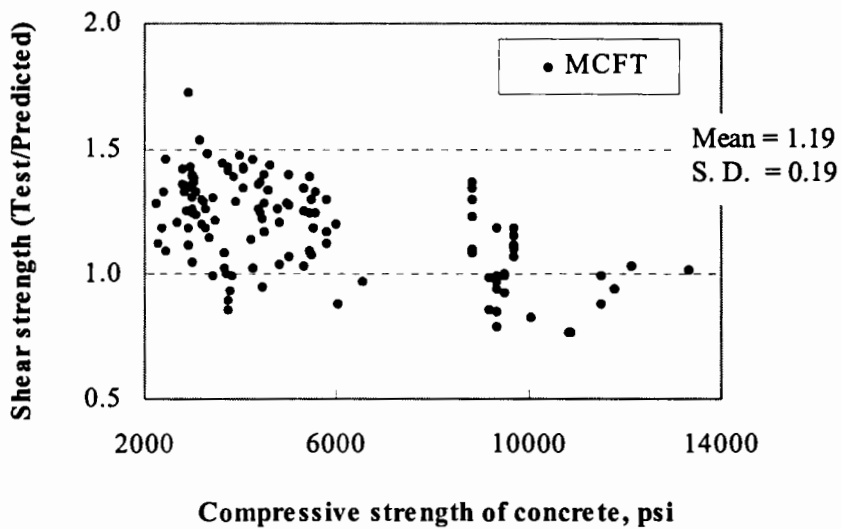


Fig.12(c). Comparison of experimental results with those predicted by MCFT - Influence of concrete strength

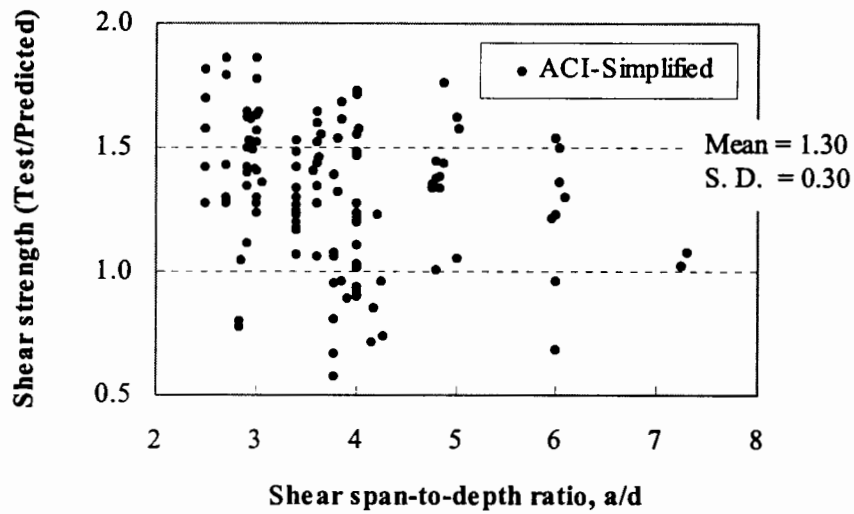


Fig.13(a). Comparison of experimental results with those predicted by ACI simplified equation - Influence of a/d ratio

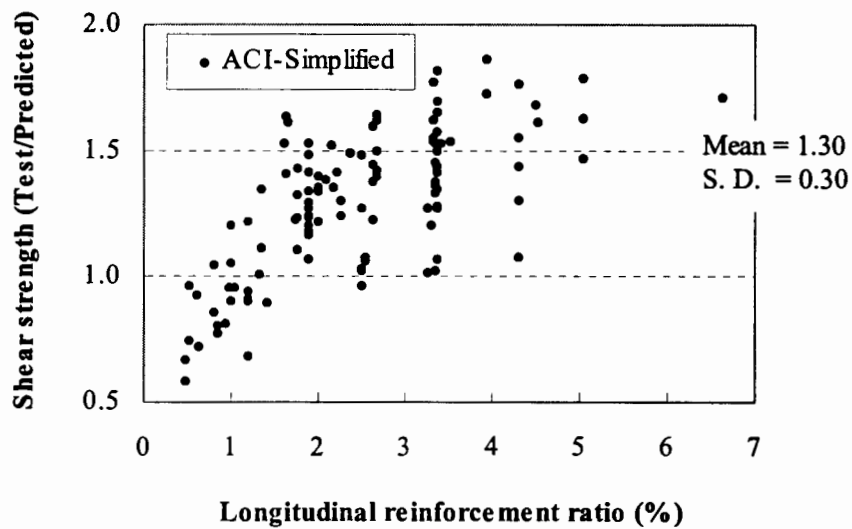


Fig.13(b). Comparison of experimental results with those predicted by ACI simplified equation - Influence of longitudinal reinforcement ratio

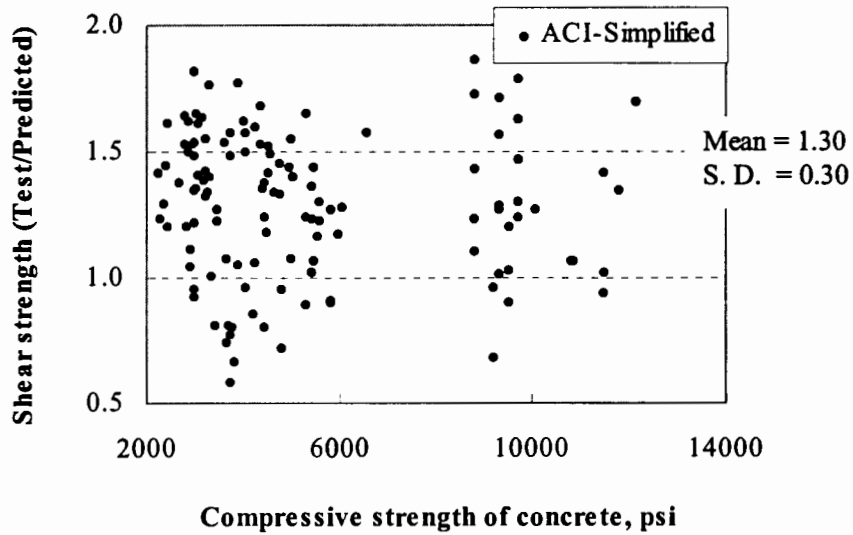


Fig.13(c). Comparison of experimental results with those predicted by ACI simplified equation - Influence of concrete strength

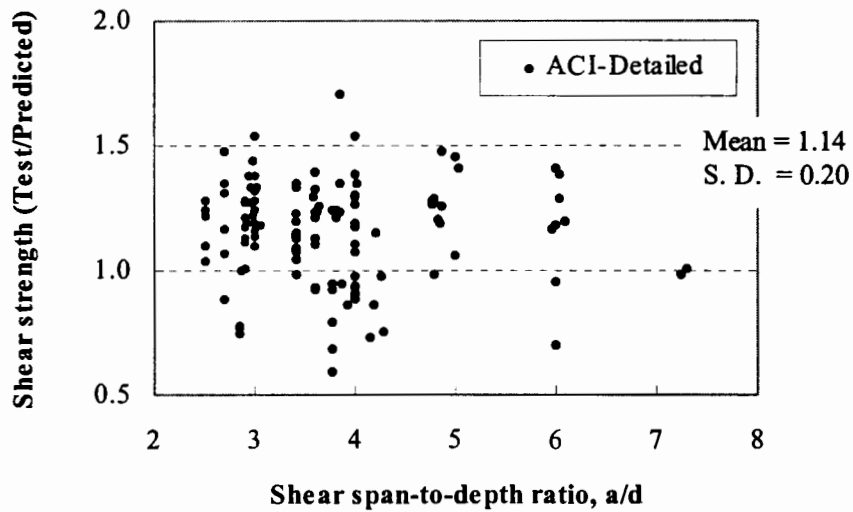


Fig.14(a). Comparison of experimental results with those predicted by ACI detailed equation - Influence of a/d ratio

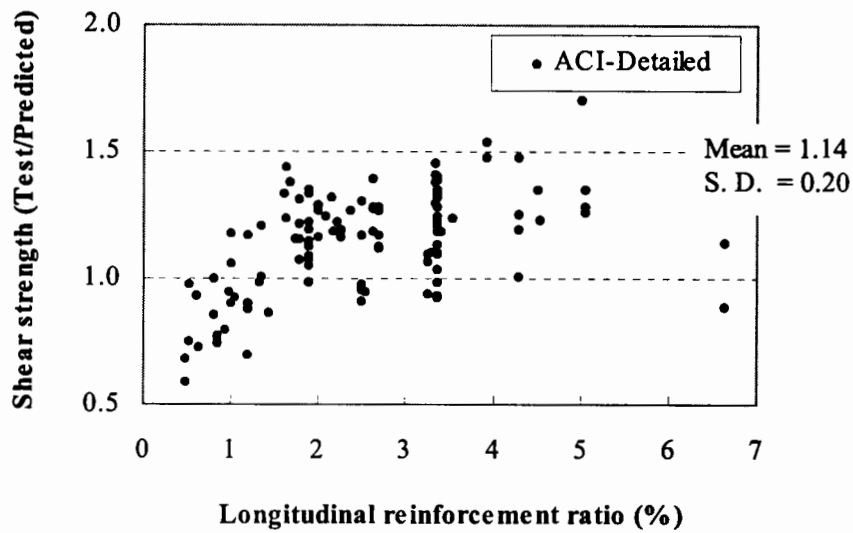


Fig.14(b). Comparison of experimental results with those predicted by ACI detailed equation - Influence of longitudinal reinforcement ratio

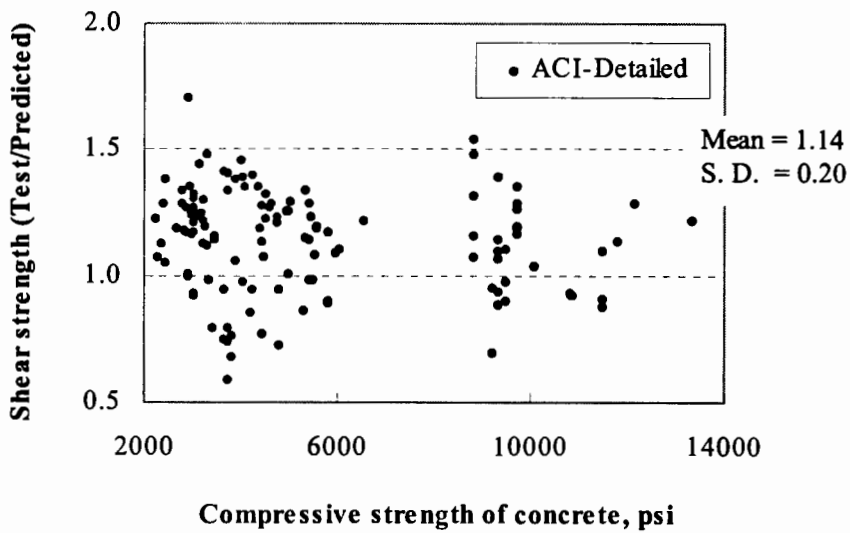


Fig.14(c). Comparison of experimental results with those predicted by ACI detailed equation - Influence of concrete strength

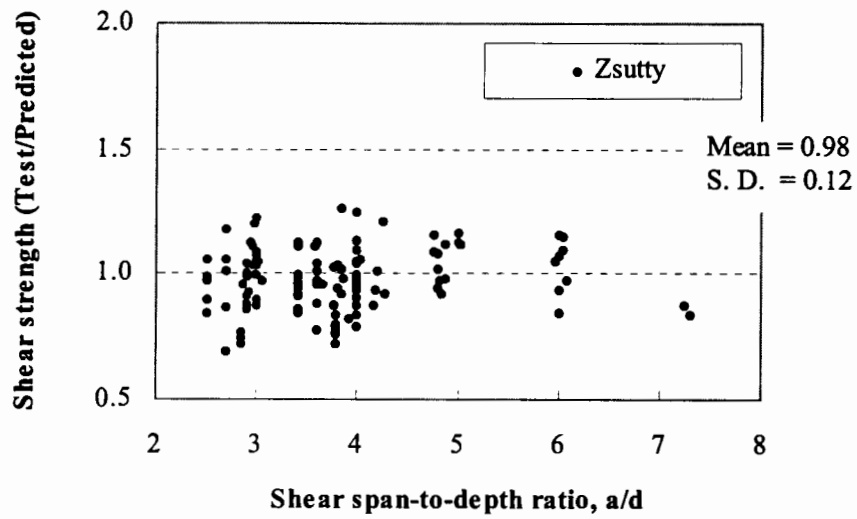


Fig.15(a). Comparison of experimental results with those predicted by Zsutty's equation - Influence of a/d ratio

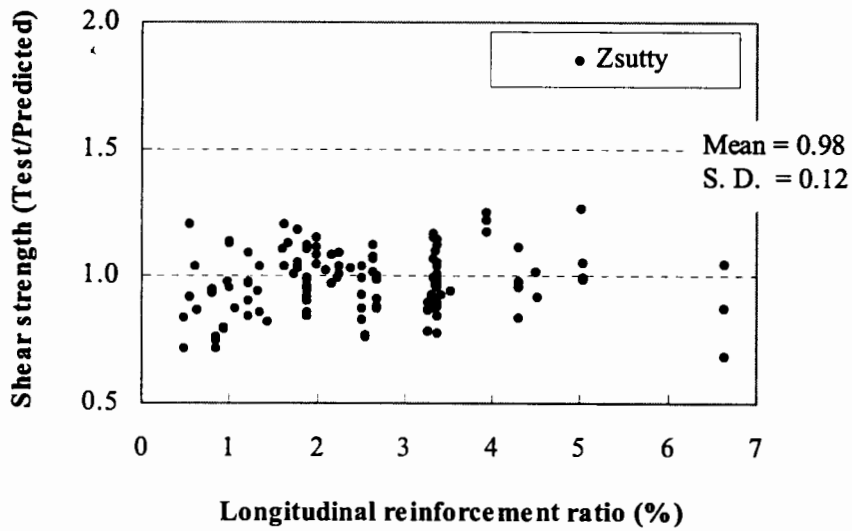


Fig.15(b). Comparison of experimental results with those predicted by Zsutty's equation - Influence of longitudinal reinforcement ratio

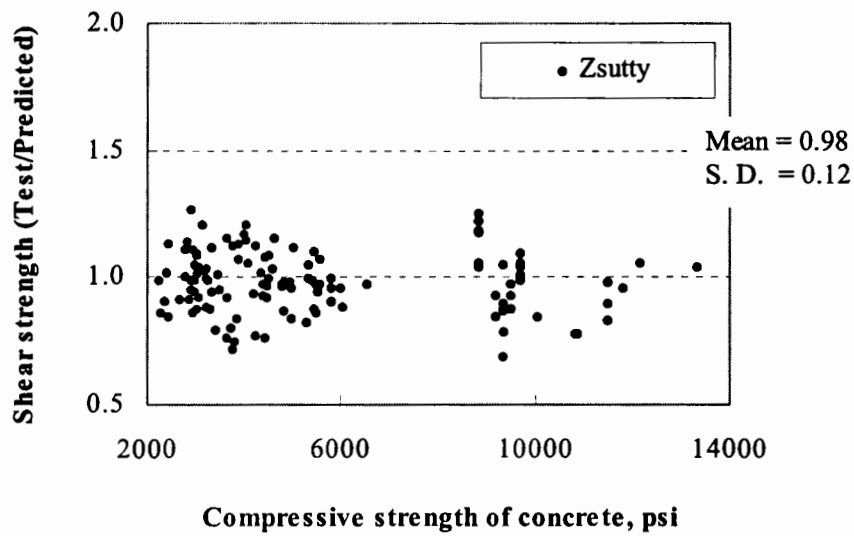


Fig.15(c). Comparison of experimental results with those predicted by Zsutty's equation - Influence of concrete strength

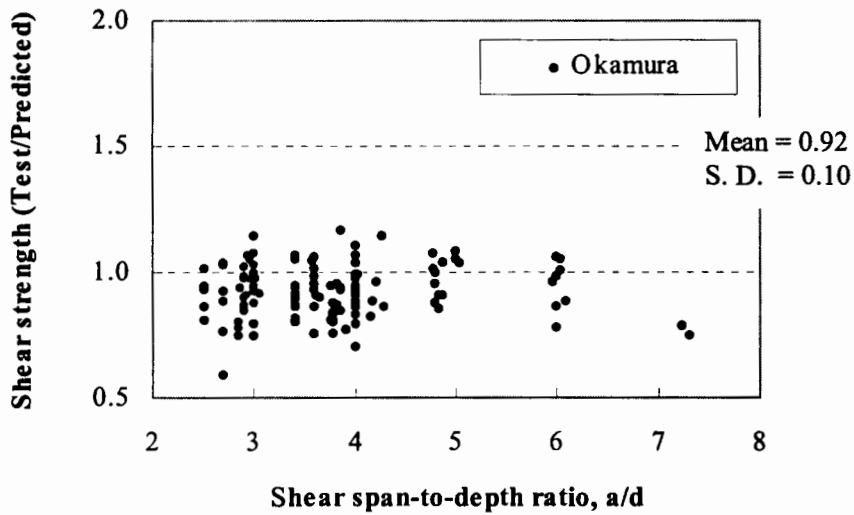


Fig.16(a). Comparison of experimental results with those predicted by Okamura's equation - Influence of a/d ratio

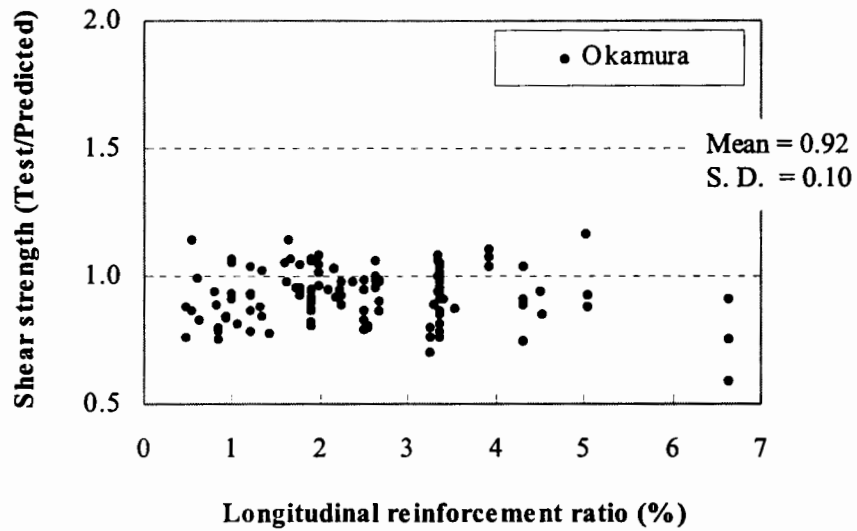


Fig.16(b). Comparison of experimental results with those predicted by Okamura's equation - Influence of longitudinal reinforcement ratio

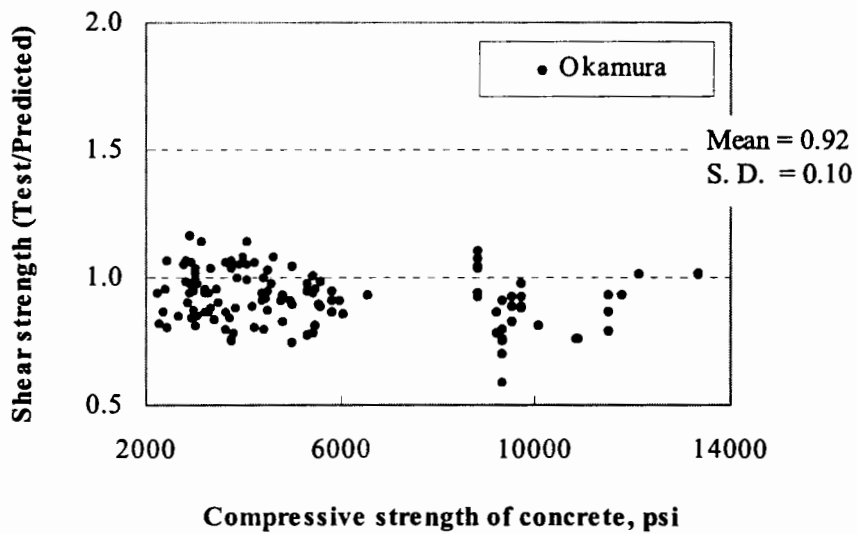


Fig.16(c). Comparison of experimental results with those predicted by Okamura's equation - Influence of concrete strength

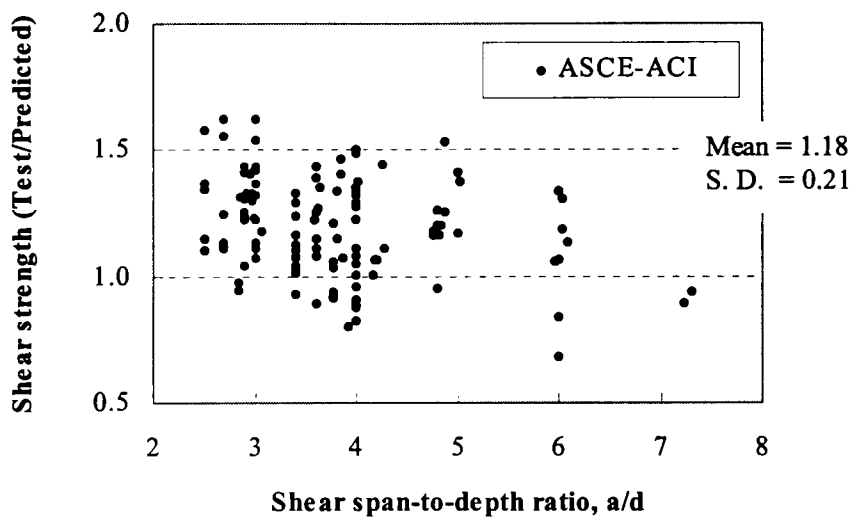


Fig.17(a). Comparison of experimental results with those predicted by ASCE-ACI equation - Influence of a/d ratio

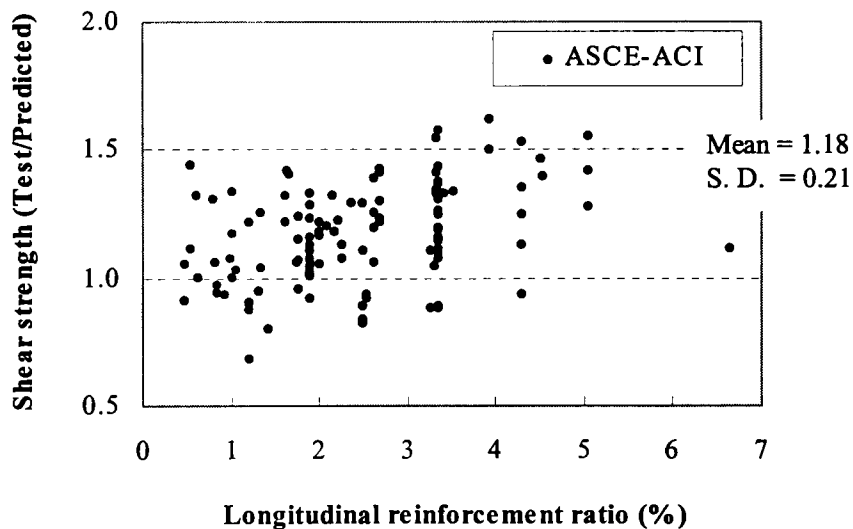


Fig.17(b). Comparison of experimental results with those predicted by ASCE-ACI equation - Influence of longitudinal reinforcement ratio

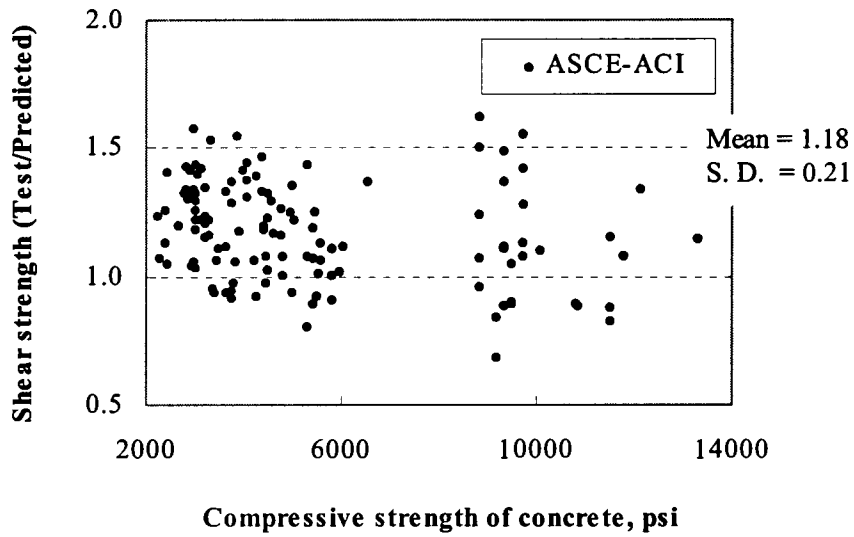


Fig.17(c). Comparison of experimental results with those predicted by ASCE-ACI equation - Influence of concrete strength

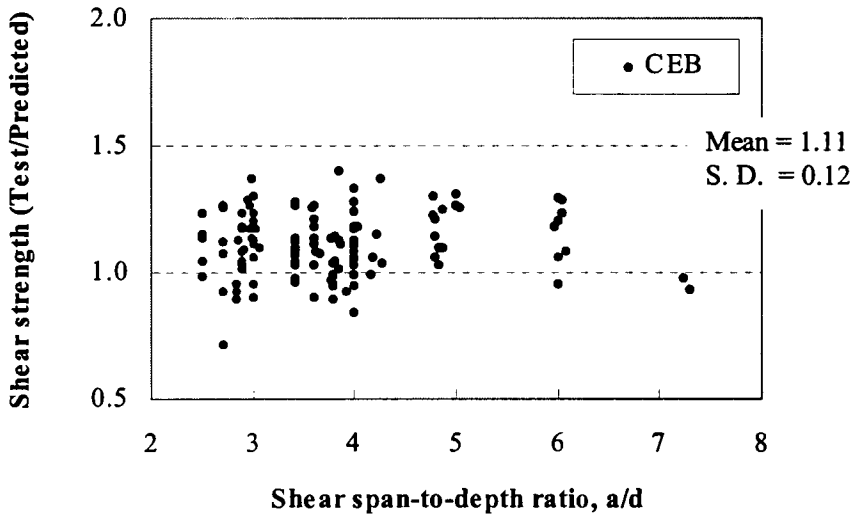


Fig.18(a). Comparison of experimental results with those predicted by CEB method - Influence of a/d ratio

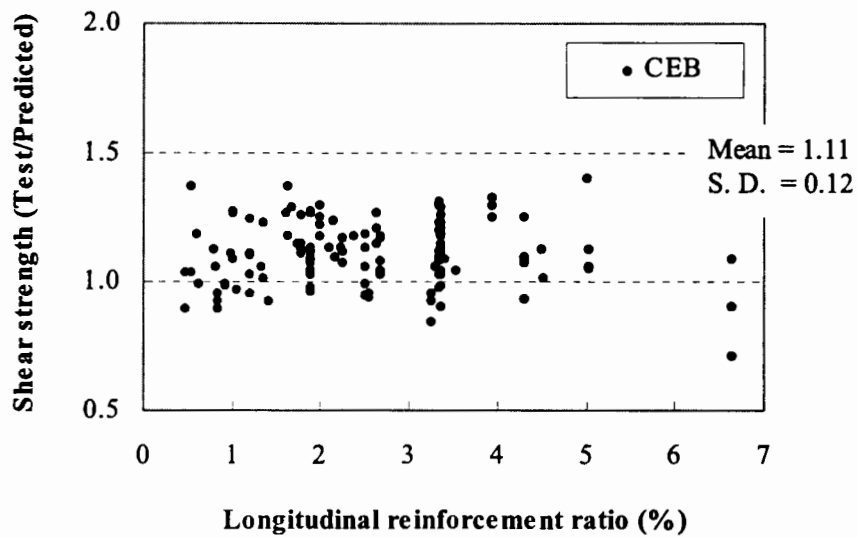


Fig.18(b). Comparison of experimental results with those predicted by CEB method - Influence of longitudinal reinforcement ratio

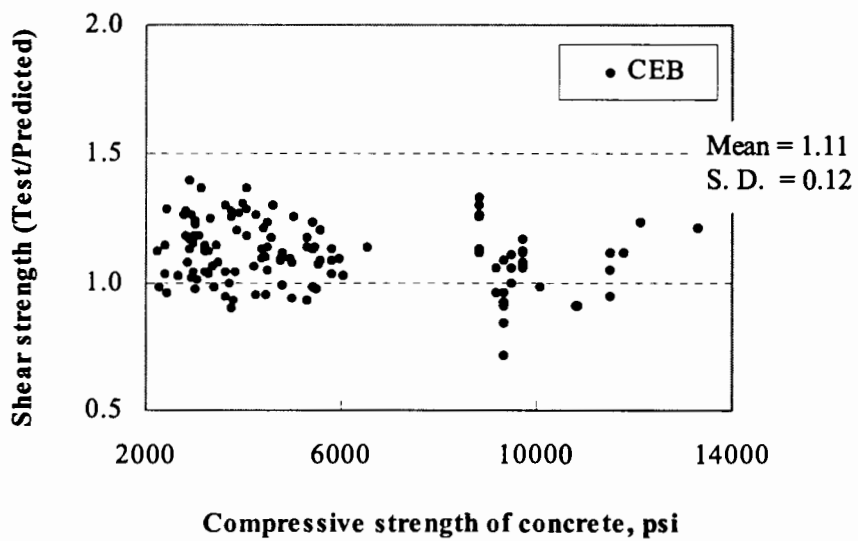


Fig.18(c). Comparison of experimental results with those predicted by CEB method - Influence of concrete strength

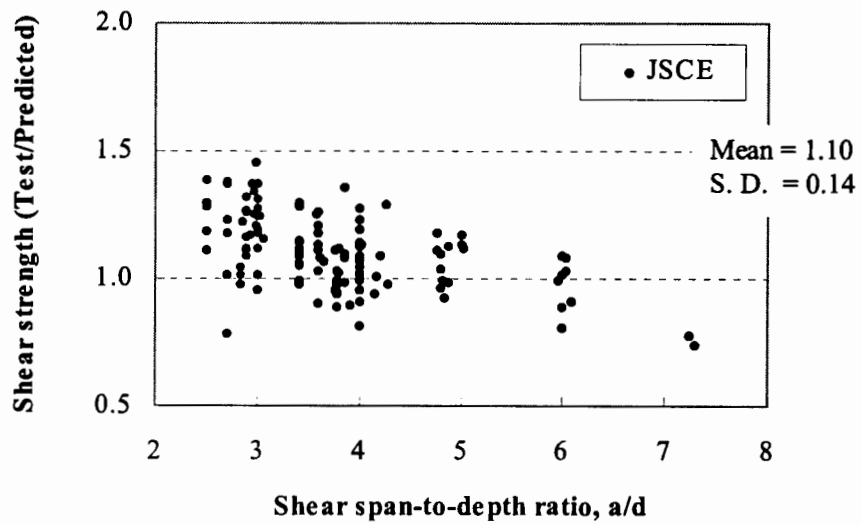


Fig.19(a). Comparison of experimental results with those predicted by JSCE method - Influence of a/d ratio

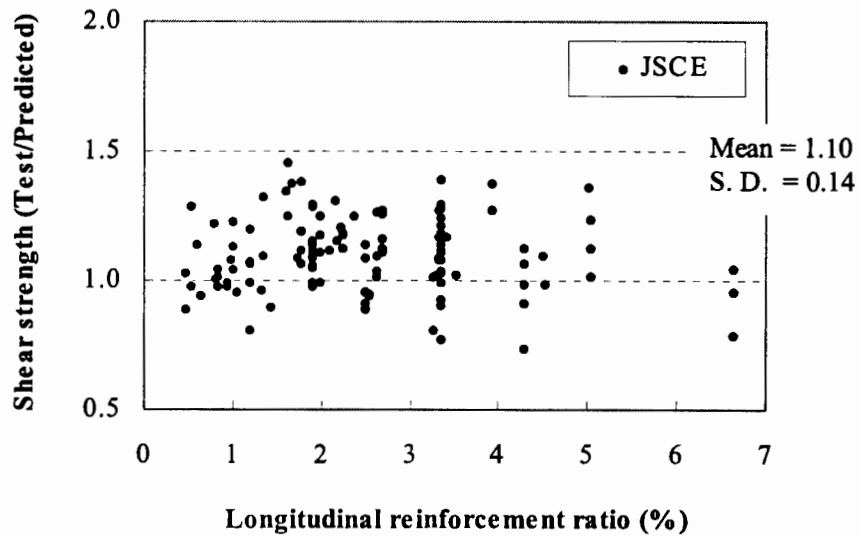


Fig.19(b). Comparison of experimental results with those predicted by JSCE method - Influence of longitudinal reinforcement ratio

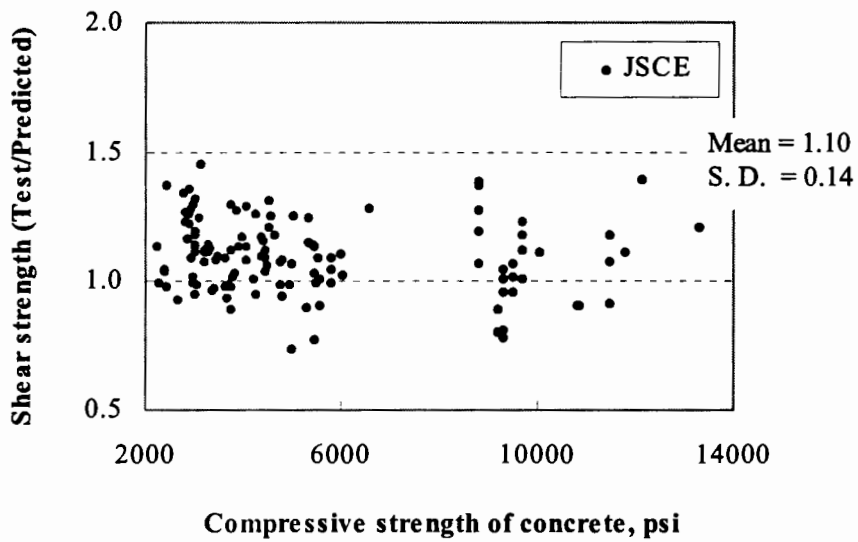


Fig.19(c). Comparison of experimental results with those predicted by JSCE method - Influence of concrete strength

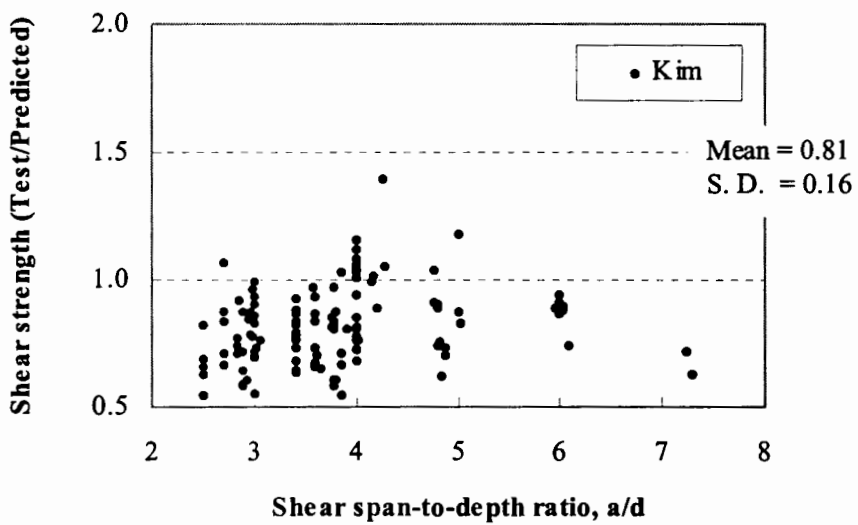


Fig.20(a). Comparison of experimental results with those predicted by Kim's equation - Influence of a/d ratio

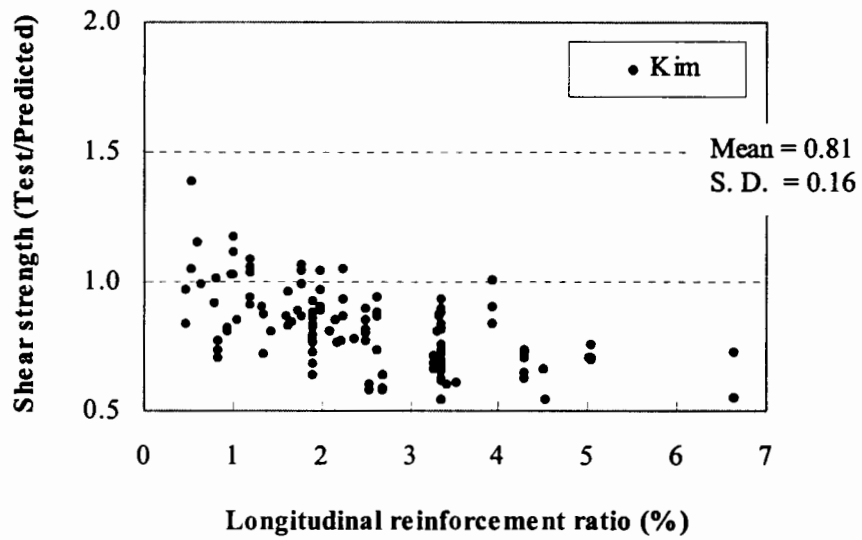


Fig.20(b). Comparison of experimental results with those predicted by Kim's equation - Influence of longitudinal reinforcement ratio

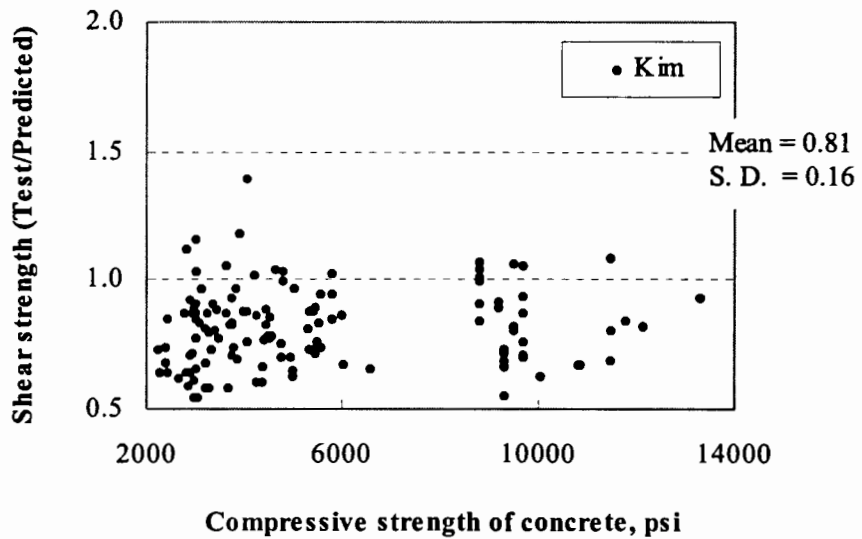


Fig.20(c). Comparison of experimental results with those predicted by Kim's equation - Influence of concrete strength

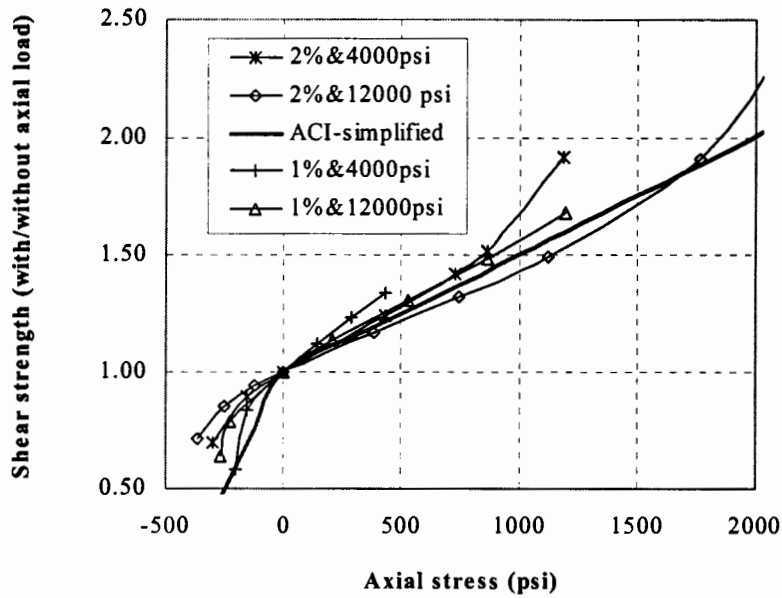


Fig. 21. Influence of axial stress on shear strength (Note: In figure, the legend 2%&4000psi indicates that $\rho = 2\%$ and $f'_c = 4000$ psi)

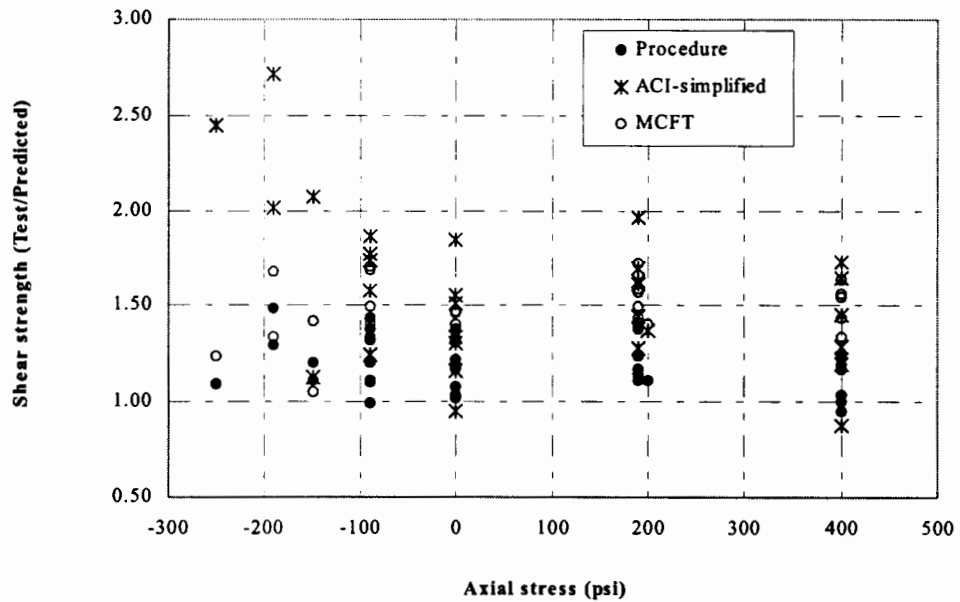


Fig. 22. Comparison of test results with those predicted by ACI, MCFT and proposed two-step procedure - Influence of axial stress on shear strength

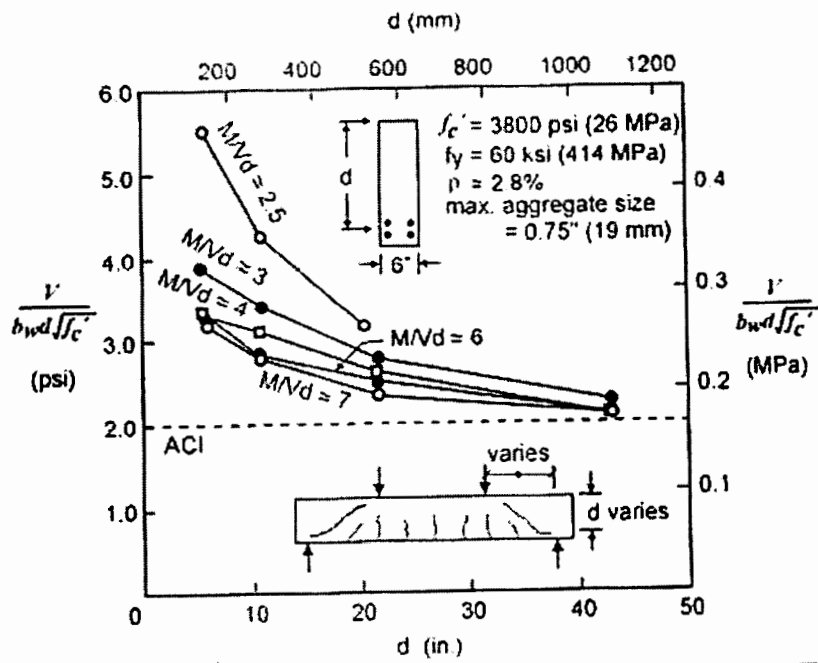


Fig. 23. Kani's test data on size effects in shear (Kani 1967)

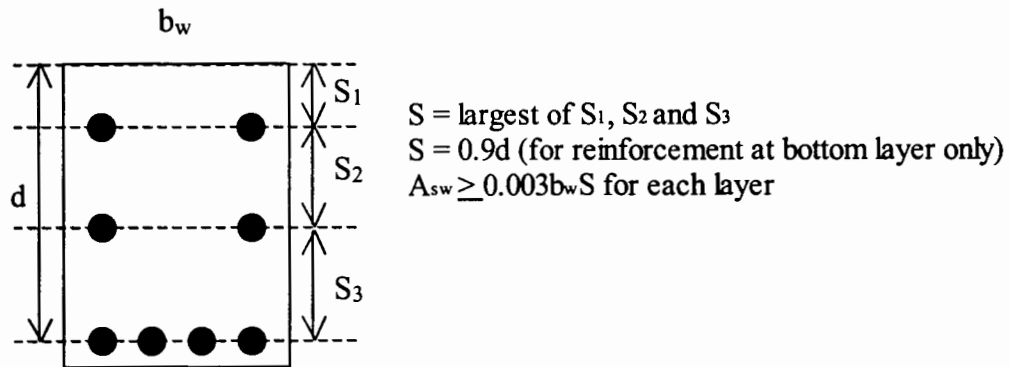


Fig. 24. Beam section with longitudinal web reinforcement in several layers

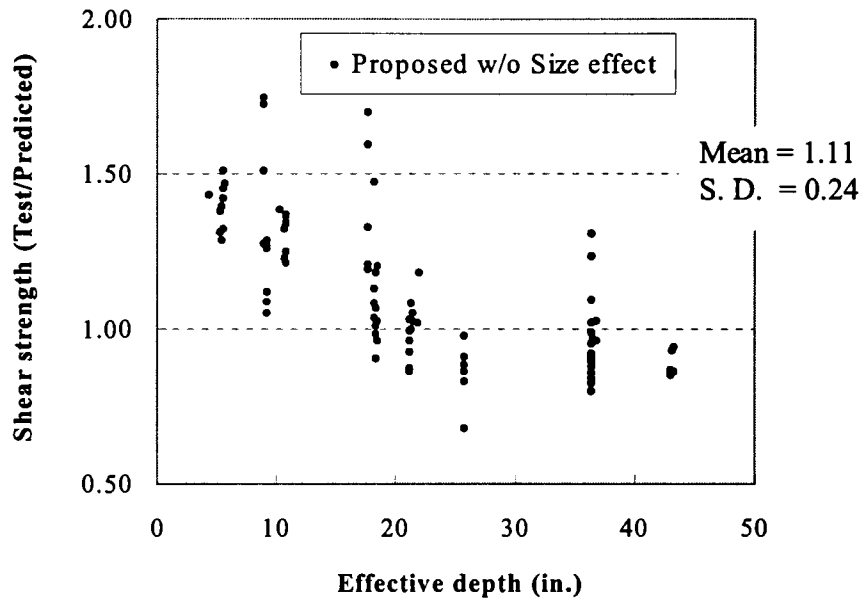


Fig. 25. Comparison of experimental results with those predicted by proposed simplified equation (Eq. 14) without size effect

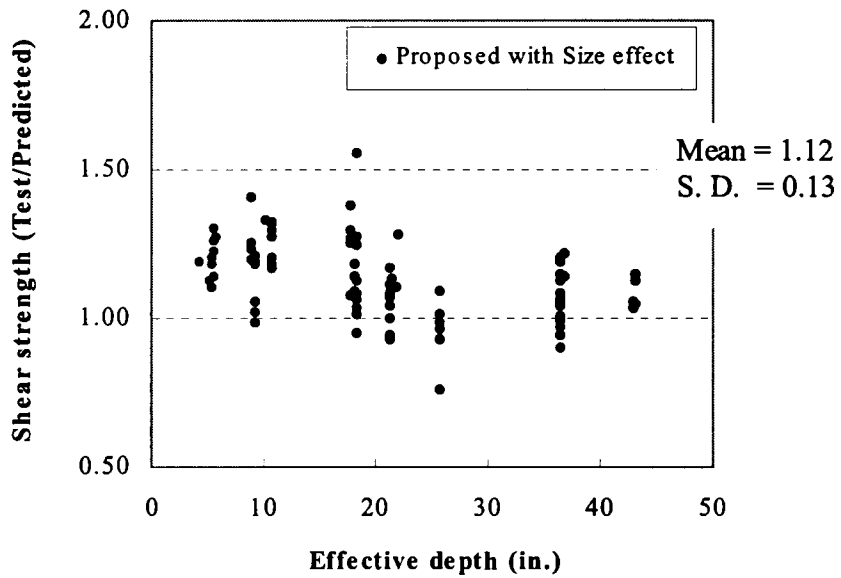


Fig. 26. Comparison of experimental results with those predicted by proposed simplified equation with size effect (Eq. 18)

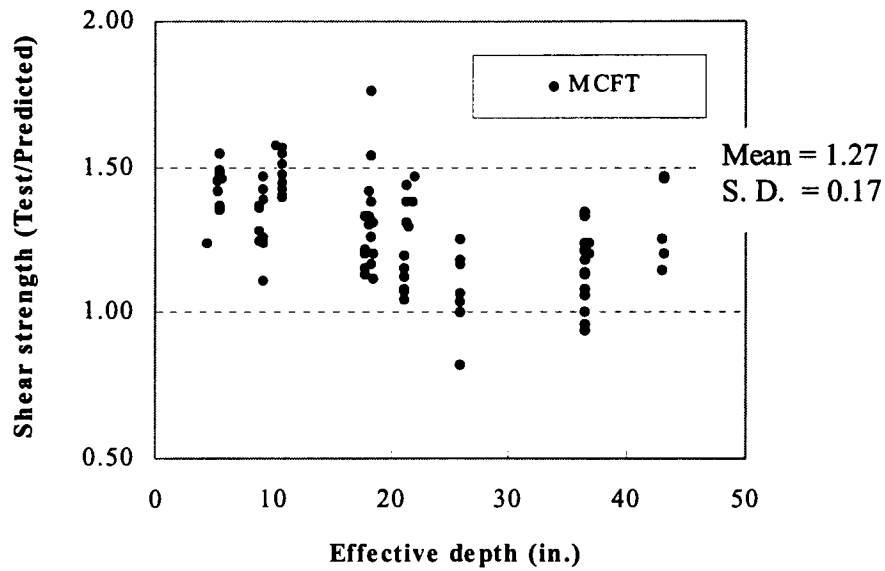


Fig. 27. Comparison of experimental results with those predicted by MCFT

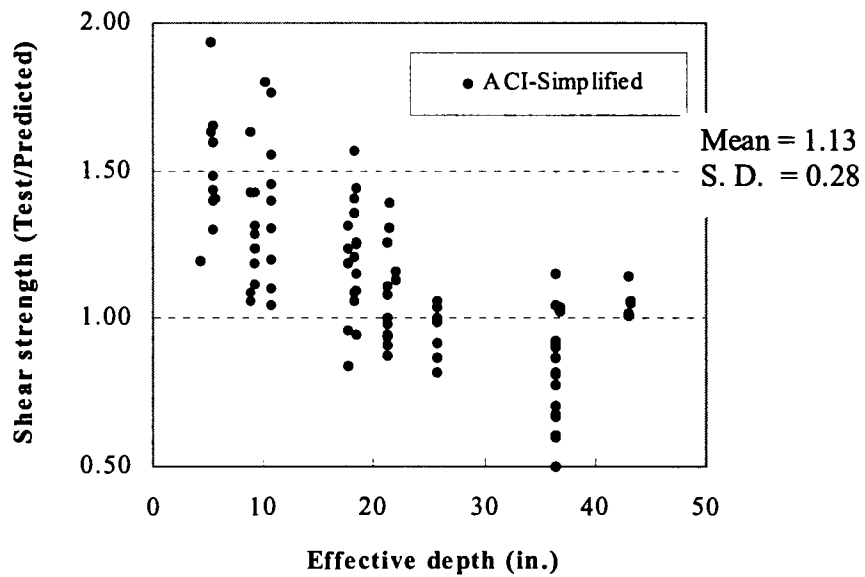


Fig. 28. Comparison of experimental results with those predicted by ACI simplified equation

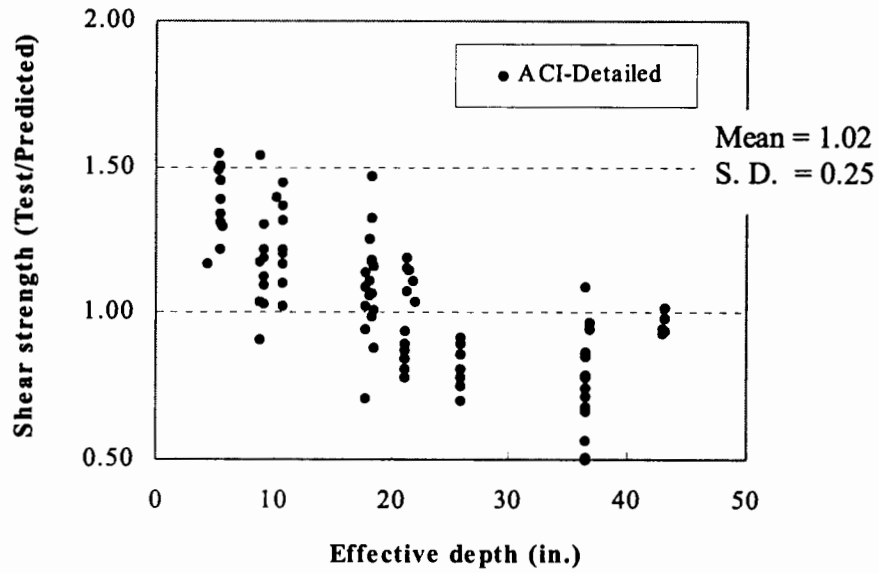


Fig. 29. Comparison of experimental results with those predicted by ACI detailed equation

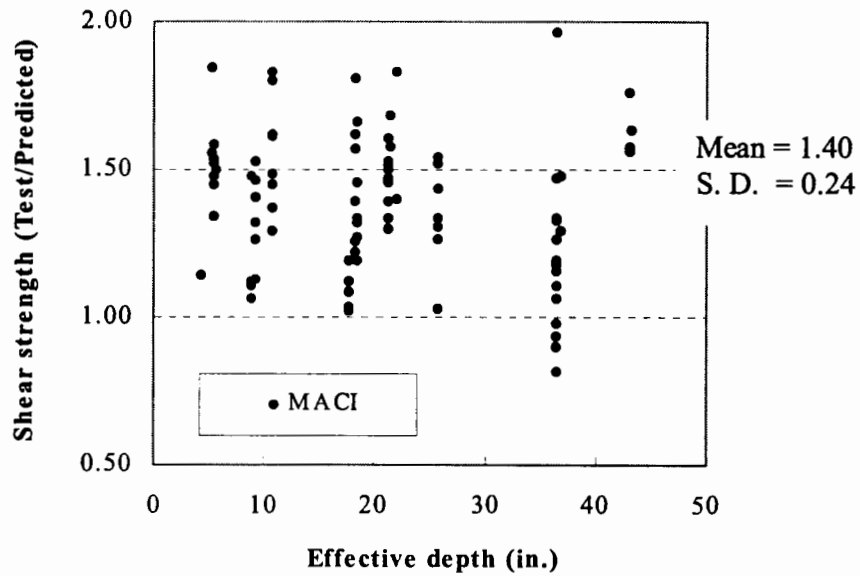


Fig. 30. Comparison of experimental results with those predicted by Modified ACI equation

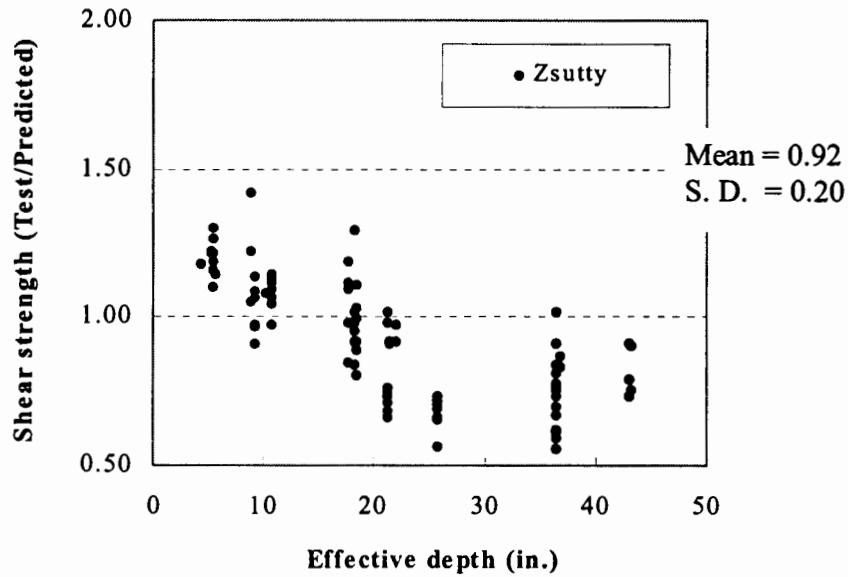


Fig. 31. Comparison of experimental results with those predicted by Zsutty's equation

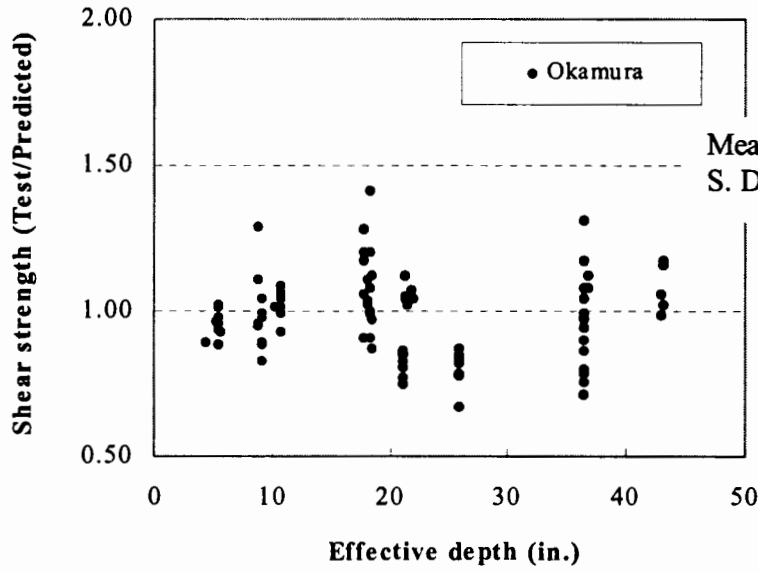


Fig. 32. Comparison of experimental results with those predicted by Okamura's equation

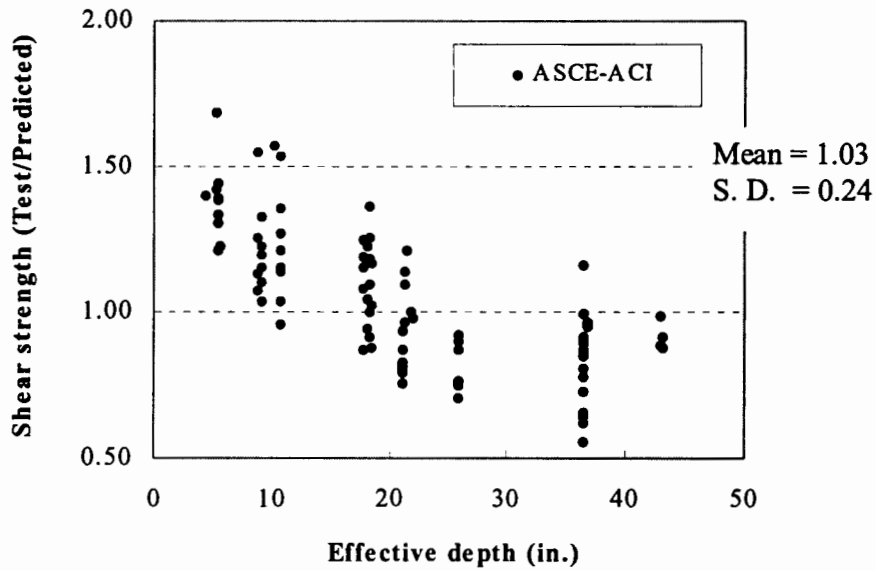


Fig. 33. Comparison of experimental results with those predicted by ASCE-ACI equation

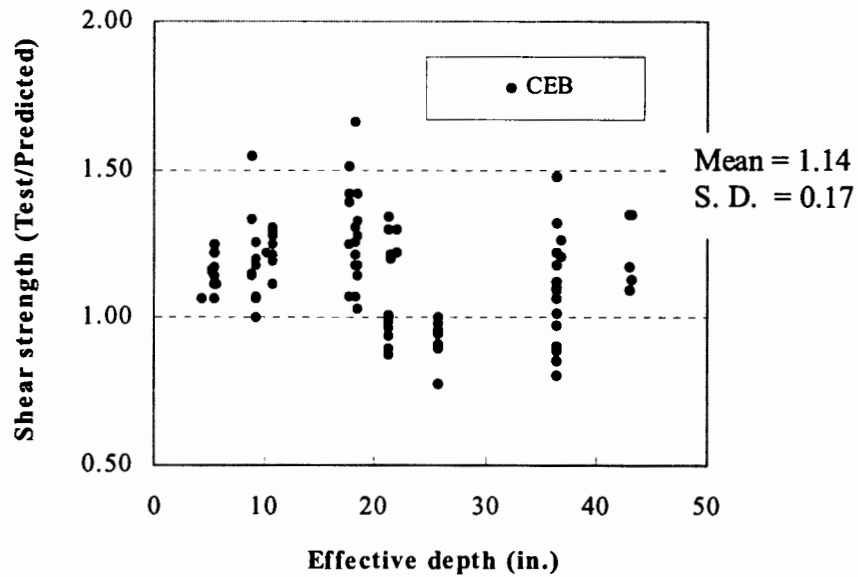


Fig. 34. Comparison of experimental results with those predicted by CEB method

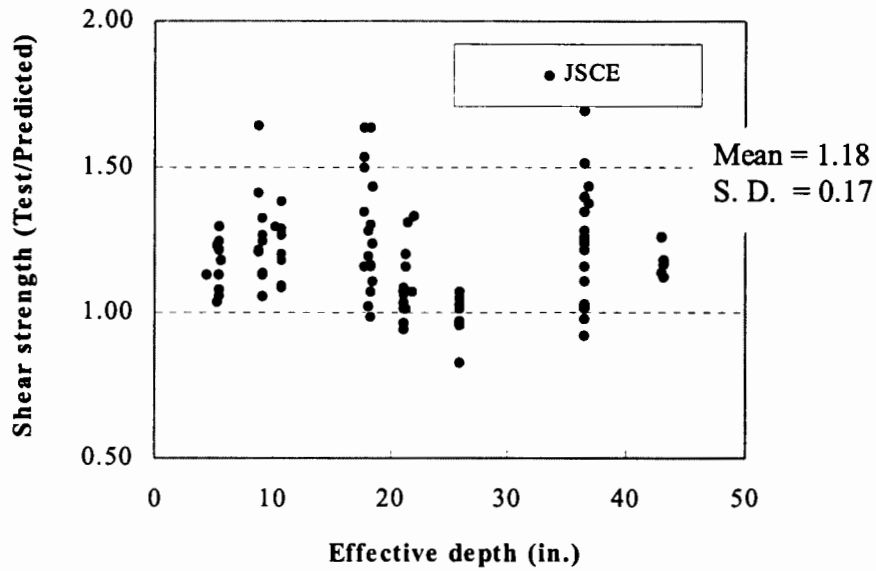


Fig. 35. Comparison of experimental results with those predicted by JSCE method

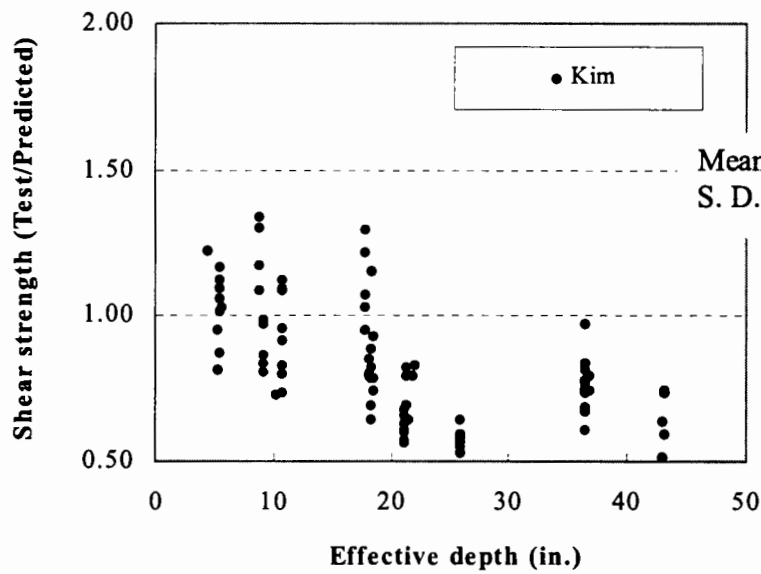


Fig. 36. Comparison of experimental results with those predicted by Kim's equation

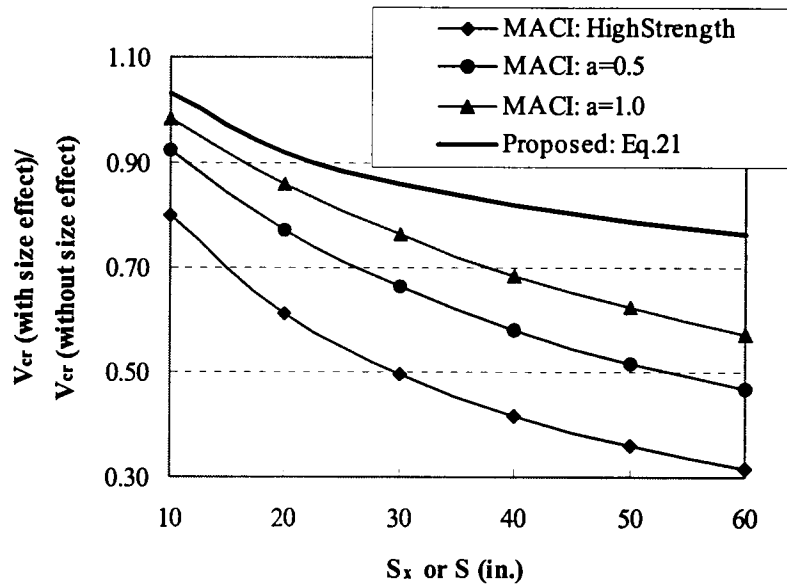
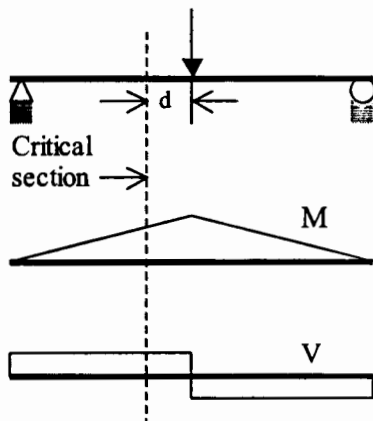
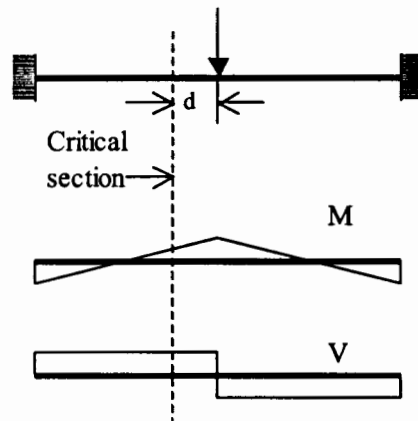


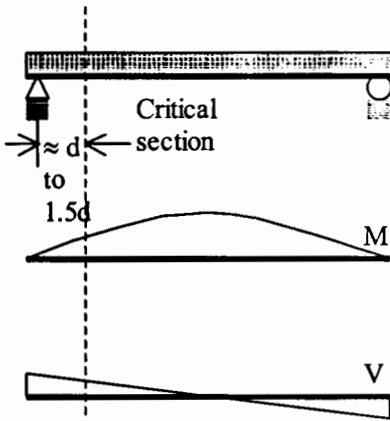
Fig. 37. Comparison of proposed simplified equation (Eq. 21) with MACI equation for size effect (Note: “a” = maximum aggregate size; a = 0 for high strength concrete)



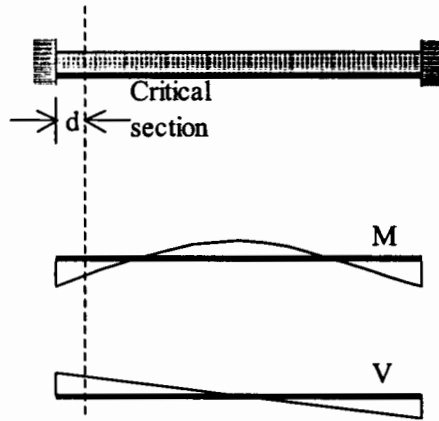
(a)



(c)

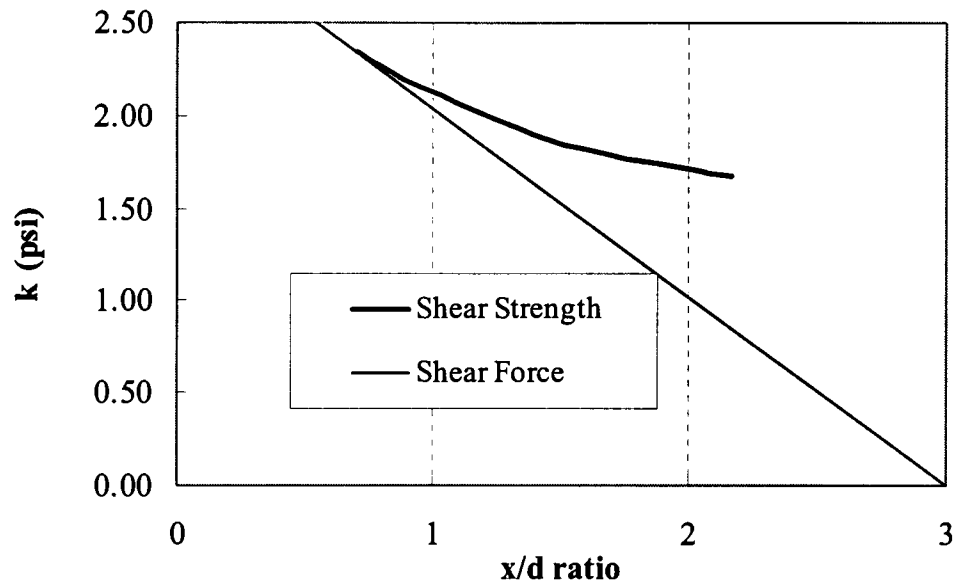


(b)

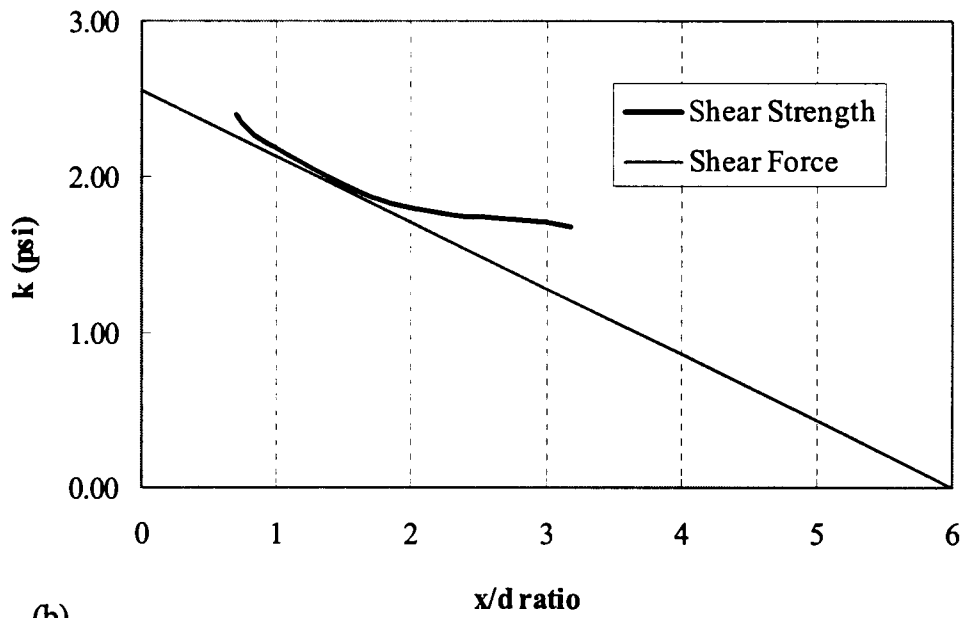


(d)

Fig. 38. Location of critical section for beams with pinned and fixed supports under point and uniform loading: (a) Simply supported beam under point loading; (c) Fixed beam under point loading; (c) Simply supported beam under uniform loading; (d) Fixed beam under uniform loading



(a)



(b)

Fig. 39. Influence of span-to-depth (L/d) ratio on location of critical section under uniform loading: (a) $L/d = 6$; (b) $L/d = 12$

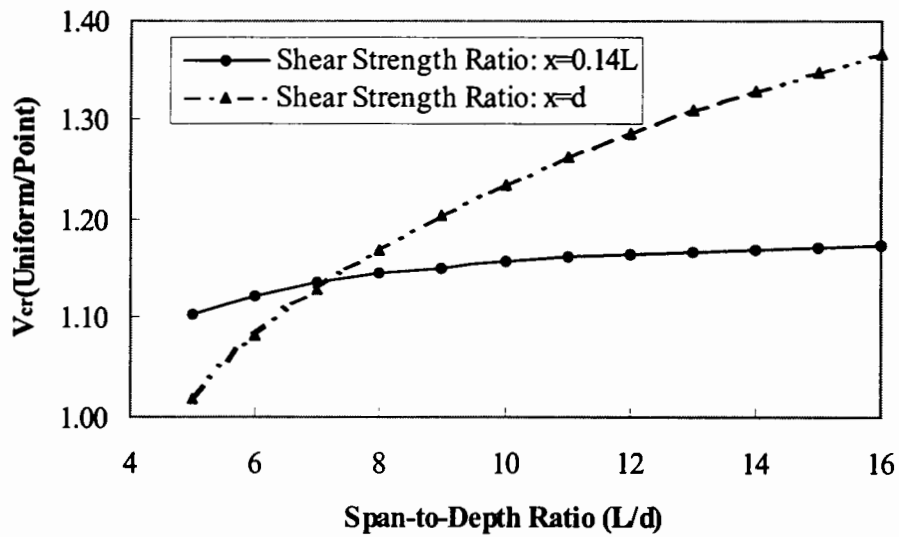


Fig. 40. Influence of type of loading on cracking shear strength

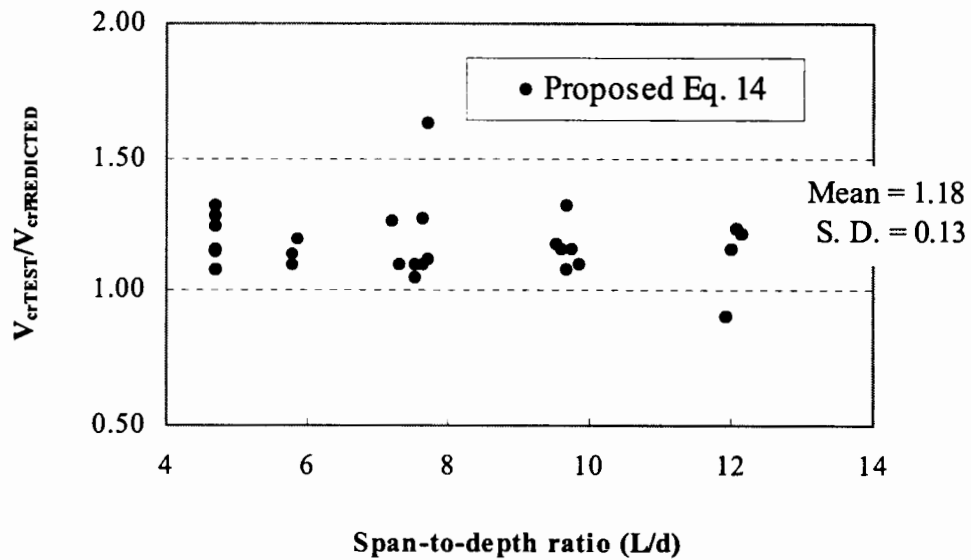


Fig. 41. Comparison of experimental results with those predicted using proposed simplified equation without size effects

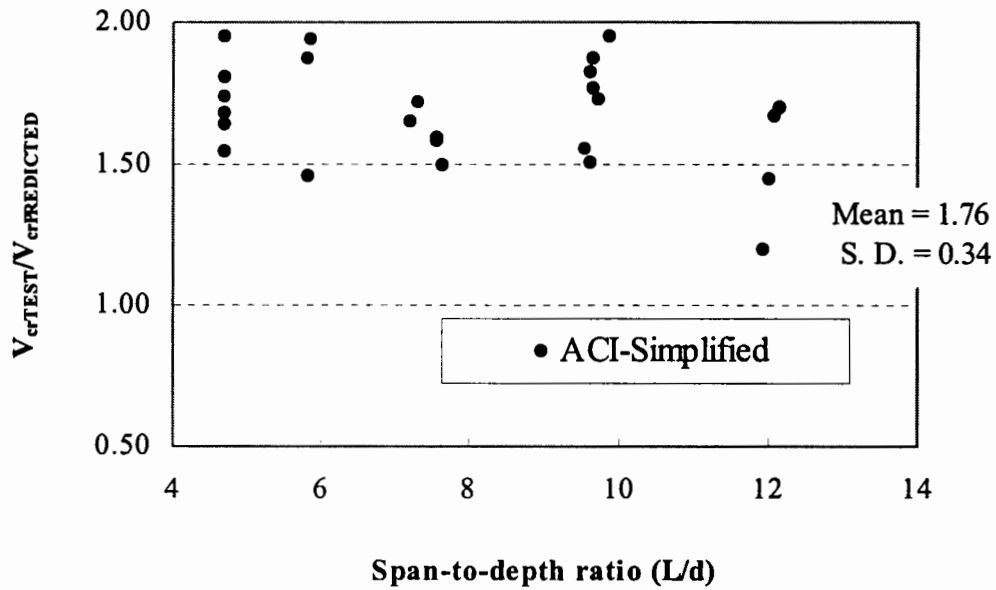


Fig. 42. Comparison of experimental results with those predicted using ACI simplified equation

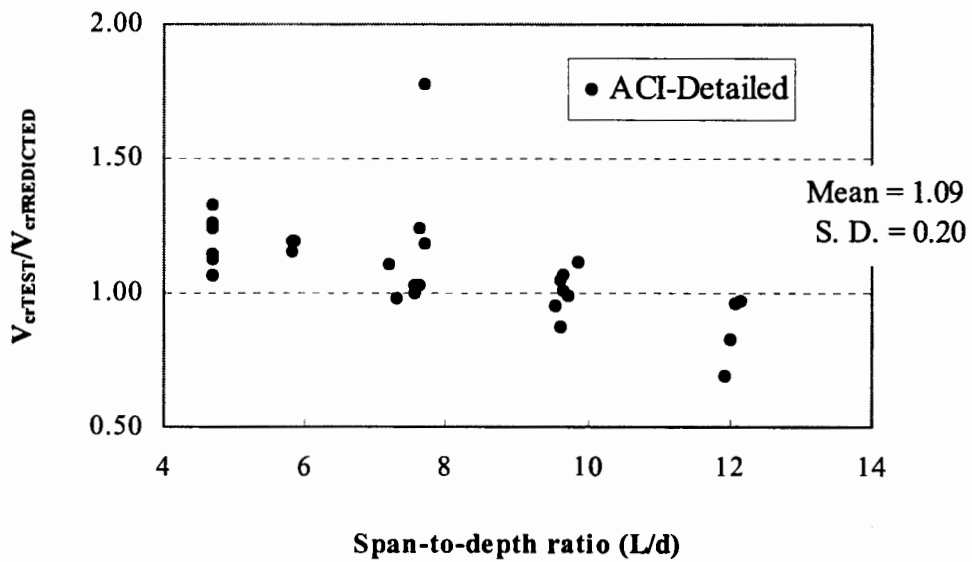


Fig. 43. Comparison of experimental results with those predicted using ACI detailed equation

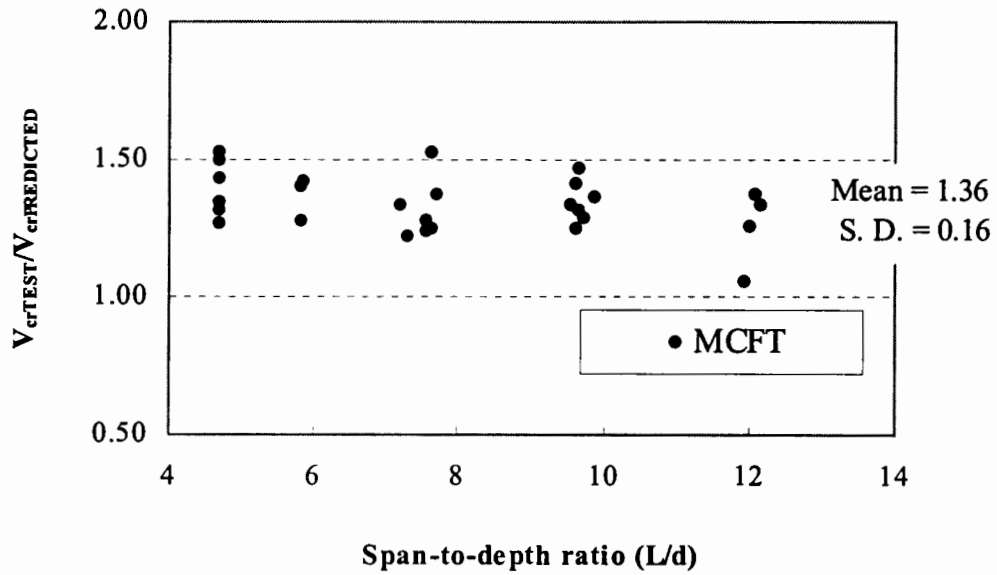


Fig. 44. Comparison of experimental results with those predicted using MCFT

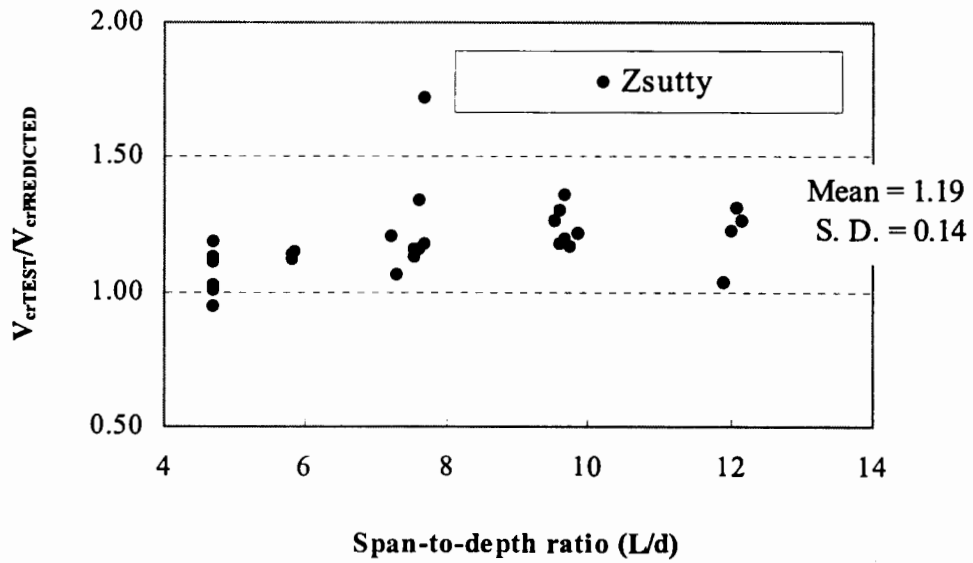


Fig. 45. Comparison of experimental results with those predicted using Zsutty's equation

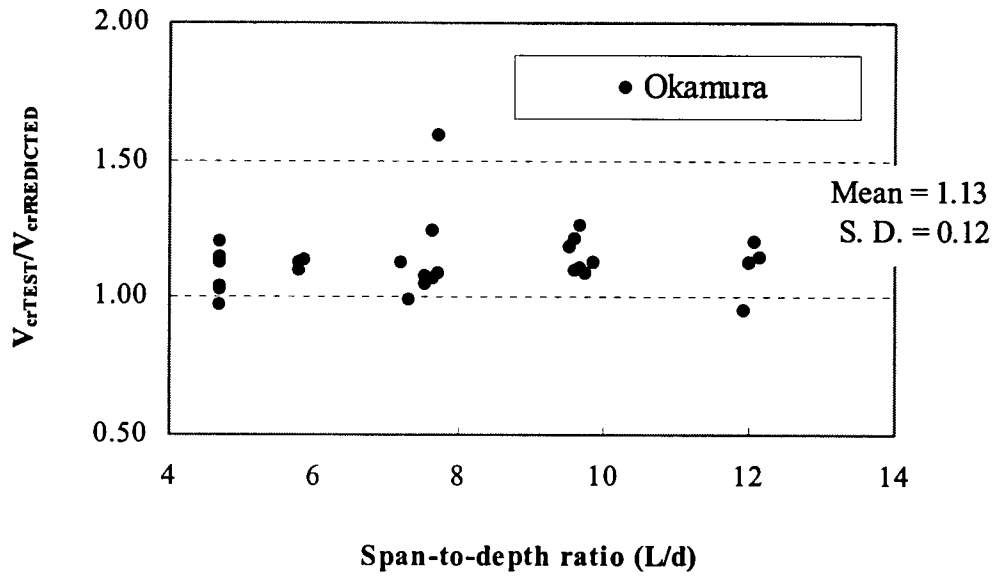


Fig. 46. Comparison of experimental results with those predicted using Okamura's equation

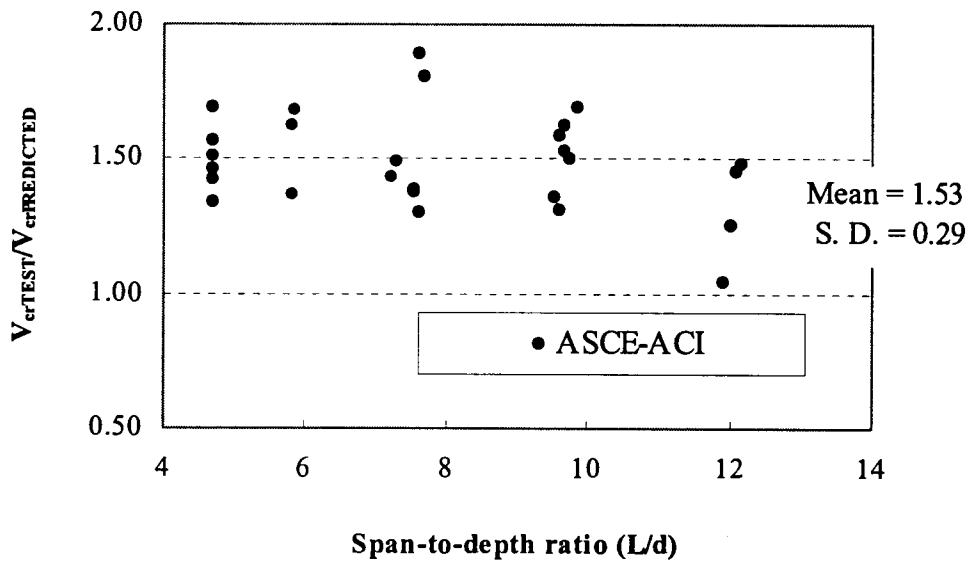


Fig. 47. Comparison of experimental results with those predicted using ASCE-ACI equation

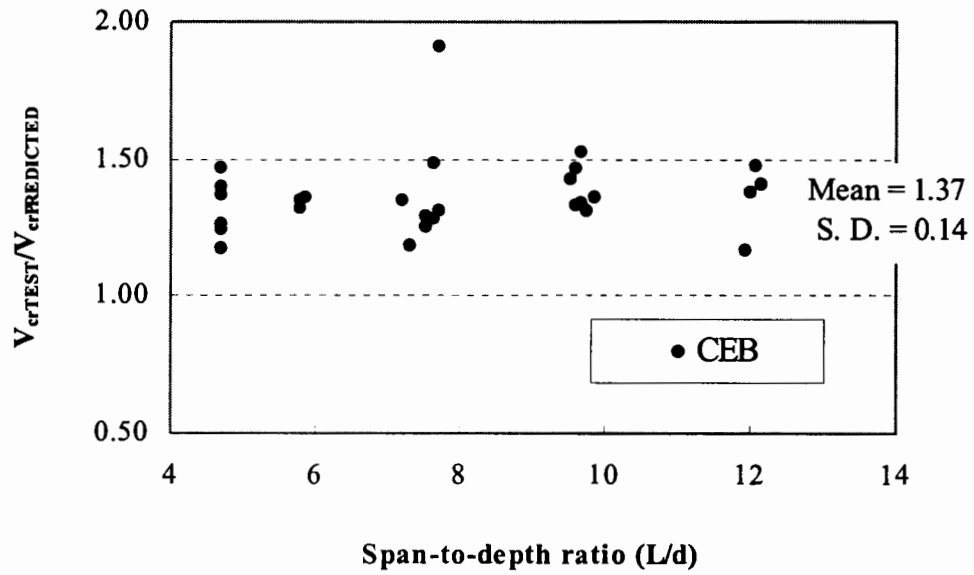


Fig. 48. Comparison of experimental results with those predicted using CEB method

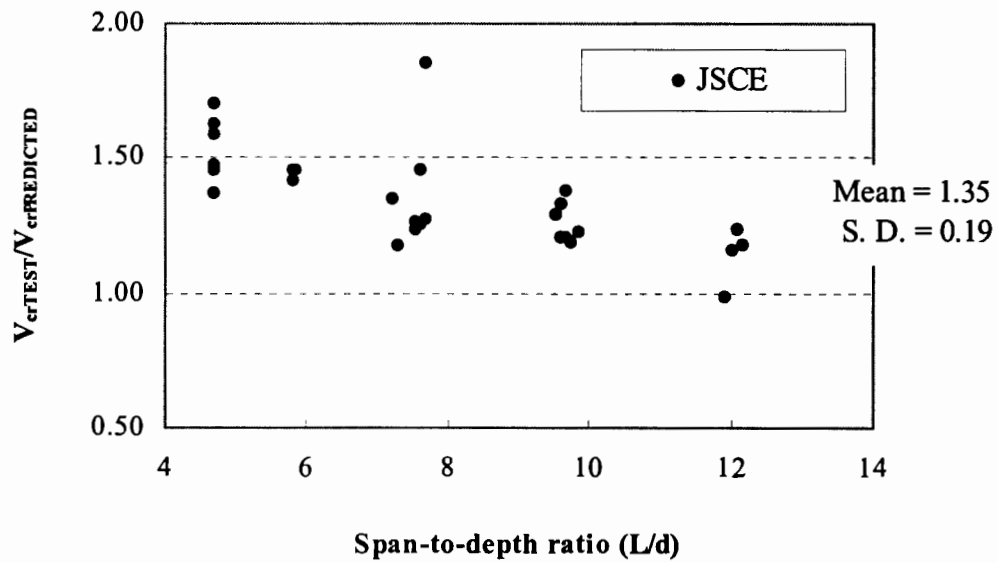


Fig. 49. Comparison of experimental results with those predicted using JSCE method

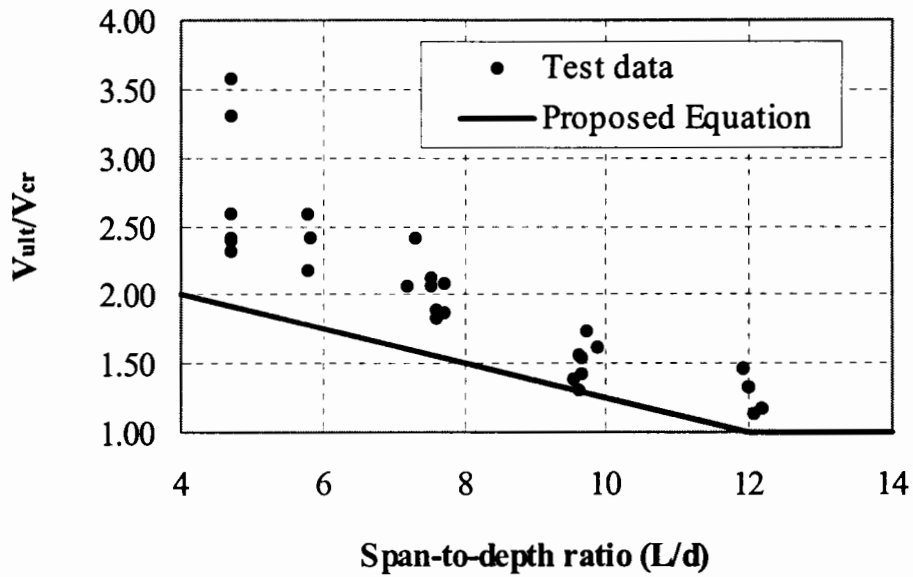


Fig. 50. Comparison of ultimate to cracking shear strength for members under uniform loading

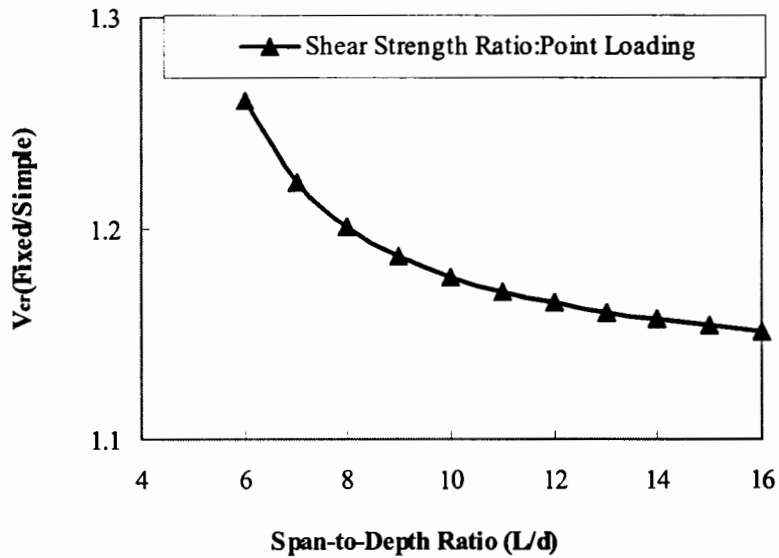


Fig. 51. Influence of support conditions on shear strength of members under point loading

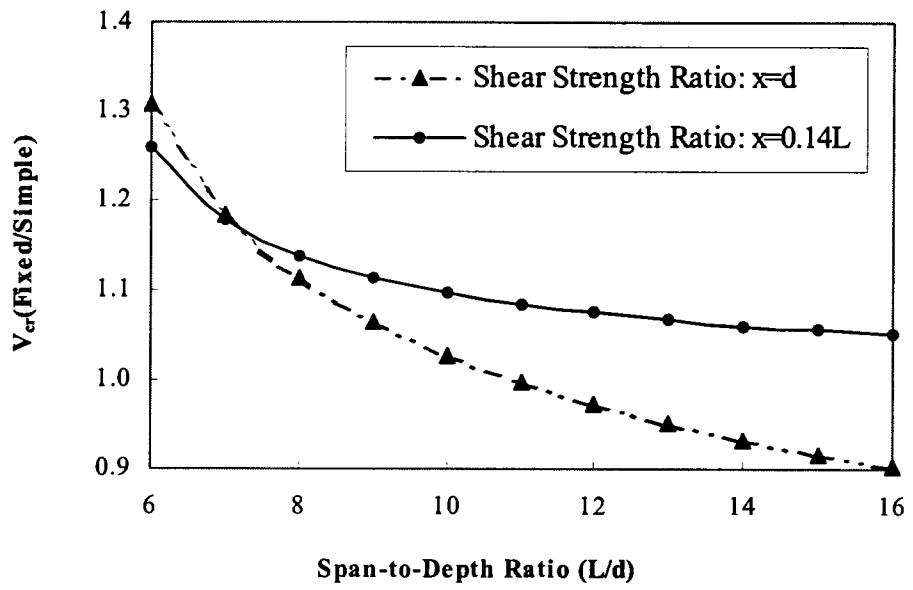


Fig. 52. Influence of support conditions on shear strength for members under uniform loading

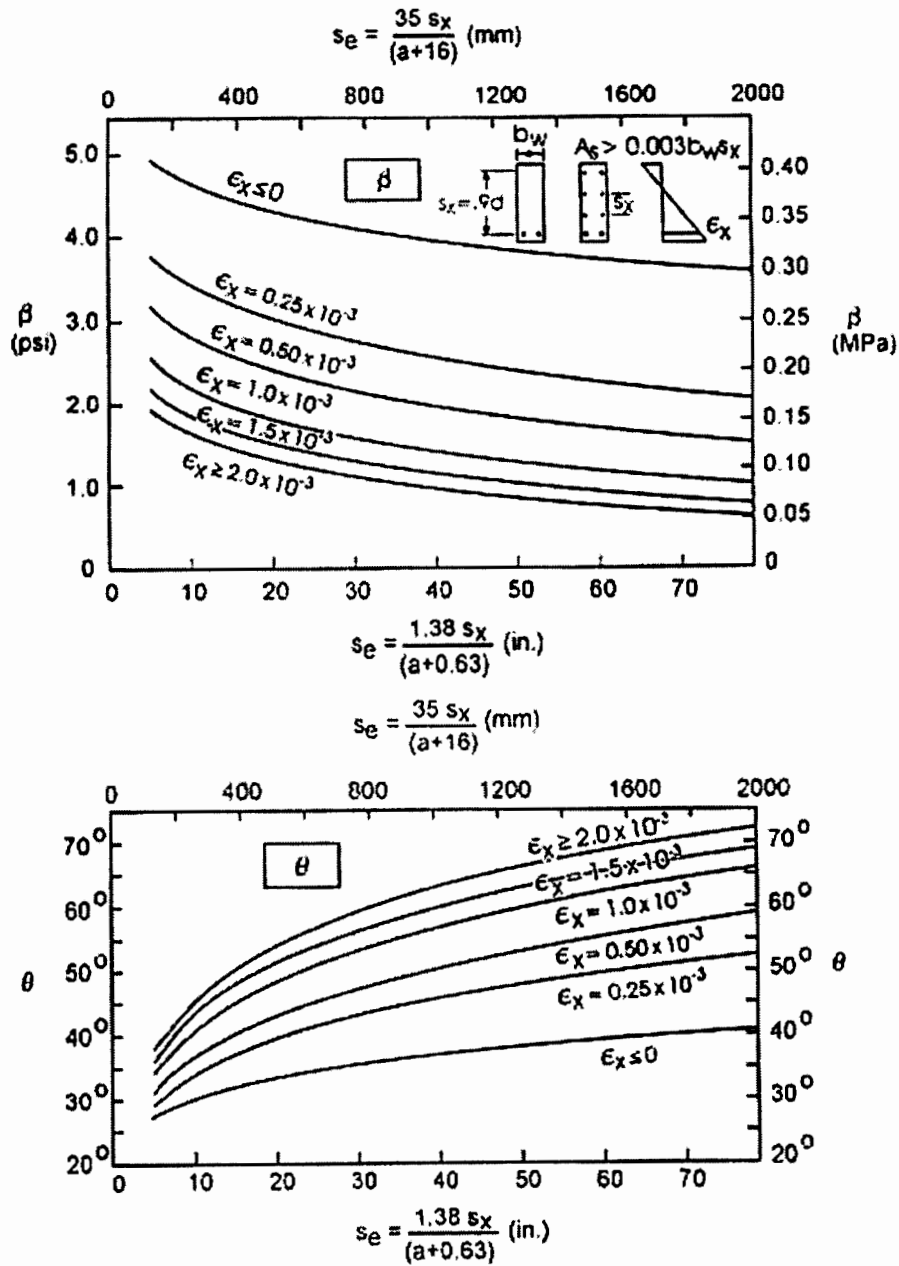


Fig. III-1. Calculation of design parameters β and θ in general shear design method (Collins et. al. 1996, Collins & Kuchma 1999)

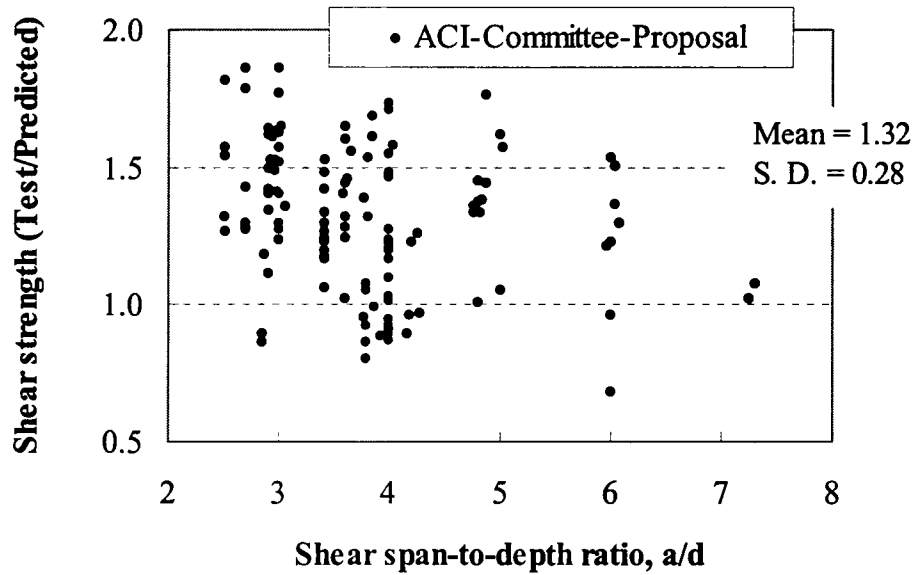


Fig. IV-1(a). Comparison of experimental results with those predicted using proposed ACI-Committee 445 Equation – Influence of a/d ratio

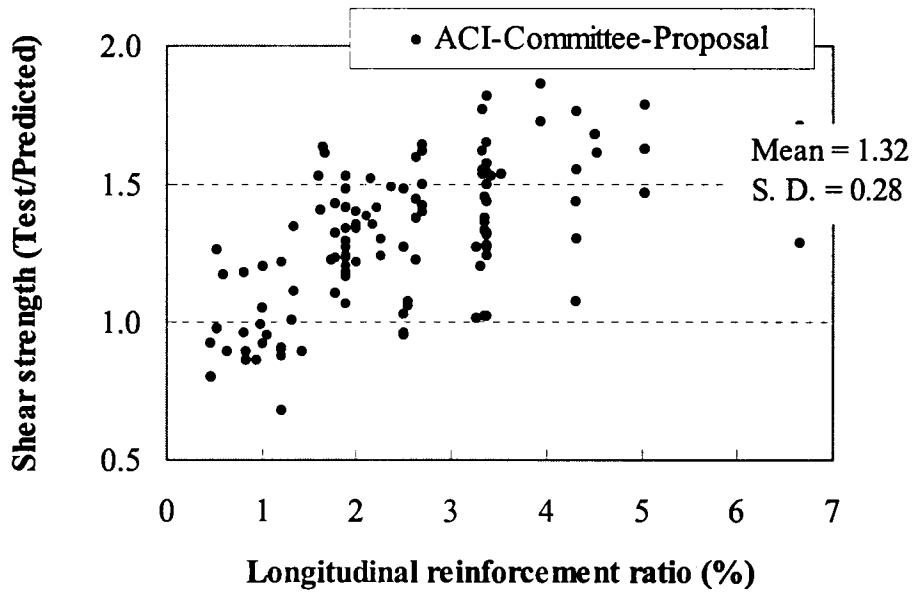


Fig. IV-1(b). Comparison of experimental results with those predicted using proposed ACI-Committee 445 Equation – Influence of longitudinal reinforcement ratio

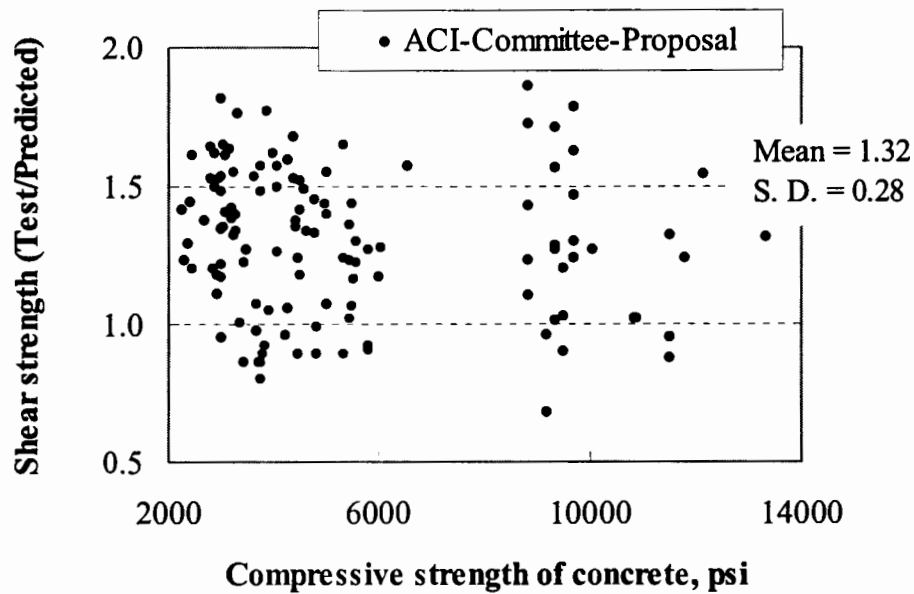


Fig. IV-1(c). Comparison of experimental results with those predicted using proposed ACI-Committee 445 Equation – Influence of Concrete Strength

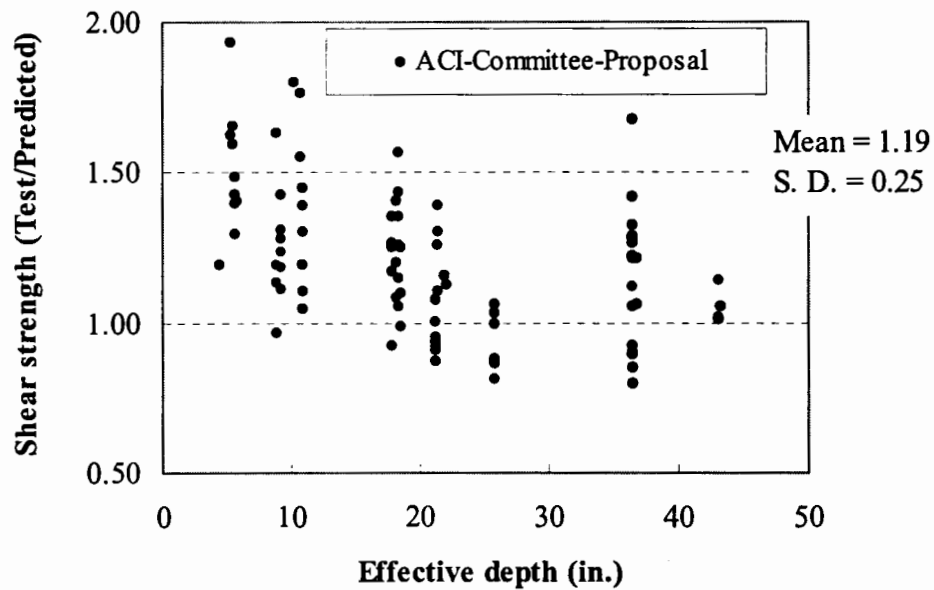


Fig. IV-2. Comparison of experimental results with those predicted using proposed ACI-Committee 445 Equation – Influence of Member Size

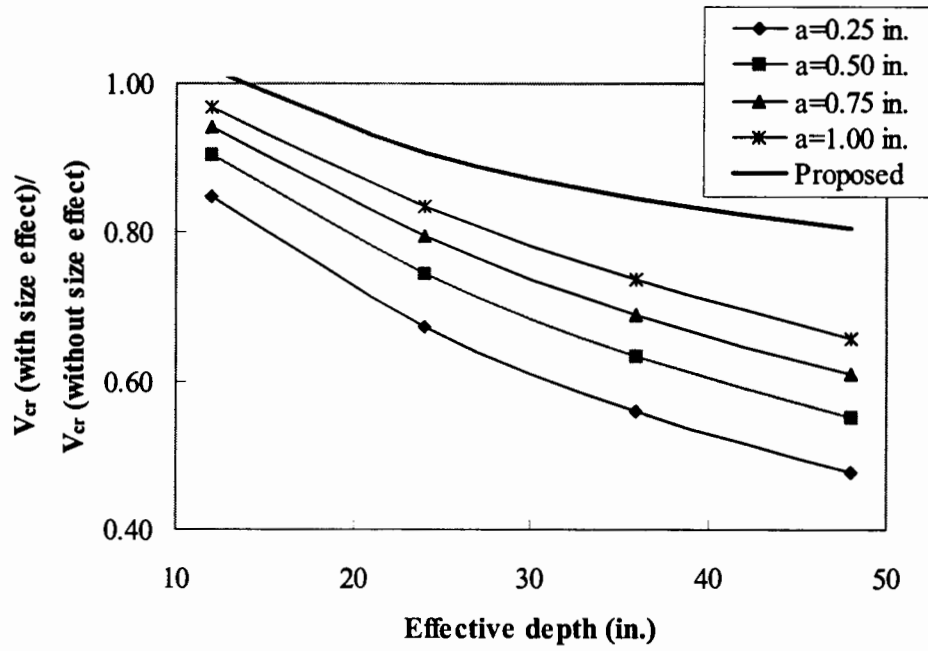


Fig. IV-3. Comparison of proposed equation with proposed ACI-Committee equation for size effect (Note: a = maximum aggregate size)

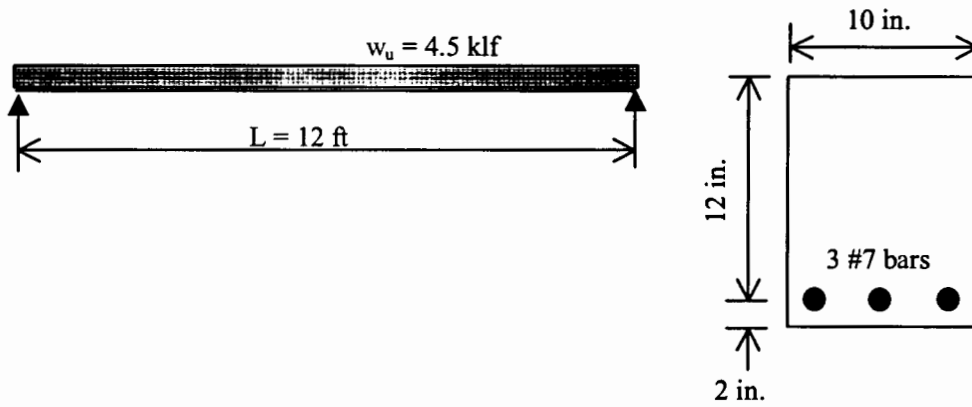


Fig. V-1

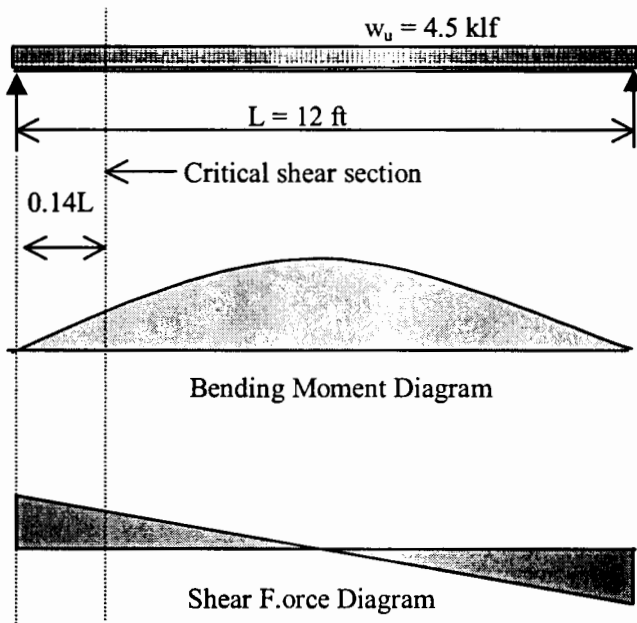


Fig. V-2

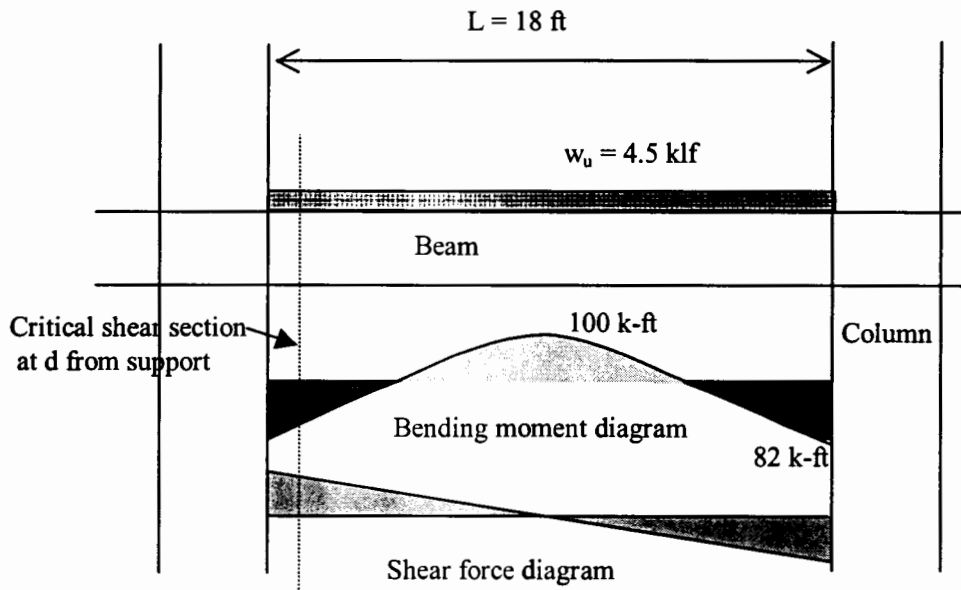


Fig. V-3

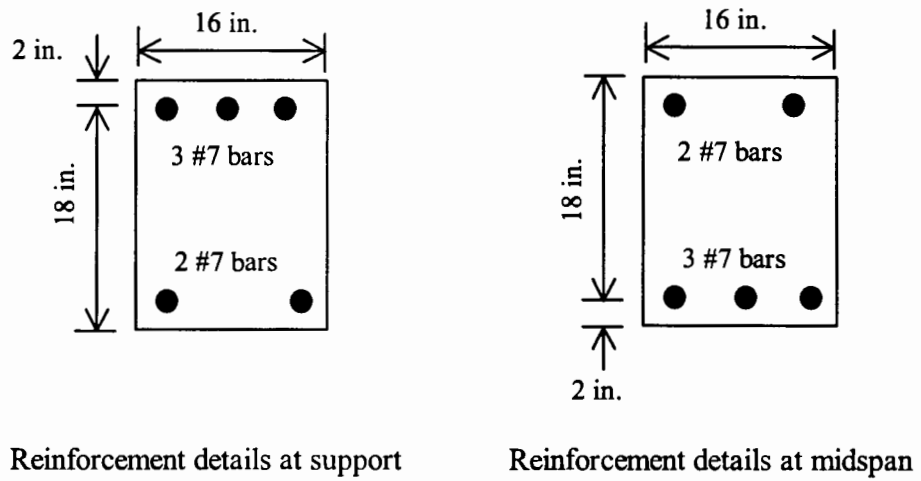


Fig. V-4